

UNIVERSITY OF CALGARY

Synthesis and Reactivity of Novel *Bis*-(pentafluorophenyl)borylated Ferrocenes

by

Bryon E. Carpenter

A THESIS

SUBMITTED TO THE FACULTY OF GRADUATE STUDIES
IN PARTIAL FULFILMENT OF THE REQUIREMENTS FOR THE
DEGREE OF MASTERS OF SCIENCE

DEPARTMENT OF CHEMISTRY

CALGARY, ALBERTA

DECEMBER, 1999

© Bryon E. Carpenter 1999



National Library
of Canada

Acquisitions and
Bibliographic Services

385 Wellington Street
Ottawa ON K1A 0N4
Canada

Bibliothèque nationale
du Canada

Acquisitions et
services bibliographiques

395, rue Wellington
Ottawa ON K1A 0N4
Canada

Your file Votre référence

Our file Notre référence

The author has granted a non-exclusive licence allowing the National Library of Canada to reproduce, loan, distribute or sell copies of this thesis in microform, paper or electronic formats.

L'auteur a accordé une licence non exclusive permettant à la Bibliothèque nationale du Canada de reproduire, prêter, distribuer ou vendre des copies de cette thèse sous la forme de microfiche/film, de reproduction sur papier ou sur format électronique.

The author retains ownership of the copyright in this thesis. Neither the thesis nor substantial extracts from it may be printed or otherwise reproduced without the author's permission.

L'auteur conserve la propriété du droit d'auteur qui protège cette thèse. Ni la thèse ni des extraits substantiels de celle-ci ne doivent être imprimés ou autrement reproduits sans son autorisation.

0-612-49601-5

Canada

Abstract

The synthesis, reactivity and characterisation of a new type of Lewis acid is the topic of this thesis. These species utilise the ferrocene skeletal motif containing a variable number of *bis*-(pentafluorophenyl)boryl moieties affixed to the cyclopentadienyl rings.

Chapter 1 presents a brief review of the relevant literature pertaining to ferrocenes and Lewis acidic boranes, in order to provide a context in which to introduce this new work. Specifically, this review summarises three broad areas of relevance to the current work: perfluoroarylboranes, activation of group IV metallocene Ziegler-Natta olefin polymerisation catalysts (methide abstraction and oxidative activation) and the synthesis and properties of ferrocenylboranes.

The synthesis, characterisation, properties and derivatisation of the two novel Lewis acids *bis*-(pentafluorophenyl)borylferrocene $\text{FcB}(\text{C}_6\text{F}_5)_2$ and 1,1'-*bis*-(pentafluorophenyl)boryl)ferrocene $\text{Fc}[\text{B}(\text{C}_6\text{F}_5)_2]_2$ provide the foundation for the work presented in Chapter 2. These unique compounds represent the first examples of perfluoroarylborylated ferrocenes. This chapter is subdivided into preparation of $\text{FcB}(\text{C}_6\text{F}_5)_2$ and $\text{Fc}[\text{B}(\text{C}_6\text{F}_5)_2]_2$ followed by reactivity and characterisation of ensuing derivatives. The X-ray structure of $\text{FcB}(\text{C}_6\text{F}_5)_2$ has been determined. A noteworthy feature of this structure was the distortion of the boron atom from coplanarity with the carbon atoms of the cyclopentadienyl ring toward the iron atom. The Lewis acidity of $\text{FcB}(\text{C}_6\text{F}_5)_2$ and $\text{Fc}[\text{B}(\text{C}_6\text{F}_5)_2]_2$ were probed with a variety of Lewis bases. $\text{Fc}[\text{B}(\text{C}_6\text{F}_5)_2]_2$ was found to interact more strongly with Lewis bases than was $\text{FcB}(\text{C}_6\text{F}_5)_2$. Of those Lewis bases surveyed only PMe_3 reacts to form stable isolable products $\text{FcB}(\text{C}_6\text{F}_5)_2\text{PMe}_3$.

and $\text{Fc}[\text{B}(\text{C}_6\text{F}_5)_2\text{PMe}_3]_2$. The X-ray crystal structures of both of these adducts were determined. Reaction of $\text{FcB}(\text{C}_6\text{F}_5)_2$ with the oxidants AgOTf , AgC_6F_5 , NOBF_4 and $\text{FcAcB}(\text{C}_6\text{F}_5)_4$ afforded the corresponding oxidised products $\text{Fc}^+\text{B}^-(\text{C}_6\text{F}_5)_2\text{OTf}$, $\text{Fc}^+\text{B}^-(\text{C}_6\text{F}_5)_3$, $\text{Fc}^+\text{B}^-(\text{C}_6\text{F}_5)_2\text{F}$, $[\text{Fc}^+\text{B}(\text{C}_6\text{F}_5)_2][\text{B}(\text{C}_6\text{F}_5)_4^-]\text{FcAc}$. The first three were fully characterised including X-ray structure determinations. $[\text{Fc}^+\text{B}(\text{C}_6\text{F}_5)_2][\text{B}(\text{C}_6\text{F}_5)_4^-]\text{FcAc}$ was not amenable to further purification and was therefore spectroscopically characterised only. Treatment of $\text{Fc}[\text{B}(\text{C}_6\text{F}_5)_2]_2$ with a selection of small anions was undertaken. The product resulting from chloride addition was the most tractable of those examined. Reaction chemistry of $\text{FcB}(\text{C}_6\text{F}_5)_2$, $\text{Fc}[\text{B}(\text{C}_6\text{F}_5)_2]_2$, $\text{Fc}^+\text{B}^-(\text{C}_6\text{F}_5)_2\text{OTf}$ and $\text{Fc}^+\text{B}^-(\text{C}_6\text{F}_5)_3$ with Cp_2ZrMe_2 was explored. $\text{Fc}[\text{B}(\text{C}_6\text{F}_5)_2]_2$ and $\text{Fc}^+\text{B}^-(\text{C}_6\text{F}_5)_2\text{OTf}$ effectively activated Cp_2ZrMe_2 , however, pentafluorophenyl and triflate transfer back to the cationic zirconium centre was facile. Finally, electrochemical analyses of $\text{FcB}(\text{C}_6\text{F}_5)_2$, $\text{Fc}[\text{B}(\text{C}_6\text{F}_5)_2]_2$, $\text{FcB}(\text{C}_6\text{F}_5)_2\text{PMe}_3$, $\text{Fc}[\text{B}(\text{C}_6\text{F}_5)_2\text{PMe}_3]_2$ and $\text{Fc}^+\text{B}^-(\text{C}_6\text{F}_5)_3$ are presented. The experimental details of the molecules described and characterised in Chapter 2 are the topic of Chapter 3.

Acknowledgements

I would like to extend my gratitude to Dr. Warren E. Piers for his supervision and direction during the past two years of my Masters program. He has challenged my way of approaching chemistry and has instilled in me principles that will be with me for many years to come. Warren is a good teacher and friend. Thank you.

I would like to thank Dr. Masood Parvez for his crystallographic expertise in solving structures and interpreting X-ray data include herein. Thanks to Dr. A. Scott Hinman for the equipment used to collect electrochemical data and useful discussions in regards to interpretation of this data.

I would like to thank the University of Calgary and the Department of Chemistry for their financial support in the form of teaching assistantships and research scholarships while studying.

I would like to thank Dr. Dan Parks, Dr. Clifford Williams, Dr. Geoff Irvine, Preston Chase, James Blackwell, Kevin Cook and other present and past members of the Piers Group for their friendship in and out of the lab and many discussions over coffee. We had a great time working together in the lab.

I am grateful for all the people in my life that have contributed to my success over the whole of my university career. My wife Wendy, of the past eight months, has loved and encouraged me throughout my Masters program. My parents, Gordon and Doris Carpenter, for their sacrifice and love throughout my life. My sister (Charmaine), my wife's parents (Reina and Dave Kreeze), friends from Centre Street Church and everyone that has sacrificed so much for my success throughout my life and post-secondary career. Thank you.

To my wife and my parents.

Table of Contents

Abstract	iii
Acknowledgements	v
Table of Contents	vii
List of Tables	x
List of Figures.....	xii
List of Abbreviations	xiii
1 Chapter 1	1
1.1 Introduction.....	1
1.2 Perfluoroarylboranes.....	1
1.3 Ferrocenylboranes	7
1.4 The Goals	15
2 Chapter 2: <i>Bis</i>-(pentafluorophenyl)borylated Ferrocene	16
2.1 Introduction.....	16
2.2 <i>Bis</i>-(pentafluorophenyl)borylferrocene (1).....	17
2.2.1 Synthesis and characterisation of with FcB(C₆F₅)₂ (1)	17
2.2.2 Reaction Behaviour of FcB(C₆F₅)₂ (1)	31
2.2.2.1 Lewis Base reactions with FcB(C₆F₅)₂ (1)	31
2.1.1.1 Oxidation Chemistry of FcB(C₆F₅)₂ (1).....	36
2.2.3 1,1'-<i>Bis</i>-(pentafluorophenyl)boryl ferrocene (2).....	50
2.3.1 Synthesis and characterisation of Fc[B(C₆F₅)₂]₂ (2)	50
2.3.2 Reaction Behaviour of Fc[B(C₆F₅)₂]₂ (2)	54
2.3.2.1 Lewis Base reactions with Fc[B(C₆F₅)₂]₂ (2)	54
2.3.2.2 Reactions of Fc[B(C₆F₅)₂]₂ (2) with anions.	59
2.4 Activation studies of dimethylzirconocene	61
2.5 Electrochemical studies	63
2.6 Quantitative assessment of the Lewis acid strength of 1 and 2.	68
2.7 Conclusions.....	71
2.8 Future Considerations	73
3 Chapter 3: Experimental Methods.....	74
3.1 General Considerations.....	74
3.2 Preparation of Mono-borylated Ferrocene and Related Compounds	78
3.2.1 Preparation of <i>Bis</i>-(pentafluorophenyl)borylferrocene FcB(C₆F₅)₂ (1).	78
3.2.1.1 Method A - Direct Borylation of Ferrocene	78
3.2.1.2 Method B - Mercury Salt Metathesis Route.....	79

3.2.1.3	Method C – “Friedel-Crafts” Type Borylation.....	80
3.2.2	Preparation of Ferrocenium <i>Bis</i> -(pentafluorophenyl)(trifluoromethanesulfonyl)borate ($\text{Fc}^+\text{B}^-(\text{C}_6\text{F}_5)_2\text{OTf}$) (4).....	80
3.2.3	Preparation of Ferrocenium Tris(pentafluorophenyl)borate ($\text{Fc}^+\text{B}^-(\text{C}_6\text{F}_5)_3$) (5).....	81
3.2.4	Preparation of Cobaltocenium Ferrocenyl Tris(pentafluorophenyl)-borate (6)	82
3.2.5	Preparation of <i>Bis</i> -(pentafluorophenyl)borylferrocene Trimethylphosphine adduct $\text{FcB}(\text{C}_6\text{F}_5)_2\cdot\text{PMe}_3$ (3).....	82
3.2.6	Preparation of $\text{Fc}^+\text{B}^-(\text{C}_6\text{F}_5)_2\text{F}$ (8).....	83
3.2.7	Preparation of $[\text{FcB}(\text{C}_6\text{F}_5)_2\cdot\text{PMe}_3]^+[\text{BF}_4]^-$ (12)	84
3.2.8	Reaction of 1 with Acetylferrocenium Tetrakis(pentafluorophenyl)-borate	84
3.2.9	Reaction of 1 with Tetrabutylammonium Tetrafluoro-borate $[\text{NBu}_4]^+[\text{BF}_4]^-$	85
3.3	Preparation of <i>Bis</i>-borylated Ferrocene and Related Compounds.....	85
3.3.1	Preparation of 1,1'- <i>Bis</i> -(bis-(pentafluorophenyl)boryl)ferrocene $\text{Fc}[\text{B}(\text{C}_6\text{F}_5)_2]_2$ (2)	85
3.3.1.1	Method A - Mercury Salt Metathesis Route.....	85
3.3.1.2	Method B - Zinc Salt Metathesis Route	86
3.3.2	Preparation of 1,1'- <i>Bis</i> -(trimethylphosphino- <i>bis</i> -(pentafluorophenyl)boryl)ferrocene $\text{Fc}[\text{B}(\text{C}_6\text{F}_5)_2\cdot\text{PMe}_3]_2$ (15)	87
3.3.3	Preparation of 1,1'- <i>Bis</i> -(chloromercuric)ferrocene ($\text{Fc}[\text{HgCl}]_2$) (13)	87
3.4	Preparation of other reagents	88
3.4.1	Preparation of Tetrabutylammonium Tetrakis(pentafluorophenyl)-borate (16)	88
3.4.2	Preparation of Acetylferrocenium Tetrakis(pentafluorophenyl)-borate (10)	89
3.5	Reactivity studies	90
3.5.1	Activation Studies with Dimethylzirconocene	90
3.5.1.1	General Procedure	90
3.5.1.1.1	Borane 1.....	90
3.5.1.1.2	Borane 2.....	90
3.5.1.1.3	Zwitterion 4	91
3.5.1.1.4	Zwitterion 5	91
3.5.2	Borane 1 with Lewis Bases	92
3.5.2.1	General Procedure	92
3.5.2.1.1	Acetonitrile (CH_3CN).....	92
3.5.2.1.2	Trimethylphosphine (PMe_3)	93
3.5.3	Borane 2 with Lewis Bases	93

3.5.3.1	General Procedure	93
3.5.3.1.1	Acetylferrocene	94
3.5.3.1.2	Acetonitrile (14)	94
3.5.3.1.3	Trimethylphosphine (15)	94
3.5.4	Borane 2 with Anions X ⁻	95
3.5.4.1	General Procedure	95
3.5.4.1.1	Reaction with Trityl Hydroxide.....	95
3.5.4.1.2	Reaction with Tetraphenylphosphonium Chloride [Ph ₄ P] ⁺ [Cl] ⁻	95
3.5.4.1.3	Reaction with copper(II)methoxide (Cu(OMe) ₂)	96
3.6	General reaction of Lewis acids with crotonaldehyde.....	96
3.6.1	FcB(C ₆ F ₅) ₂ (1) with crotonaldehyde	96
3.6.2	Fc[B(C ₆ F ₅) ₂] ₂ (2) with crotonaldehyde	98
3.6.3	BBr ₃ with crotonaldehyde	98
3.6.4	AlCl ₃ with crotonaldehyde	98
3.6.5	SnCl ₄ with crotonaldehyde	98
3.7	Electrochemical Experiments – Cyclic Voltammetry (CV).....	98
3.8	Crystallographic Data Collection and results	100
4	References.....	101
5	Appendix I: Crystal Structure Data.....	106
5.1	Table 5-1: Crystal Data Collection and Refinement Parameters for 1, 3, 4 and 5.....	106
5.2	Table 5-2: Crystal Data Collection and Refinement Parameters for 7, 13 and 15.....	107
5.3	Crystal Data Obtained for 1.....	108
5.4	Crystal Data Obtained for 3.....	115
5.5	Crystal Data Obtained for 4.....	119
5.6	Crystal Data Obtained for 5.....	125
5.7	Crystal Data Obtained for 7.....	129
5.8	Crystal Data Obtained for 12.....	136
5.9	Crystal Data Obtained for 15.....	140

List of Tables

Table 2-1: ^{19}F NMR meta/para chemical shift differences and ^{11}B NMR resonances of selected pentafluorophenylboron compounds.	23
Table 2-2: Selected Bond Distances (\AA) and Angles ($^\circ$) and Dihedral Angles ($^\circ$) for 1	26
Table 2-3: Variable temperature ^1H NMR spectral data for the reaction of 1 and CH_3CN (1.0:1.1) in d_6 -toluene.	32
Table 2-4: Selected interatomic distances (\AA) and angles ($^\circ$) for adduct 3	34
Table 2-5: Selected Bond Distances (\AA) and Angles ($^\circ$) and Dihedral Angles ($^\circ$) for 4	38
Table 2-6: Selected Bond Distances (\AA) and Angles ($^\circ$) and Dihedral Angles ($^\circ$) for 5	42
Table 2-7: Selected Bond Distances (\AA) and Angles ($^\circ$) for 12	49
Table 2-8: Selected Bond Distances (\AA) and Angles ($^\circ$)for 15	57
Table 2-9: Electrochemical data observed for 1, 2, 3, 5, 15	64
Table 2-10: ^1H NMR chemical shift differences ($\Delta\delta$) of crotonaldehyde on complexation with various Lewis acids. ^a	69
Table 2-11: Lewis acid scale based on $\Delta\delta_{\text{H}3}$ resonances of crotonaldehyde.	70
Table 3-1: Variable temperature ^1H NMR data for the reaction of 1 and CH_3CN (1:1.1) in d_6 -toluene.	93
Table 3-2: CV experiment data.....	98
Table 5-1: Crystal Data Collection and Refinement Parameters for 1, 3, 4 and 5	105
Table 5-2: Crystal Data Collection and Refinement Parameters for 7, 13 and 15	106
Table 5-3: Atomic Parameters x, y, z and U(eq) for 1	107
Table 5-4: Hydrogen Parameters x, y, z and U(eq) for 1	108
Table 5-5: Interatomic Distances (\AA) and Angles ($^\circ$) for 1	109
Table 5-6: Atomic Parameters x, y, z and U(eq) for 3	114
Table 5-7: Hydrogen Parameter x, y, z and U(eq) for 3	115
Table 5-8: Interatomic distances (\AA) and Angles ($^\circ$) for 3	115
Table 5-9: Atomic Parameters x, y, z and U(eq) for 4	118
Table 5-10: Hydrogen Parameters x, y, z and U(eq) for 4	119
Table 5-11: Interatomic Distances (\AA) and Angles ($^\circ$) for 4	119

Table 5-12: Atomic Parameters x, y, z and U(eq) for 5.....	124
Table 5-13: Hydrogen Parameters x, y, z and U(eq) for 5.....	125
Table 5-14: Interatomic Distances (\AA) and Angles ($^{\circ}$) for 5	125
Table 5-15: Atomic Parameters x, y, z and U(eq) for 7.....	128
Table 5-16: Hydrogen Parameters x, y, z and U(eq) for 7.....	129
Table 5-17: Interatomic Distances (\AA) and Angles ($^{\circ}$) for 7	130
Table 5-18: Atomic Parameters x, y, z and U(eq) for 12.....	135
Table 5-19: Hydrogen Parameters x, y, z and U(eq) for 12.....	136
Table 5-20: Interatomic Distances (\AA) and Angles ($^{\circ}$) for 12	137
Table 5-21: Atomic Parameters x, y, z and U(eq) for 15.....	139
Table 5-22: Hydrogen Parameters x, y, z and U(eq) for 15.....	140
Table 5-23: Selected Interatomic Distances (\AA) and Angles ($^{\circ}$) for 15.....	141

List of Figures

Figure 2.1: ^1H NMR spectrum of 1 in C_6D_6	21
Figure 2.2: ^{19}F NMR spectrum of 1 in C_6D_6	22
Figure 2.3: ^{11}B NMR spectrum of 1 in C_6D_6	24
Figure 2.4: ORTEP diagram of 1_A (thermal ellipsoids at 50% probability level). Important structural features: $\text{Fe}(1)\cdots\text{B}(1)$, 2.924 Å; Cp, Cp' tilt angle $\text{Cp}_{cent}\text{Fe}1\cdots\text{Cp}'_{cent}$, 173.6°; ϕ (deviation from eclipsed, $\text{C}(13)\text{Cp}_{cent}\text{Cp}'_{cent}\text{C}(18)$, deg), 0.7°.....	25
Figure 2.5: A view down through the Cp_{cent} of both Cp rings for structure 1_B . Note the deviation from the eclipsed conformation of the Cp rings, $\phi = 9.0^\circ$	28
Figure 2.6: a) Two resonance forms of boron substituted Cp rings; b) interatomic distances of the functionalised Cp ring in 1	29
Figure 2.7: UV/Visible spectrum of 1 in 1,2-dichloroethane. λ_{max} , nm (ϵ): 230 (1.33 x 10^4). Note charge transfer band at 230 nm corresponding to a symmetry-allowed metal to ligand (d to p) transition.....	30
Figure 2.8: ORTEP diagram of 3	34
Figure 2.9: UV/Visible spectrum of 1 and 3 in 1,2-dichloroethane. Note charge transfer band at 230 nm present for 1 and lack of CT band for 3	35
Figure 2.10: ORTEP diagram of 4	37
Figure 2.11: ^1H NMR spectrum of 5 in CD_2Cl_2 . Note the paramagnetically shifted and broadened signals (cf. ^1H NMR of 1).....	40
Figure 2.12: ORTEP diagram of 5	41
Figure 2.13: ORTEP diagram of 8	44
Figure 2.14: ORTEP diagram of 12	48
Figure 2.15: ^1H NMR spectrum of 2 in C_6D_6 . Note the apparent triplet for H_β	53
Figure 2.16: ORTEP diagrams of 15	57
Figure 2.17: CV of 1 (1 mM) in TFT. Electrolyte 16 [Bu_4N][$\text{B}(\text{C}_6\text{F}_5)_4$] at 100 mM. $E_H(1) = +450$ mV (cf. FcH/FcH^+).....	65
Figure 2.18: CV of 2 (1 mM) in TFT. Electrolyte 16 [Bu_4N][$\text{B}(\text{C}_6\text{F}_5)_4$] at 100 mM. $E_H(2) = +420$ mV (cf. Fc/Fc^+).....	65
Figure 2.19: (a) CV of 3 and (b) 15 in TFT at 1mM. Electrolyte 16 [Bu_4N][$\text{B}(\text{C}_6\text{F}_5)_4$] at c = 100 mM. Ag-wire QRE.....	67
Figure 2.20: CV of 5 (1 mM) in TFT. Electrolyte 16 [Bu_4N][$\text{B}(\text{C}_6\text{F}_5)_4$].	68

List of Abbreviations

δ	chemical shift (ppm)
$^\circ$	degrees
ϕ	deviation from eclipsed conformation ($^\circ$)
α	dip angle ($^\circ$)
λ	wavelength (nm)
\AA	angstrom unit, 10^{-10} metre
Ac	acetyl group, $-\text{C}(\text{O})\text{CH}_3$
C	Celsius
C_6D_6	d_6 -benzene
C_6F_5	pentafluorophenyl group
Cp	η^5 -cyclopentadienyl ligand, C_5H_5^-
d	doublet
$E_{\text{1/2}}$	half wave potential (mV)
equiv	equivalent(s)
Et	ethyl group, $-\text{CH}_2\text{CH}_3$
Fc	Ferrocenyl group, $(\eta^5\text{-C}_5\text{H}_5)\text{Fe}(\eta^5\text{-C}_5\text{H}_4)$
Fc^+	Ferrocenium, $[(\eta^5\text{-C}_5\text{H}_5)_2\text{Fe(III)}]^+$
iPr	isopropyl group, $-\text{CH}(\text{CH}_3)_2$
J	coupling constant
m	mulitplet
Me	methyl group, $-\text{CH}_3$

MHz	megaHertz
<i>n</i> -Bu	<i>n</i> -butyl group, -(CH ₂) ₃ CH ₃
NMR	nuclear magnetic resonance
ORTEP	Oakridge Thermal Ellipsoid Plot
OTf	triflate or trifluoromethanesulfonate (-OSO ₂ CF ₃)
Ph	phenyl group, -C ₆ H ₅
ppm	parts per million
s	singlet
t	triplet
<i>t</i> Bu	tertiary-butyl group, -C(CH ₃) ₃
TFT	α,α,α-trifluorotoluene (C ₆ H ₅ CF ₃)
THF	tetrahydrofuran
UV	ultraviolet
Vis	visible
WHM	width at half maximum

1 Chapter 1

1.1 Introduction

Since the discovery of ferrocene (FcH)^{1,2} in the early 1950s a great deal of effort has been expended to understand the chemistry of this and other metallocenes. Ferrocene is one of the most documented metallocene compounds³ and the breadth of information available is far beyond the scope of this thesis review.³⁻⁶ The synthesis and reaction chemistry of perfluoroarylboryl ferrocene compounds is of interest to us. Prior to detailing our findings, a general overview of perfluoroarylboranes and borylferrocenes will be discussed briefly. The combination of these two topics will lead us into perfluoroarylboryl ferrocenes. The background information will provide a basis for undertaking the new chemistry presented in Chapter 2.

1.2 Perfluoroarylboranes⁷

The chemistry of boron-containing compounds has been studied in depth, as evidenced by the great amount of literature that is devoted to this group 13 element. Three-coordinate boron-containing compounds, boranes, are considered electron-deficient in their neutral state (6 valence electrons), capable of accepting another pair of electrons to complete the octet for boron. A Lewis acid, by definition, is an electron pair acceptor. This electron deficiency is the basis for describing boranes as Lewis acids.

Boron trihalides (BX_3) are difficult to handle as they are quite volatile and moisture sensitive. These properties led to the interest in perfluoroalkylboranes ($\text{B}(\text{R}_f)_3$) in the 1950s. The boron–carbon bonds of these compounds ($\text{B}(\text{R}_f)_3$) were expected to be

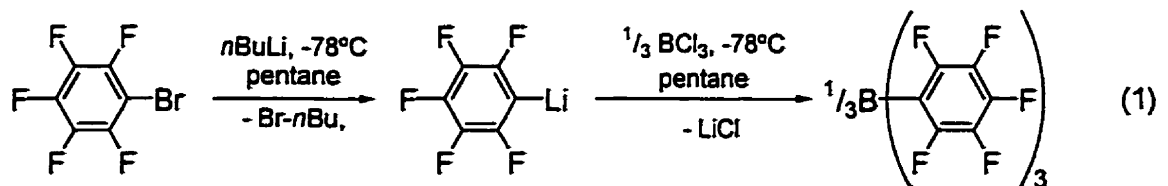
more hydrolytically stable than $B-X$ ($X = \text{halide}$) bonds. Alkylboranes $B(R_f)_3$ were expected to have comparable Lewis acid strengths by virtue of the electron-withdrawing ability of the fluorine atoms attached to the alkyl groups. These reagents, however, were found to be thermally unstable at elevated temperatures due to α - and β -fluoride transfer to boron and loss of a carbene or alkene. The empty p_z -orbital of boron requires occupation to increase the thermal stability of alkyl boranes, by decreasing the possibility of fluoride transfer. Ligands that $p(\pi)$ -donate (like amides or phosphides with an available lone pair in the p_z -orbital) can supply the necessary electrons to boron to allow the isolation of alkyl borane molecules. For example, the amides of $B(CF_3)(NMe_2)_2$ donates electron pairs through π -interaction with the empty p_z -orbital of the boron.⁷

Pentafluorophenylboranes were first reported in the early 1960s by Massey, with the development of tris(pentafluorophenyl)borane ($B(C_6F_5)_3$), and Chambers with (pentafluorophenyl)haloboranes $X_nB(C_6F_5)_{3-n}$ ($X = \text{Cl/F}$, $n = 1$ or 2). The Lewis acid properties of these compounds were not fully exploited, though, until the 1980s. The π -donation from perfluorophenyl (C_6F_5) rings and the lack of perfluoroalkyl groups on boron stabilize these compounds from fluoride transfer. The π -interaction does not seem to hamper the reactive nature of these Lewis acids, as the C_6F_5 rings are also σ -electron-withdrawing.

The utility of pentafluorophenylboranes has come to a place of prominence over the past twenty years. Yamamoto and Ishihara recently reviewed the use of arylboron reagents in organic synthetic transformations.⁸ There have been other reviews on the application and preparation of perfluorophenylboranes^{7,9,10} but only the highlights applicable to the topic of this thesis will be discussed. They are: (a) Lewis acid like,

$B(C_6F_5)_3$, as an activator for group IV alkyl-metallocenes to generate reactive Ziegler-Natta catalyst systems, and (b) *tetrakis*-(pentafluorophenyl)borate ($B(C_6F_5)_4^-$) as a weakly coordinating anion to support reactive cationic species.

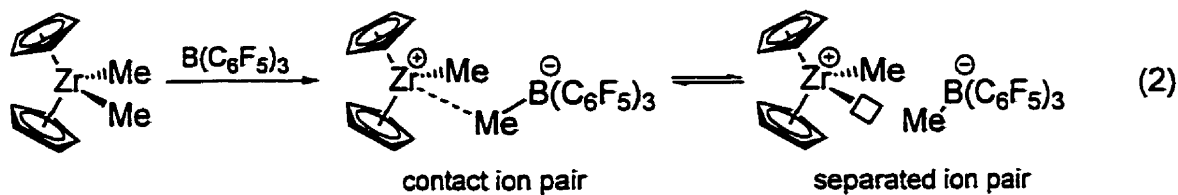
Tris-(pentafluorophenyl)borane¹¹ was first prepared by mixing pentafluorophenyl lithium and boron trichloride in pentane at low temperature (Equation 1). This borane is described as a highly electrophilic Lewis acid possessing thermal stability and a greater resistance to hydrolysis than perfluoroalkylboranes. Hydrolysis does occur, though very slowly to eliminate pentafluorobenzene (C_6F_5H) and the borinic acid $HOB(C_6F_5)_2$. Green and Doerr recently reported the isolation and structure of the monoqua adduct of $B(C_6F_5)_3$.¹² Massey and Park, upon reaction of $B(C_6F_5)_3$ and other trihaloboranes with amines, determined spectroscopically that the Lewis acidity of $B(C_6F_5)_3$ is intermediate between that of BCl_3 and BF_3 ; BCl_3 is the stronger Lewis acid.¹³ Coordination of crotonaldehyde ($CH_3CHCHCHO$) to different boranes has been utilised as a means of quantifying the Lewis acid strength and confirms the placement of $B(C_6F_5)_3$ between BCl_3 and BF_3 observing the degree of change in chemical shift of the aldehyde resonance by 1H NMR spectroscopy.^{14,15}



Chemical and physical properties of $B(C_6F_5)_3$ led Marks and coworkers to the investigate the borane as a cocatalyst for homogeneous Ziegler-Natta olefin polymerisation.¹⁶ As this area of research is considerable this topic of catalyst activation will be discussed only as it pertains to the scope of this thesis. Activation of a Ziegler-

Natta olefin polymerisation precatalyst generally proceeds by the opening of a coordination site at the metal centre by abstraction of an alkide with a strong Lewis acid cocatalyst. The counteranion in these systems must be weakly coordinating to allow the metal centre to maintain an open ligation site for olefin coordination. The cocatalyst methylalumoxane (MAO), prepared by mixing water and trimethylaluminum, has traditionally been used as a methide (CH_3^-) group abstractor from group IV alkylmetallocenes. A large excess of MAO (10^3 to 10^4 equivalents *cf.* metallocene) is necessary to afford optimal catalyst activity for olefin polymerization.

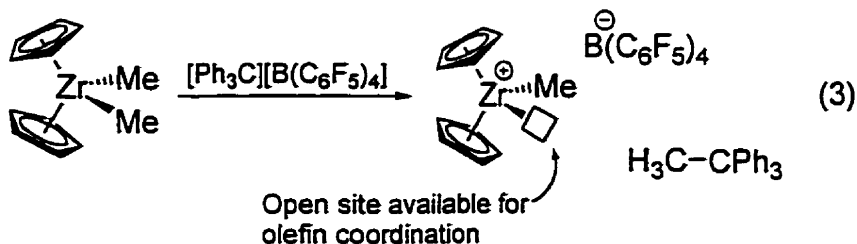
The structure of the Lewis acid species of the MAO mixture responsible for this action is not well defined or understood. Using a Lewis acid of known structure allows for less ambiguity while studying the activation process. Treatment of dimethylzirconocene (Cp_2ZrMe_2) with $\text{B}(\text{C}_6\text{F}_5)_3$ generates an active “cation-like” catalyst (Equation 2).¹⁶ Here the Lewis acid serves to abstract the methide by backside attack and withdraws it from the metal centre to form the counterion $\text{MeB}(\text{C}_6\text{F}_5)_3^-$.



The product formed is a contact ion pair with the methide bridging, unsymmetrically, between the zirconium cation ($\text{Cp}_2(\text{Me})\text{Zr}^+$) and the borane, although it is more strongly associated to the borane.¹⁶ The competition between the two Lewis acids, the borane and the zirconium cation, for the methide affects the dissociation pathway, *i.e.*; freeing a coordination site for olefin approach to the zirconium cation species (separated ion pair). Generally, the greater the cation-anion separation the more

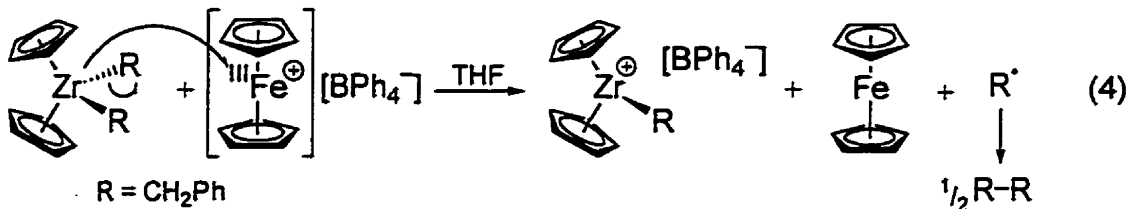
active the catalyst system should be as there is greater opportunity for olefin to coordinate to Zr metal centre. Once olefin (e.g. ethene) coordinates to zirconium, at the open ligation site, enchainment can occur by olefin insertion into the remaining Zr-Me bond; polymerization proceeds.

Another means of methide abstraction is by the use of trityl or triphenylcarbonium cation (Ph_3C^+), isoelectronic to $\text{B}(\text{C}_6\text{F}_5)_3$, to afford 1,1,1-triphenylethane and an active catalyst species (Equation 3). The supporting counterion, often *tetrakis*-(pentafluorophenyl)borate ($\text{B}(\text{C}_6\text{F}_5)_4^-$) is a weakly coordinating anion, (*cf.* $\text{MeB}(\text{C}_6\text{F}_5)_3^-$), rendering the catalyst more reactive to olefin coordination and polymerisation. The methide abstraction product does not bridge between the zirconium and trityl cation as in Equation 2, but is removed from the coordination sphere of the metal as a neutral molecule.



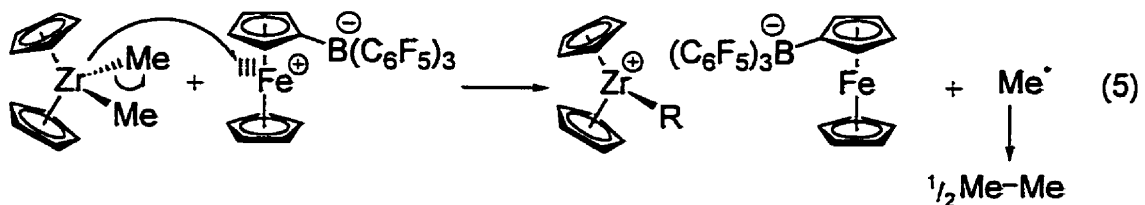
Generation of cationic metal catalysts is attainable by methide abstraction with a strong Lewis acid (e.g., $\text{B}(\text{C}_6\text{F}_5)_3$ or Ph_3C^+), as mentioned above. Another method for preparing the desired cation species is by electron transfer bond homolysis of a metal/alkyl (M-R) bond to form M^+ and an alkyl radical using a one-electron oxidant. The most accessible electrons for removal by oxidation of the Cp_2ZrMe_2 are in the highest occupied molecular orbital (HOMO) which is a combination of the b_2 -molecular orbital of zirconocene ($\text{Cp}_2\text{Zr}^{2+}$) and the sp^3 -hybridised molecular orbitals of the methides (CH_3^-). Oxidative M-R bond cleavage of d^0 metal complex $\text{Cp}_2\text{Zr}(\text{R})_2$ to afford an alkyl

radical (R^\bullet) and a metal cation $Cp_2Zr^+(R)$, was reported by Jordan and coworkers (Equation 4).¹⁷⁻²⁰ Cationic silver(I) (Ag^+) and the ferrocenium ion ($Cp_2Fe(III)^+$ or Fc^+) have been shown to act as one-electron oxidants to cleave alkyl-metal bonds in these systems.¹⁷⁻²⁰ The one-electron transfer oxidation method of catalyst activation has not been used as the byproducts formed, ferrocene/silver metal and alkane ($R^\bullet \rightarrow \frac{1}{2} R$), are not easily removed from the polymer product mixture.



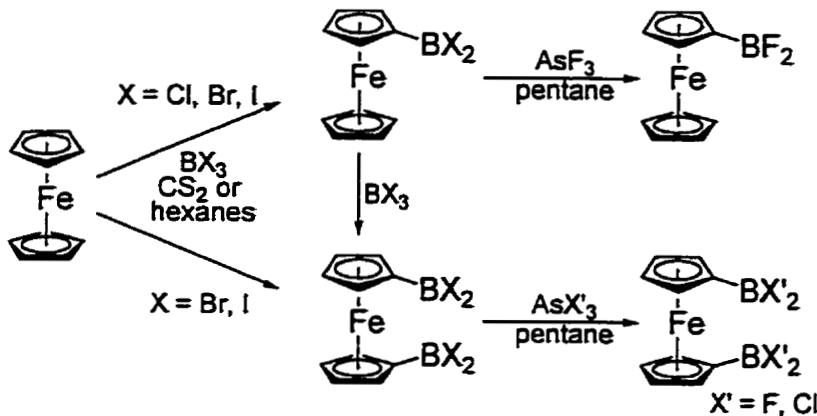
With these methods of catalyst activation in mind, two different types of molecules were considered as targets in this thesis. First a novel Lewis acid having a ferrocenyl fragment in place of one of the perfluorophenyl rings of $B(C_6F_5)_3$ to form a perfluoroarylborylferrocene was identified as a target. This type of Lewis acid may be capable of abstracting a methide from zirconium. Ferrocenyl based boron Lewis acids contain oxidisable iron centres. If the iron (II) of the ferrocene substituent could be oxidised to $Fe(III)$, and a zwitterion formed by coordination of an additional ligand to the boron centre, the resulting zwitterion may be useful toward electron-transfer activation of Zr-Me bonds. This is the second type of molecule we are interested in as a target synthon. The borate fragment, of the resulting ferrocenylborate, could act as a weakly coordinating counterion for the cationic catalyst; the neutral byproduct ferrocene would be incorporated into the anion moiety (Equation 5). Prior to looking at the desired targets

for this thesis, ferrocenyl boranes must be discussed to put the work we are interested in into context.



1.3 Ferrocenylboranes

Borylated ferrocenes were first prepared by the reaction of boron trihalides and ferrocene in the early 1970s (Scheme 1).²¹ Reaction of BBr_3 or BI_3 with ferrocene in boiling carbon disulfide (CS_2) or hexanes affords either the monoborylated or 1,1'-diborylated ferrocenes, under controlled conditions.²²⁻²⁴ Entry into the chloride derivative FcBCl_2 proceeds in essentially the same way with BCl_3 ,^{22,23,25,26} however $\text{Fc}[\text{BCl}_2]_2$ is not accessible *via* this route. The latter is generated by the halide exchange reactions of AsCl_3 with $\text{Fc}[\text{BX}_2]_2$ ($X = \text{Br}/\text{I}$).^{22,24} The FcBF_2 and $\text{Fc}(\text{BF}_2)_2$ are accessible from any other haloboranes (Cl, Br or I) mentioned, with the use of AsF_3 as the fluoride source in pentane solutions.²²⁻²⁴ With these dihaloborylferrocenes in hand a number of derivatives can be prepared by exchange reactions of the halide (X) with a substituent (R) to afford FcBR_2 ($R = \text{NMe}_2$,^{23,26} NEt_2 , OEt , SMe_2 , Me ^{23,24}). Addition of an excess of BX_3 to FcBX_2 affords 1,3,1'-*tris*- and 1,3,1',3'-*tetrakis*-(dihaloboryl)ferrocene.²⁷

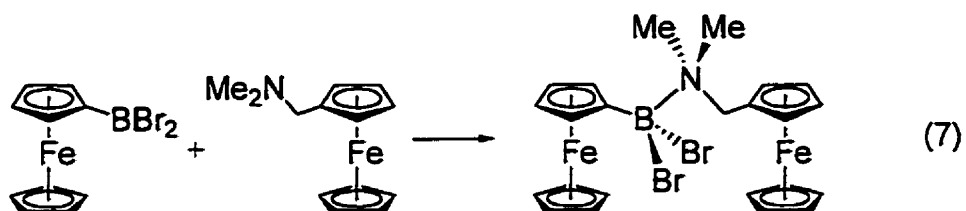


Scheme 1 : Synthesis of dihaloborylferrocenes²¹

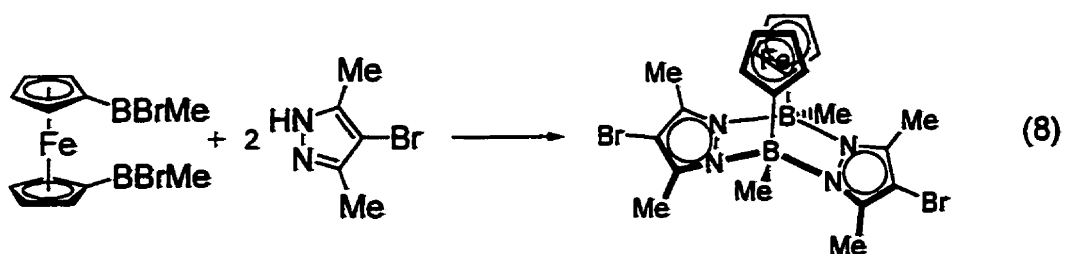
Lithioferrocenes can be used as another entry into borylated ferrocene compounds. Dilithioferrocene is not isolable as a base-free compound, but requires the presence of *N,N,N,N*-tetramethylethylenediamine ($\text{FcLi}_2\cdot(\text{TMEDA})_n$) to stabilize the lithiums present in the molecule. Monolithioferrocene (FcLi), in contrast, does exist as an isolable base-free species. One potential disadvantage of employing dilithioferrocene as a potential synthon is that the necessary TMEDA molecules pose a threat when borylating FcLi_2 as they can bind to the boron atoms as Lewis bases. Monolithioferrocene (FcLi) has been shown to react with BF_3 to form the homoleptic product, BFc_3 .²⁸⁻³⁰ The product BFc_3 is a three coordinated boron centre with Fc groups attached as aromatic ligands. Following oxidation of the by-product from the reaction, an additional product isolated from the homoleptic reaction was formed, the zwitterion $\text{Fc}^+\text{B}^-\text{Fc}_3$. One of the ferrocenyl moieties has been oxidized to ferrocenium (Fc^+) and the boron is tetrahedral anionic (Equation 6).³¹



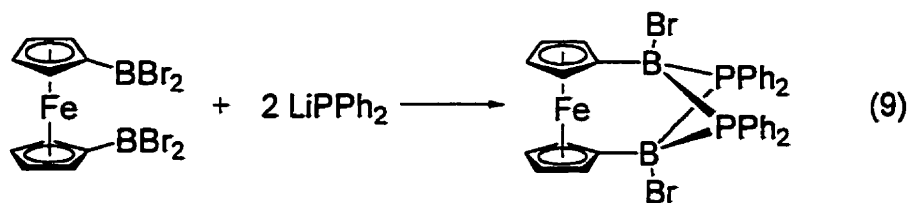
Wagner *et al.* report the use of FcBBr_2 and $\text{FcCH}_2\text{NMe}_2$ as a starting point for generation of a B-N bridged bimetallic compounds (Equation 7).³² The amine binds strongly to the boron to form a stable dative B-N bond, even up to 100°C. The bridging unit ($\text{CH}_2\text{N}-\text{B}$) is isoelectronic to, and sterically resembles, a propylene bridge between the two ferrocene centres. Formation of the $\text{CH}_2\text{N}-\text{B}$ bridges is of interest as carbon-based propylene bridges are difficult to form under such mild conditions; highly reactive organolithium and organomagnesium reagents can destroy the delicate mononuclear building block.



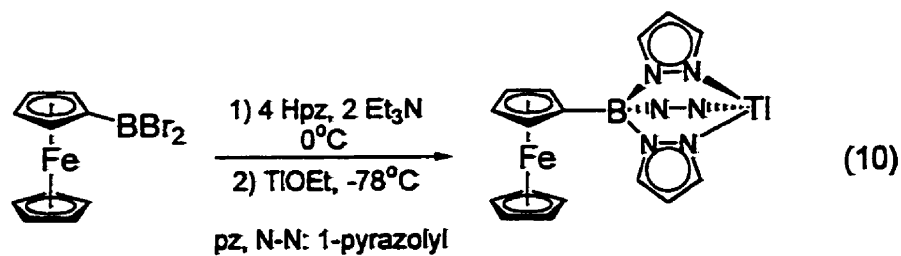
An *ansa*-ferrocene system possessing B-N bonds is formed at low temperature by the reaction of 1,1'-bis-(bromo(methyl)boryl)ferrocene and 4-bromo-3,5-dimethyl-pyrazole (Equation 8).^{33,34} Wagner *et al.* suggests that the isoelectronic effect is important for bridged systems as the B-N bond may be a replacements for C-C linkages; they exhibited similar structural and chemical properties. These B-N bond are also stable up to 100°C as observed by ^1H NMR in d_6 -toluene. Synthetic problems of C-C bond formation may be overcome by using such a donor-acceptor relationship.^{33,35}



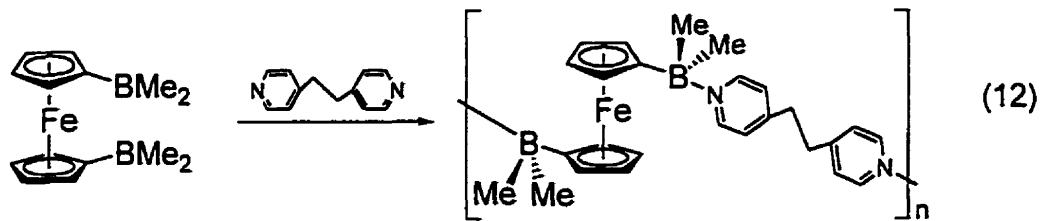
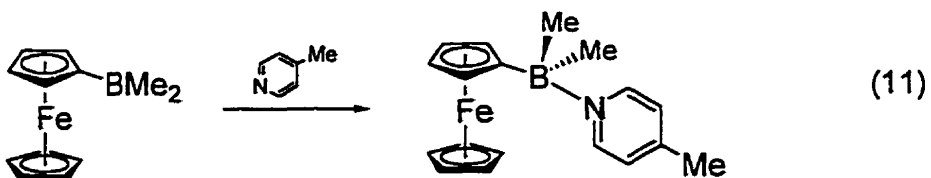
Boron-phosphorus bonds are also similar to those of C-C bonds. The interesting feature of the phosphinoboryl-substituted ferrocene compound $\text{Fc}[\text{B}(\text{PPh}_2)(\text{Br})]_2$ is the bridging-phosphide ($\mu\text{-PPh}_2$) between the two boron centres (Equation 9).^{34,36,37} Lithium amide reacts with $\text{Fc}(\text{BBrR})_2$ but no bridging amides are observed spectroscopically in the product. Novel ligands for other organometallic compounds may be generated by use of these kinds of donor-acceptor type systems.



Ferrocene-based *tris*-(1-pyrazole)borates have also been prepared and show reactivity with other metals to generate oligonuclear organometallic complexes, containing more than one type of metal, for potential application towards organometallic polymers.³⁸ When FcBBr_2 is mixed with pyrazole (Hpz) and triethylamine (Et_3N) in toluene at 0°C , the acid product is generated which can be converted to the thallium salt via reaction with thallium ethoxide (Equation 10).³⁸ This work opened the door to a number of other products from both mono- and 1,1'-bis(dibromoboryl)ferrocene. Extended structures and “polymers” were observed in both the solid and solution states to support the proposed di- and tri-metallic assemblies.³⁹

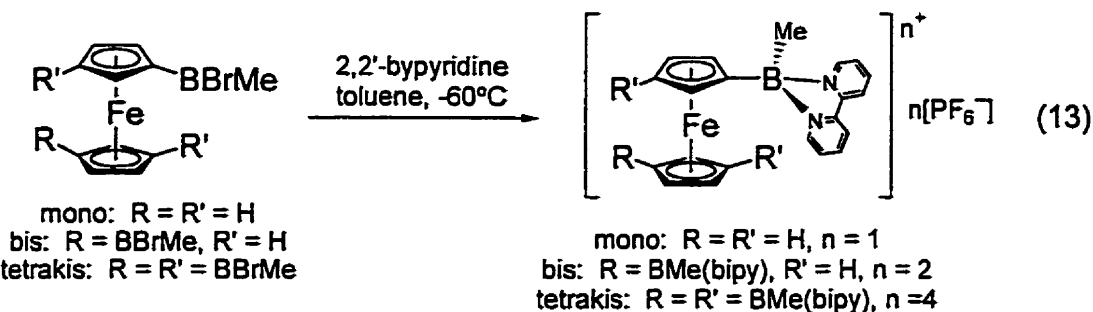


A number of pyridine Lewis bases coordinate to both *mono-* and *bis*-(dimethylboryl)ferrocene. The resultant organometallic polymers are susceptible to depolymerisation (rupture of the dative B-N bonds) at elevated temperatures. Wagner *et al.* undertook this work to generate some organometallic-based polymers and to investigate the electronic communication between the ferrocene units.⁴⁰ Two examples of linear pyridine (i.e. *para*-substituted pyridines) adducts are shown below (equations 11 and 12).

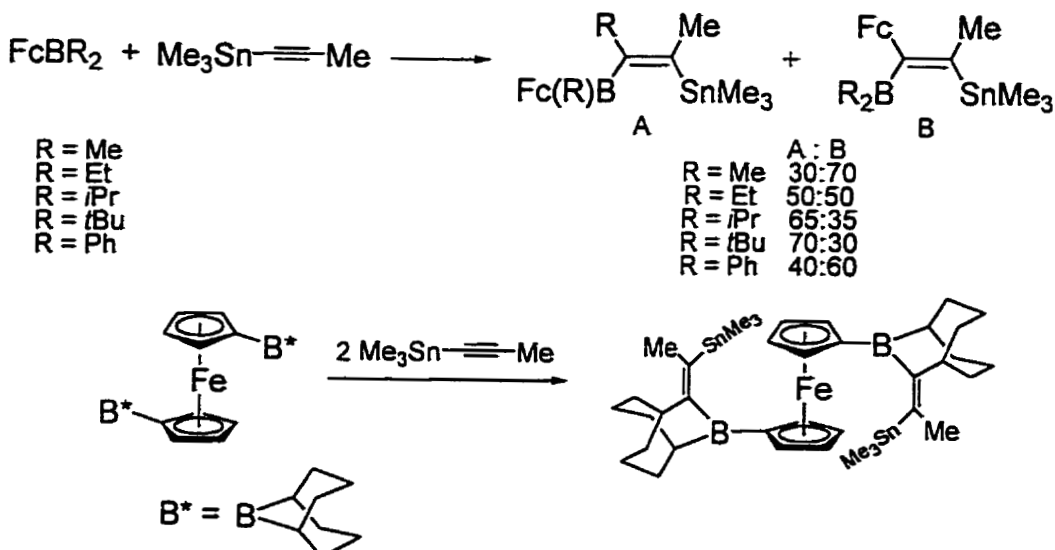


Another pyridine that binds to boron is the bidentate 2,2'-bipyridine (bipy) forming 2,2'-bipyridylboronium salts.⁴¹ 2,2'-Bipyridylboronium salts have been prepared from *mono*-, 1,1-*bis*- and 1,1',3,3'-*tetrakis*-(bromo(methyl)boryl)ferrocene (Equation 13) and electrochemical and X-ray structure analyses were carried out. These bipyridine adducts exhibit multiple redox processes as the borate-group can adopt +1, 0 or -1 charge, and the ferrocene core can switch between Fe(II) and Fe(III). The 1,1',3,3'-*tetrakis*-(bipy(methyl)boryl)ferrocene adduct is capable of tolerating both a one-electron reversible oxidation at the iron centre and up to an eight electron reversible reduction at the (bipy)methylboryl ligand. The electronic flexibility of this molecule and its

incorporation into a dendrimeric complex to serve as electron sponge is a possible application the Wagner group is interested in.⁴¹



Wrackmeyer and coworkers have investigated 1,1-organoboration of trimethyl-1-propynyltin ($\text{Me}_3\text{Sn}-\text{C}\equiv\text{CCH}_3$) by reactions with different diorganoborylferrocenes (FcBBr_2).⁴² They examined the regioselectivity of the ferrocenyl (Fc) and organo (R) groups, attached to the resulting stannylnalkene in the 1,1-position (Scheme 2). The organo groups utilized were methyl (Me), ethyl (Et), *isopropyl* (*i*Pr), *t*-butyl (*t*Bu) and phenyl (Ph). It was found that ferrocene transfers preferentially to the alkene, except in the *t*Bu case (Scheme 2). Statistically an organo group should transfer in a 2:1 ratio but this was not observed. Also, the reaction of $\text{Me}_3\text{Sn}-\text{C}\equiv\text{CCH}_3$ with 1,1'-bis(9-bora-bicyclo[3.3.1]nonyl)ferrocene, prepared from dilithioferrocene and methoxy-9-BBN, affords only the methylene ring expanded product and Fc transfer to the alkene was not observed (Scheme 2).⁴²



Scheme 2 : Reactions of organoborylferrocenes with trimethyl-1-propynyltin

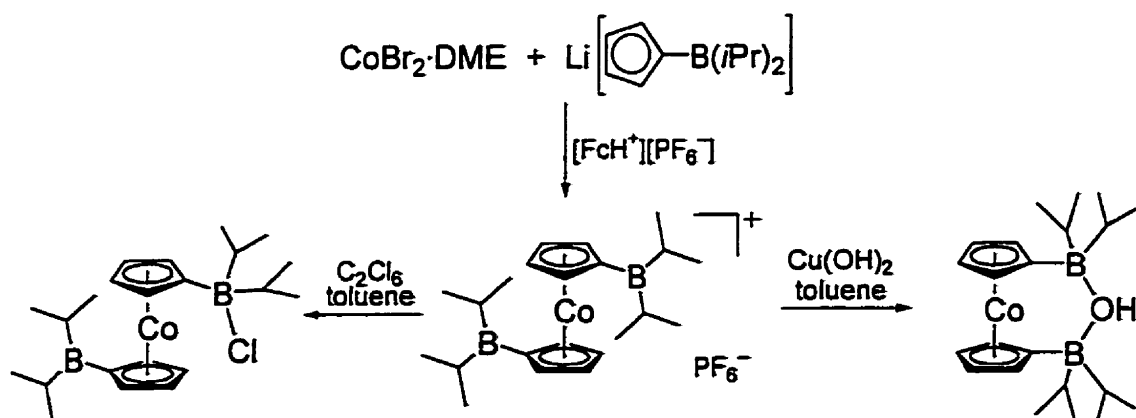
[1]Ferrocenophanes, or *ansa*-ferrocenes with a single atom connecting the two Cp rings, have been of interest to the Manners research group for a number of years.⁴³ The reaction behaviour of these compounds, particularly their ability to undergo ring opening polymerisation affording high molecular weight poly(ferrocene)s, is of interest. A boron-bridged [1]ferrocenophane can be prepared from dilithioferrocene-TMEDA and $(\text{Me}_3\text{Si})_2\text{NBCl}$ to make $[\text{I}](\mu\text{-BN}(\text{SiMe}_3)_2)\text{Fc}$. Ring opening polymerisation of $[\text{I}](\mu\text{-BN}(\text{SiMe}_3)_2)\text{Fc}$ occurs at 180°C to affords a poly(boraferrocene) with boron atoms connecting the ferrocene units.* The structure of $[\text{I}](\mu\text{-BN}(\text{SiMe}_3)_2)\text{Fc}$ clearly show significant ring strain and bending of the ferrocene-boron cycle.

Cobaltocene (Cp_2Co) is a 19-electron metallocene as a neutral molecule. Cobalt belongs to Group 9 which is to the right of the iron group. Oxidation of Cp_2Co generates cobaltocenium (Cp_2Co^+) which is isoelectronic with ferrocene. In the interest of anion binding by use of bidentate Lewis acid systems, Herberich *et al.* prepared a compound

* Braunschweig, H.; Dirk, R.; Müller, M.; Nguyen, P.; Resendes, R.; Gates, D. P.; Manners, I. *Angew. Chem. Int. Ed. Engl.* 1997, 36, 2338-2340.

isoelectronic to *bis*-borylated ferrocene. 1,1'-*Bis*-(diisopropylboryl)cobaltocenium hexafluorophosphate $[\text{Co}(\text{CpB}(i\text{Pr})_2)_2]^+[\text{PF}_6]^-$ was generated from $\text{CoBr}_2\cdot\text{DME}$ and lithium diisopropylborylcyclopentadienide. Oxidation of the 19-electron product afforded the diamagnetic $[\text{Co}(\text{CpB}(i\text{Pr})_2)_2]^+[\text{PF}_6]^-$ product (Scheme 3).⁴⁴ This is another means of generating a boryl-functionalized metallocene, where direct borylation of the metallocene is not successful, that is, borylation of the Cp ligand prior to metallocene formation.⁴⁴ Herberich *et al.* describe their early work on the isolation of borylated cyclopentadienides for preparing metallocenes by this method.⁴⁵ Bochmann *et al.* have also reported many boryl (BR_2)- and borato (BR_3)-substituted Cp ligands useful for making complex metallocene systems.⁴⁶

The anion binding capabilities of many *bis*-borylated compounds, utilizing them as molecular pincers, has been an area of interest for some time. Herberich *et al.* demonstrated the anion binding nature of the cationic molecule $[\text{Co}(\text{CpB}(i\text{Pr})_2)_2]^+$.⁴⁴ They showed that hydroxide and chloride anions can be bound by this *bis*-borylate in a symmetrical and unsymmetrical manner, respectively (Scheme 3).^{44,47}



Scheme 3: Preparation and anion binding of the 1,1'-*bis*-(diisopropylboryl)cobaltocenium cation.

Ferrocenyl boranes are susceptible to coordination of Lewis bases and anions at the boron centres. The Lewis acid strength allows for dative and covalent bonds to form readily. Many novel products are available and yet to be discovered. Preliminary forays into the chemistry of ferrocenylboranes have alluded to a rich and diverse chemistry. Further investigation of their reaction behaviour may reveal new and exciting differences between these compounds and traditional Lewis acids.

1.4 The Goals

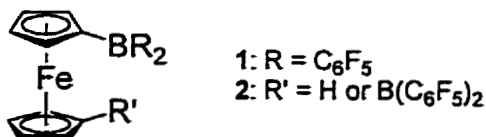
With catalyst activation at the forefront of our interest we became attracted to generating some novel highly Lewis acidic perfluoroarylborylferrocenes for use as potential activators by way of methide abstraction from model precatalysts. The oxidizable nature of the ferrocene core may allow for some zwitterionic ferrocenium borates to be formed. By activation of precatalysts through electron transfer oxidation of a Zr-Me bond, the borate of the zwitterion could act as a built-in counterion.

To the best of our knowledge there have been no reports in the literature of bis(perfluoroaryl)borylferrocenes. In Chapter 2 the preparation, characterisation and reactivity of two *bis*-(pentafluorophenyl)borylated ferrocenes and their derivatives will be presented.

2 Chapter 2: *Bis-(pentafluorophenyl)borylated Ferrocene*

2.1 Introduction

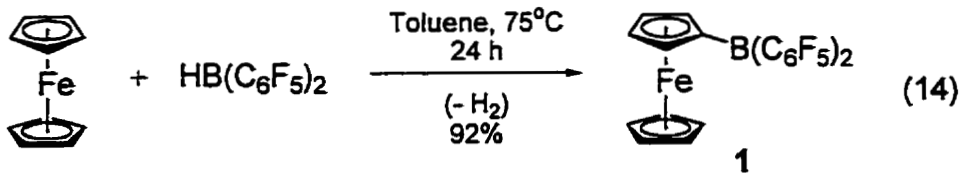
The aromatic cyclopentadienyl (Cp) rings of the sandwich molecule ferrocene^{1,2} engage in similar chemistry to that of the planar molecule benzene.^{5,21} Electrophilic additions, a well established reaction mode for arenes, are also possible for ferrocene which possesses a comparably electron rich aromatic system, in the form of its cyclopentadienyl ligands. The primary difference between benzene and ferrocene is the presence of the central iron atom and its sensitivity towards oxidation. Ferrocene is readily oxidised in the presence of a number of oxidants to the ferrocenium cation, which as a result is resistant to electrophilic addition reactions. Consequently, standard methods that have been developed for derivatising benzene are not successful for ferrocene. Electrophilic substitutions, therefore, can only be carried out under nonoxidising conditions (e.g. lithiation, borylation, mercuration and Friedel-Crafts acylation).²¹ The mechanisms of such transformations have been examined and metal mediation is believed to be important for most electrophilic addition reactions. The borylation of ferrocene is an example of an electrophilic addition reaction that we have investigated. Our interest in these systems stemmed from a desire to generate a new type of borane Lewis acid, perfluoroarylborated ferrocenes. Furthermore, it was envisaged that this new class of compound and its derivatives may find application in the activation of Ziegler-Natta olefin polymerization catalysts.



2.2 Bis-(pentafluorophenyl)borylferrocene (1)

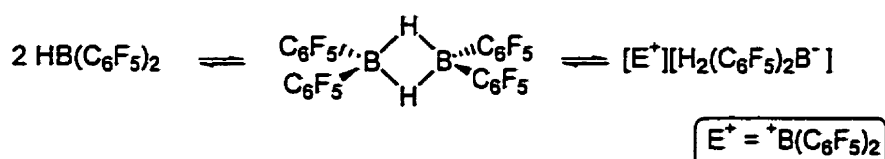
2.2.1 Synthesis and characterisation of with FcB(C₆F₅)₂ (1)

The generation of *bis*-(pentafluorophenyl)borylferrocene (1) occurs when ferrocene (FcH) reacts with *bis*-(pentafluorophenyl)borane (HB(C₆F₅)₂)⁴⁸ in a warm toluene solution. The orange FcH solution turns dark maroon over the course of 24h with the concomitant consumption of FcH. After the toluene is removed *bis*-(pentafluorophenyl)borylferrocene (1) is collected as a crystalline, maroon solid in high yield (92%) (Equation 14). This reaction proceeds cleanly as hydrogen gas is the only possible by-product. Any unreacted FcH is removed from the product mixture by sublimation to afford 1 in high purity as judged by ¹H and ¹⁹F NMR spectroscopy. Compound 1 is highly moisture-sensitive and must be handled under inert atmosphere conditions. The B-C_{Cp} bond is readily hydrolysed to generate FcH and the borinic acid (HOB(C₆F₅)₂).

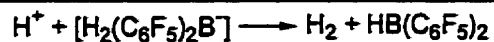
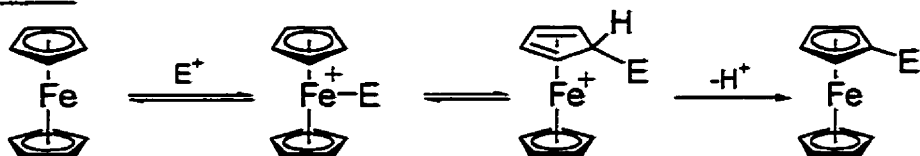


The proposed mechanisms for the generation of 1 by borylation of ferrocene are shown below in Scheme 4. We are uncertain as to the exact mechanism that is operating for equation 14, however, the two delineated below are not unreasonable and may be acting separately or in tandem. As seen, monomeric HB(C₆F₅)₂ exists in an equilibrium

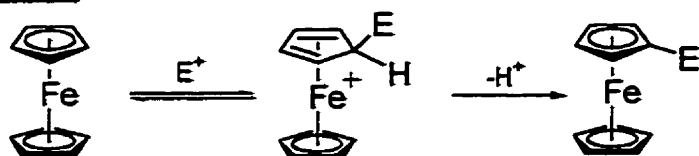
with its dimeric form in solution.⁴⁸ The $[\text{HB}(\text{C}_6\text{F}_5)_2]_2$ dimer may generate, if only a catalytic amount, the electrophilic ${}^+\text{B}(\text{C}_6\text{F}_5)_2$ (E^+) by hydride abstraction to afford the borate anion $\text{H}_2\text{B}(\text{C}_6\text{F}_5)_2^-$. The iron centre is most likely involved in coordinating the E^+ , followed by E^+ transfer to the endo-face of the Cp ring (Route A).³ Exocyclic ring addition of the E^+ could also occur as it is likely susceptible to attack by the π -electrons of the aromatic Cp ring (Route B). In contrast to Route A, Route B does not involve direct metal mediation of the incoming electrophile to facilitate the reaction. Endocyclic loss of a proton according to route B is possible but not through a metal mediated process.⁴⁹ The resulting H^+ probably combines with the borate $[\text{H}_2\text{B}(\text{C}_6\text{F}_5)_2]^-$ to form hydrogen gas as the only by-product.



Route A

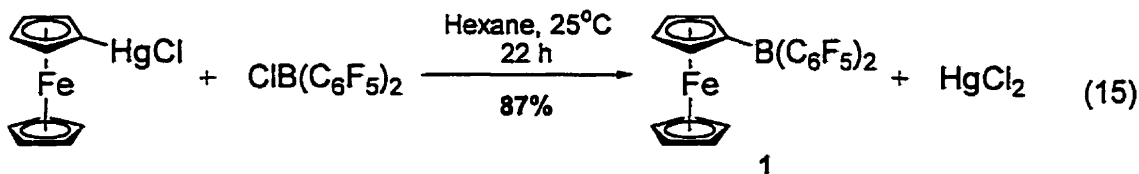


Route B



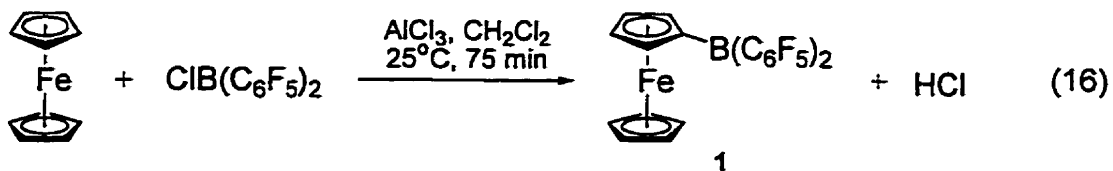
Scheme 4: Proposed mechanisms for the electrophilic hydacoborylation of FcH .

Borane **1** may also be prepared by an alternative metathetical salt reaction of bis-(pentafluorophenyl)chloroborane ($\text{ClB}(\text{C}_6\text{F}_5)_2$)⁵⁰ and (chloromercuric)ferrocene (FcHgCl).⁵¹ This method requires extended reaction times, typically overnight, though occurs at ambient temperature (Equation 15). Mercury(II) chloride precipitates out of the maroon hexane solution and is easily filtered away. Compound **1** is isolated cleanly after removing the residual amount of unreacted $\text{ClB}(\text{C}_6\text{F}_5)_2$ by sublimation, affording **1** in high yield. Although effective, the toxic nature of organomercury reagents and the prior synthesis of the requisite mercury substrate detract from the appeal of this approach.



As demonstrated borylation of ferrocene may be effected by addition of $\text{HB}(\text{C}_6\text{F}_5)_2$ to FcH (Equation 14), or by salt metathesis through FcHgCl and $\text{ClB}(\text{C}_6\text{F}_5)_2$ (Equation 15). Unfortunately, $\text{HB}(\text{C}_6\text{F}_5)_2$ is a rather expensive reagent to use and the toxicity of organomercurials is undesirable. In an attempt to circumvent these concerns, Friedel-Craft methodology was employed in an endeavour to borylate FcH directly with $\text{ClB}(\text{C}_6\text{F}_5)_2$. Friedel-Crafts acetylation of arenes has been well documented and occurs 3×10^6 times faster for FcH than it does for benzene.³ Application of this approach toward the synthesis of **1** was attempted (Equation 16) yet only 54% of **1** was detected in the product mixture by ^1H NMR spectral analysis. Despite a number of attempts to optimise the generation of **1** via this route, the low isolated yield detracted from this method and therefore further investigation was suspended. Given the facility of $\text{B}-\text{C}_\text{p}$ bond rupture in **1** as evidenced by the high hydrolytic sensitivity of the compound it is not unreasonable to propose that the HCl by-product generated in equation 16 may

homolyse the B-C_{Cp} bond to reverse the reaction back to the starting materials FcH and ClB(C₆F₅)₂.



The ¹⁹F, ¹H and ¹³C NMR spectra of 1 all indicated a C_s-symmetrical geometry characteristic of a *mono*-substituted ferrocene. The ¹H NMR spectrum (Figure 2.1) shows three signals, in a 5:2:2 ratio, assigned to the unsubstituted Cp ring protons (δ 4.03 ppm), the α - and β -protons of the borylated Cp ring, respectively. The anticipated coupling patterns for H _{α} and H _{β} were doublets resulting from 3-bond H _{α} -H _{β} coupling and a consequence of the symmetry of the molecule, however a pseudotriplet (or an apparent triplet) appears for each. The apparent triplets for H _{α} (2,5-position) and H _{β} (3,4-position) pairs reside at δ 3.95 and 4.51 ppm, respectively. These assignments are consistent with those reported by Slocum and Ernst from their trimethylsilylferrocene ¹H NMR spectroscopic study.⁵² The protons do not couple as simple doublets but exhibit pseudo-triplet behaviour best described by the AA'BB' four spin system. The pair of α -protons are chemically equivalent but magnetically inequivalent; the same is true of the β -proton pair.²³ Herbstein *et al.* conducted a low temperature study of a *mono*-substituted ferrocene system, α,α -diferrrocenylmethylium cation ([Fc₂CH]⁺[BF₄])⁻, and observed the separation of the pseudotriplets into broadened doublets at -70°C.⁵³ Siebert *et al.* also reported the ¹H NMR spectrum of dibromoborylferrocene (FcBBr₂) as exhibiting an AA'BB' spin system giving rise to pseudotriplets for the α - and β -protons. This observation is a common phenomenon for the cyclopentadienyl protons of *mono*-

substituted metallocenes.²³ The α -protons of 1 are coupled to the quadrupolar boron nucleus resulting in significant line broadening.

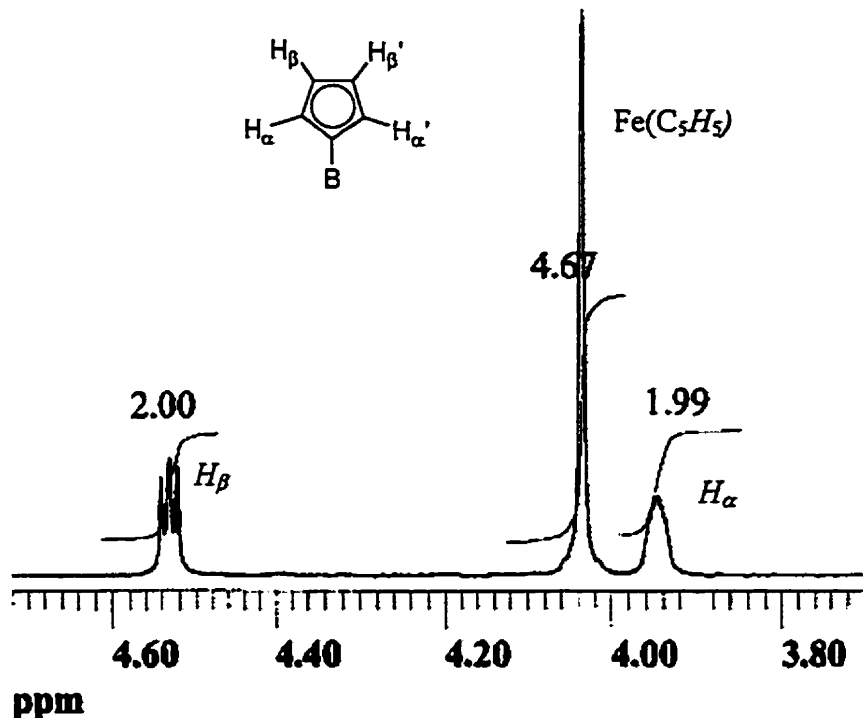


Figure 2.1: ^1H NMR spectrum of 1 in C_6D_6 .

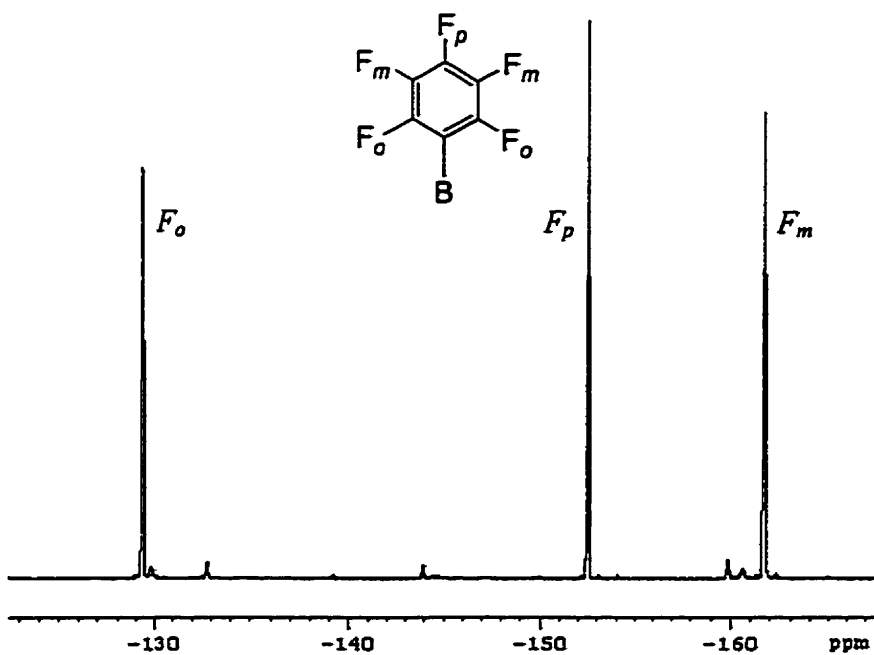


Figure 2.2: ¹⁹F NMR spectrum of **I** in C₆D₆.

The ¹⁹F NMR spectrum shows three distinct signals for the *ortho* (δ -129.3 ppm), *meta* (δ -152.5 ppm) and *para* (δ -161.7 ppm) fluorine atoms in a 2:1:2 ratio, respectively (Figure 2.2). The charge and coordination environment of boron attached to pentafluorophenyl (C₆F₅) rings is found to directly correlate to the chemical shift difference between the *para* and *meta*-fluorine ($\Delta(m,p\text{-F})$) in the ¹⁹F NMR spectrum.⁵⁴ Consequently, the important empirically derived relation was developed. A chemical shift difference $\Delta(m,p\text{-F})$ of > 12 ppm indicates a three-coordinate neutral boron centre. As the boron becomes tetrahedral and anionic $\Delta(m,p\text{-F})$ tends towards 3 ppm. Marks *et al.* reported a weakly coordinated methylborane to a zirconium cation [Cp₂ZrMe⁺][MeB(C₆F₅)₃⁻] to have $\Delta(m,p\text{-F})$ of 5.5 ppm in support of the anionic borane.^{54,55} Ferrocenyl borane **I** has a $\Delta(m,p\text{-F})$ of 9.2 ppm indicative of a neutral borane but not strictly three-coordinate. This value was the first indication that something was

unusual about borane 1. Perhaps a more sensitive probe of the electronic and coordination environment about the boron is ^{11}B NMR spectroscopy.

Table 2-1: ^{19}F NMR meta/para chemical shift differences and ^{11}B NMR resonances of selected pentafluorophenylboron compounds.

Compound	$\Delta(m,p\text{-F})$ (ppm)	^{11}B δ (ppm)	Reference
$\text{HB}(\text{C}_6\text{F}_5)_2$	18.3	60.1	a
$\text{B}(\text{C}_6\text{F}_5)_3$	16.3	80	b
$\text{PhB}(\text{C}_6\text{F}_5)_2$	12.6	72.6 ^g	c
$\text{FcB}(\text{C}_6\text{F}_5)_2$, 1	9.2	53.0	this work
FcBBr_2	-	46.7	d
$[\text{Cp}_2\text{ZrMe}]^+$ $[\text{MeB}(\text{C}_6\text{F}_5)_3]^-$	5.5	NA	e
$[\text{N}_3\text{Zr}]^+$ $[\text{MeB}(\text{C}_6\text{F}_5)_3]^-$	4.4	NA	f
$\text{Li}[\text{B}(\text{C}_6\text{F}_5)_4]$	3.7	-17.3	b

^a Parks, D. J.; Spence, R. E. v. H.; Piers, W. E. *Angew. Chem. Int. Ed. Engl.* 1995, 34, 809-811. ^b Massey, A. G.; Park, A. J. *J. Organomet. Chem.* 1966, 5, 218-225. ^c Deck, P. A.; Beswick, C. L.; Marks, T. J. *J. Am. Chem. Soc.* 1998, 120, 1771-1784. ^d Ruf, W.; Renk, T.; Siebert, W. Z. *Naturforsch.* 1976, 31b, 1028-1034. ^e Yang, X.; Stern, C. L.; Marks, T. J. *J. Am. Chem. Soc.* 1991, 113, 3623-3625. ^f Horton, A. D.; With, J. D.; van der Linden, A. J.; Weg, H. v. d. *Organometallics* 1996, 15, 2672-2674. ^g $\text{PhB}(\text{C}_6\text{F}_5)_2$ prepared according to reference (c); ^{11}B NMR (64 MHz, d_6 -toluene, δ): 72.6 (bs, WHM = 750 Hz).

Boron NMR spectroscopy can be used to probe the charge and coordination environment about a boron atom. There are two NMR active isotopes of boron; ^{10}B (18.83 %, I = 3) and ^{11}B (81.17 %, I = $3/2$). The most common boron NMR experiment exploits the ^{11}B nucleus due to the higher natural abundance, greater sensitivity to NMR experiments and lower spin quantum number (I = $3/2$). The chemical shift of boron in ^{11}B NMR spectroscopy has proven very useful in characterisation of boron environments, specifically charge and coordination about it. Chemical shifts of $\delta > 20$ ppm are characteristic of a neutral, three-coordinate geometry; $20 > \delta > 0$ ppm, neutral, four

coordinate; and $\delta < 0$ ppm, tetrahedral, anionic boron. For borane **1** the ^{11}B NMR spectrum shows a broadened singlet at 53.0 ppm and the width at half maximum is 700 Hz (Figure 2.3). Table 2-1 presents ^{11}B NMR data for **1** and related pentafluorophenyl-substituted boron molecules for comparative purposes. $\text{B}(\text{C}_6\text{F}_5)_3$ has a chemical shift of δ 80 ppm and is neutral three-coordinate, whereas the weakly coordinating $\text{B}(\text{C}_6\text{F}_5)_4^-$ anion resonance resides at δ -17.5 ppm. As was indicated by the ^{19}F NMR experiment, ^{11}B NMR also suggests an unusual environment for the boron of **1**. The boron is perturbed from the trigonal neutral environment somehow.

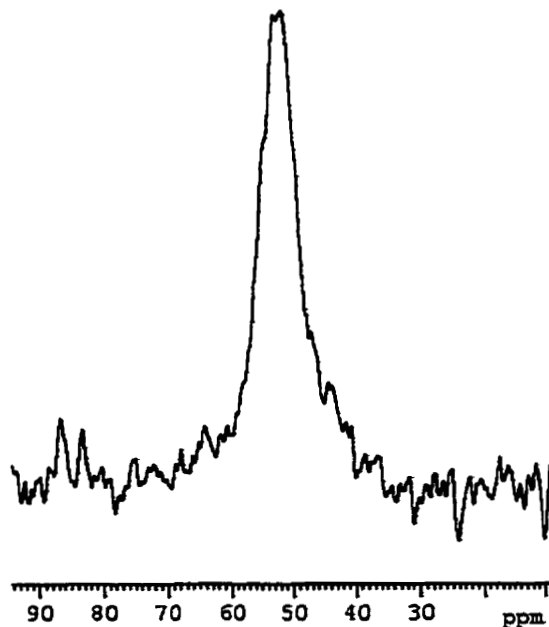


Figure 2.3: ^{11}B NMR spectrum of **1** in C_6D_6 .

Taken together, the NMR data suggested that the boron is attached to one of the Cp rings but the boron is not entirely three-coordinate neutral. Crimson red X-ray quality crystals of **1** were grown from a hexamethyldisiloxane solution at low temperature (-35°C) over two days. Hexamethyldisiloxane was used as **1** exhibits very

high solubility in nonpolar solvent like hexane or benzene. A structure was found in keeping with that reported by Wagner *et al.*⁵⁶ for dibromoborylferrocene.²³ Compound 1 crystallised in the $P_{2_1}2_12_1$ space group with two crystallographically independent molecules (1_A and 1_B) in the asymmetric unit. Figure 2.4 shows the ORTEP diagram of only one of those molecules, 1_A . Selected bond distances and angles are given in Table 2-2.

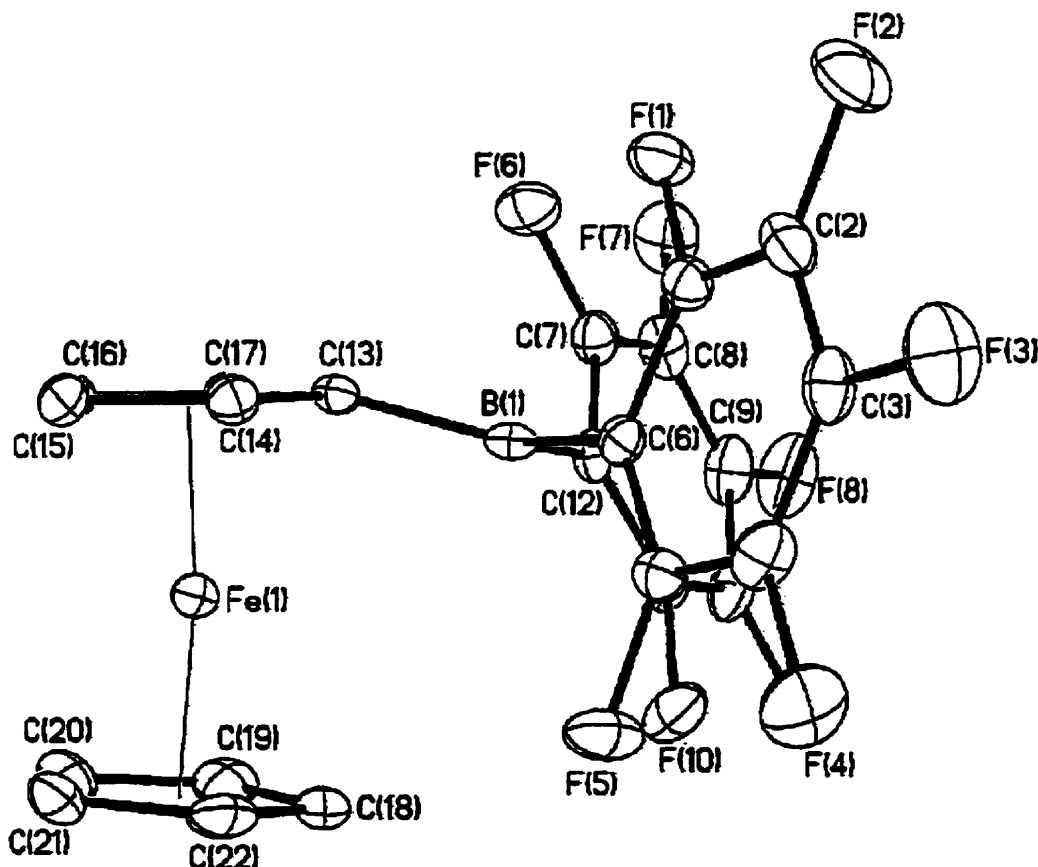


Figure 2.4: ORTEP diagram of 1_A (thermal ellipsoids at 50% probability level). Important structural features: $Fe(1) \cdots B(1)$, 2.924 Å; C_p, C_p' tilt angle $Cp_{cent}Fe1-Cp'_{cent}$, 173.6° ; ϕ (deviation from eclipsed, $C(13)-Cp_{cent}-Cp'_{cent}-C(18)$, deg), 0.7° .

Table 2-2: Selected Bond Distances (\AA) and Angles ($^\circ$) and Dihedral Angles ($^\circ$) for **1**.

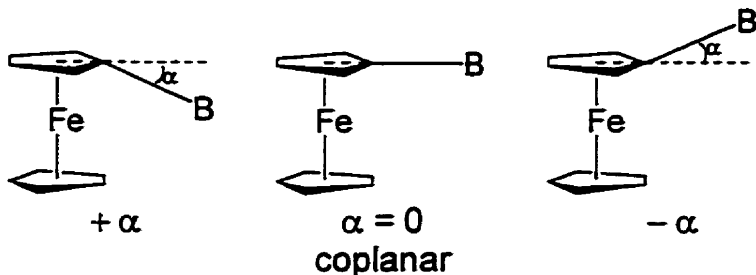
1_A^a			
B(1) – C(6)	1.604(4)	C(14) – C(15)	1.414(3)
B(1) – C(12)	1.584(4)	C(15) – C(16)	1.418(3)
B(1) – C(13)	1.501(4)	C(16) – C(17)	1.407(4)
C(13) – C(14)	1.444(3)	C(13) – C(17)	1.448(3)
C(6)-B(1)-C(12)	118.4(2)	B(1)-C(13)-C(14)	124.9(2)
C(6)-B(1)-C(13)	118.0(2)	B(1)-C(13)-C(17)	126.0(2)
C(12)-B(1)-C(13)	122.5(2)	C(14)-C(13)-C(17)	105.6(2)
C(6)-B(1)-C(13)-C(14)	-22.2	B(1)-C(13)-C(14)-C(15)	-160.8
C(12)-B(1)-C(13)-C(17)	14.5	B(1)-C(13)-C(17)-C(16)	160.5
$\alpha^b = 16$		$\phi^c = 0.7$	
1_B			
B(2) – C(28)	1.596(3)	C(36) – C(37)	1.414(3)
B(2) – C(34)	1.583(4)	C(37) – C(38)	1.420(3)
B(2) – C(35)	1.501(4)	C(38) – C(39)	1.405(3)
C(35) – C(36)	1.448(3)	C(35) – C(39)	1.454(3)
C(28)-B(2)-C(34)	118.7(2)	B(2)-C(35)-C(36)	125.6(2)
C(28)-B(2)-C(35)	120.3(2)	B(2)-C(35)-C(39)	125.6(2)
C(34)-B(2)-C(35)	120.1(2)	C(36)-C(35)-C(39)	105.5(2)
C(28)-B(1)-C(36)-C(37)	-22.2	B(1)-C(35)-C(36)-C(37)	-161.6
C(34)-B(1)-C(35)-C(39)	19.4	B(1)-C(35)-C(39)-C(38)	161.0
$\alpha^b = 15.5$		$\phi^c = 9.0$	

^aA and B refer to two crystallographically independent molecules. ^b $\alpha = \text{Cp}_{\text{centroid}}-\text{C}_i-\text{B}$.

^c ϕ = deviation from eclipsed conformation of Cp rings.

The B-C bond lengths to the perfluorophenyl rings⁵⁷ and to the cyclopentadienyl ring⁵⁸⁻⁶¹ are in accordance with the literature values of similar structures.⁵⁷⁻⁶² The boron atom sits below the C(13)-C(12)-C6 plane by 0.108 and 0.096 \AA in **1_A** and **1_B**, respectively. Compound **1** exhibits a distortion of the exocyclic boron atom bent towards the Fe centre of the ferrocene core (Figure 2.4). The deviation or bending of the boron (or exocyclic atom) from being coplanar with the Cp ring attached is called the dip angle

(α); it is the angle measured from the $Cp_{cent}-C_{ipso}$ -B. Positive α arbitrarily denotes bending towards the centre of the ferrocene core and negative α is away (Scheme 5).



Scheme 5: Dip angle (α) convention used.

The dip angle α for 1 is quite significant at $+16.0^\circ$; the boron is tilted towards the iron out of the plane of the Cp ring. The distance from iron to boron ($d(Fe(1)-B(1)) = 2.924 \text{ \AA}$) is longer than their sum of atomic radii (2.89 \AA); the sum of covalent radii is 1.99 \AA . Clearly there is not likely a bond between B and Fe, but some kind of interaction is perturbing the B towards Fe. Wagner *et al.* reports the dip angle α of $FcBBr_2$ to be $+18.9^\circ$ and the $d(Fe\cdots B)$ is 2.840 .⁵⁶ The structure of the isoelectronic fulvene-cyclopentadienylferrocene carbocation (FcC^+Ph_2) reported by Behrens⁶³ is similar to those of $FcBBr_2$ and 1; $\alpha(FcC^+Ph_2)$ is $+20.7^\circ$ and the $d(Fe-C)$ is $2.715(6)\text{\AA}$. The increased steric bulk of the pentafluorophenyl rings of 1 (cf. bromides⁵⁶ of $FcBBr_2$) does decrease the $Fe\cdots B$ interaction; *i.e.*, the distance between iron and boron increases ($d(Fe(1)-B(1)) = 2.924 \text{ \AA}$) by 0.8 \AA . The major difference between the two crystallographically independent molecules is the amount of ϕ deviation of the Cp rings from being eclipsed (Figure 2.5); $\phi(I_A) = 0.7^\circ$ and $\phi(I_B) = 9.0^\circ$.

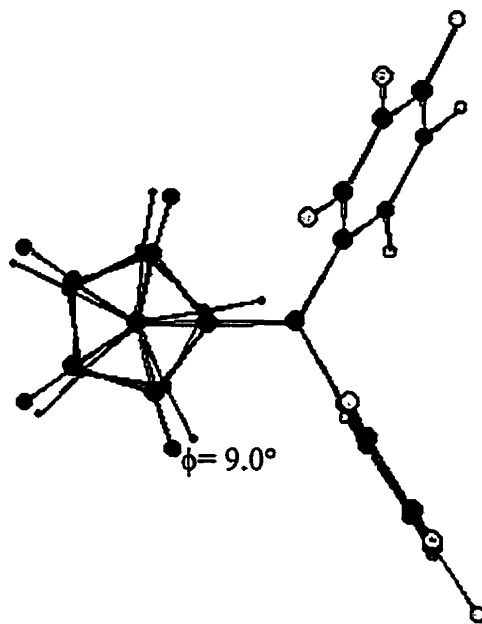


Figure 2.5: A view down through the Cp_{cent} of both Cp rings for structure 1_{B} . Note the deviation from the eclipsed conformation of the Cp rings, $\phi = 9.0^\circ$.

The functionalised Cp ring has a certain amount of fulvene character which is noted by the differing bond lengths around the ring (Figure 2.6). The three bonds on the far side of the ring between C(14) and C(17) are shortened relative to the ones adjacent to C(13). The shortened bonds range from 1.407 to 1.418 Å, whereas the bonds adjacent to C(13) are longer (1.444 and 1.448 Å) indicating less π -bond character than the rest (Figure 2.6). The B(1)-C(13) bond length is 1.501(4) Å which is intermediate between a typical $\text{B}(\text{sp}^2)\text{-C}(\text{sp}^2)$ double bond distance in a borataethene ion (*cf.* $\text{Li}[\text{CH}_2=\text{B}(\text{Mes})_2]$, 1.44 Å⁶⁴) and that of a typical $(\text{B}(\text{sp}^2)\text{-C}(\text{sp}^2))$ single B-C bond at 1.58 Å (*cf.* BPh_3 ,⁶⁵ and BMes_3 ,⁶⁶ Mes = 2,4,6-trimethylphenyl). Hence, there appears to exist some π -character

in the B(1)-C(13) bond (*i.e.*, 1.501(4) Å is more like a B=C bond). Therefore, it is apparent that the boratafulvene canonical form is an important contributor in the bonding description of **1**. The inductive electron-withdrawing ability of the $\text{B}(\text{C}_6\text{F}_5)_2$ moiety is also indicated by the short B(1)-C(13) bond distance. Moreover, the positive dip angle α lends support to the idea that iron is donating electron density to the boron, through a non-contact interaction.

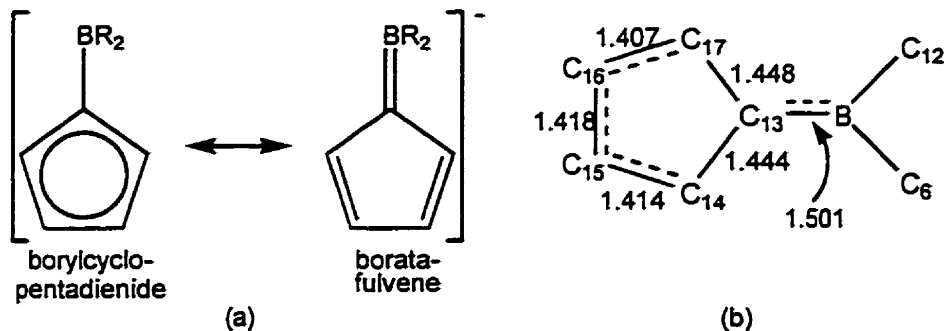


Figure 2.6: a) Two resonance forms of boron substituted Cp rings; b) interatomic distances of the functionalised Cp ring in **1**

The intense colour of **1** may be the result of a charge transfer (CT) phenomenon. CT transitions are common for highly coloured organometallic systems as electrons are excited through a symmetry-allowed transition from one molecular orbital to another. The occurrence can be either from a metal based orbital to ligand based orbital or *vice versa*. CT processes occur with high intensity as the transitions are symmetry-allowed. Typically, molar absorptivities (ϵ) greater than 5000 L/mol·cm are observed. In contrast, symmetry-prohibited transitions, for example, occur between d-orbitals of a metal, with ϵ intensities *ca.* 500 L/mol·cm.⁶⁷ The permanganate anion (MnO_4^-) is an intensely purple colour for which a CT transition (oxygen p-orbital to metal d-orbital) is observable in the visible spectrum ($\lambda_{\max} = 530 \text{ nm}$).⁶⁷ To probe the metal to ligand interaction in **1**,

ultraviolet/visible (UV/Vis) spectroscopy was employed. A solution of **1** was prepared in 1,2-dichloroethane (DCE) at low concentrations and the spectrum was collected (Figure 2.7), indicating a CT band at $\lambda_{\text{max}} = 230 \text{ nm}$, $\epsilon = 1.33 \times 10^4 \text{ L/mol}\cdot\text{cm}$. Wagner *et al.*⁵⁶ calculated the HOMO orbital of the model system, borylferrocene (FcBH_2), to be an interaction of the empty p_z -orbital of boron and the d_{z^2} or $d_{x^2-y^2}$ orbital of the ferrocene core. Wagner's molecular orbital description supports the supposition of an $\text{Fe}\cdots\text{B}$ interaction asserted earlier in this work based on spectral data analysis. Electron promotion from the iron d_{z^2} or $d_{x^2-y^2}$ -orbital to the boron p_z -orbital is most likely the origin of the CT band in **1**.

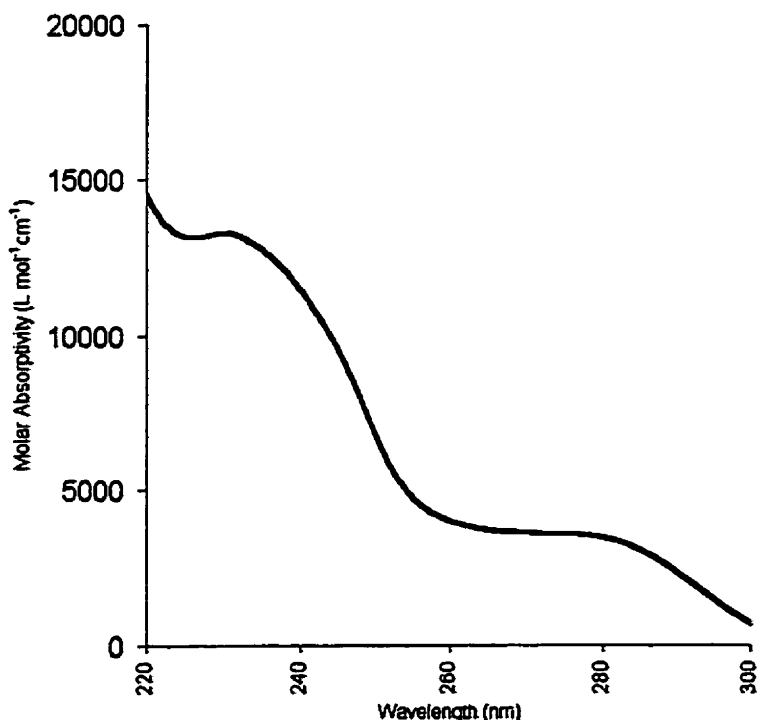
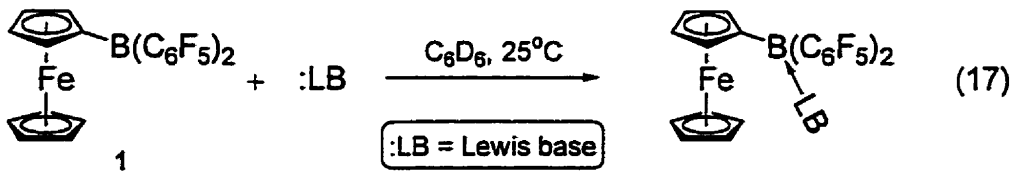


Figure 2.7: UV/Visible spectrum of **1** in 1,2-dichloroethane. λ_{max} , nm (ϵ): 230 (1.33×10^4). Note charge transfer band at 230 nm corresponding to a symmetry-allowed metal to ligand (d to p) transition.

2.2.2 Reaction Behaviour of $\text{FcB}(\text{C}_6\text{F}_5)_2$ (1)

2.2.2.1 Lewis Base reactions with $\text{FcB}(\text{C}_6\text{F}_5)_2$ (1)

To probe the reactivity of the Lewis acid centre of 1 a series of reactions with Lewis bases was undertaken on an NMR tube scale (Equation 17). All of the Lewis bases tested form strong adducts with *tris*-(pentafluorophenyl)borane⁶⁸⁻⁷⁰ and hence were deemed appropriate to be used here to gauge the relative acidity of 1 in comparison to $\text{B}(\text{C}_6\text{F}_5)_3$.



Qualitatively acetophenone,^{68,69} benzophenone, tetrahydrofuran, *N,N*-diisopropylbenzamide,⁶⁸ and acetylferrocene do not react with 1 at room temperature as observed by ¹H NMR spectroscopy and reaction colour. Acetonitrile⁷⁰ does not coordinate to 1 at room temperature, however, upon cooling a *d*₈-toluene solution of 1 containing acetonitrile to -78°C the initial maroon colour turns light yellow. The maroon colour is restored as the sample warms to room temperature. A series of variable temperature NMR experiments was undertaken to assess the lower temperature limit of CH_3CN adduct formation. Unfortunately, the lower temperature limit was determined to be below that of the freezing point of *d*₈-toluene (Table 2-3). Only a single acetonitrile resonance at each temperature is observed in the ¹H NMR spectra collected, suggesting that the coordination of CH_3CN to 1 is labile even at low temperature.

Table 2-3: Variable temperature ^1H NMR spectral data for the reaction of **1** and CH_3CN (1.0:1.1) in d_8 -toluene.

Temperature (K)	$\delta(\text{CH}_3\text{CN})$ (ppm)	$\delta(\text{H}_\beta)$ (ppm)	$\delta(\text{H}_{\text{Cp}})$ (ppm)
300	0.675	4.541	4.033
280	0.625	4.511	4.024
260	0.567	4.457	4.000
240	0.498	4.371	3.967
220	0.435	4.261	3.939
200	0.375	4.12	3.926

In contrast to acetonitrile, the stronger Lewis base trimethylphosphine (PMe_3) reacts immediately with **1** at room temperature in hexanes to form a yellow solution. This PMe_3 adduct (**3**) of **1** was isolated and characterised. The methyl group doublet of the coordinated phosphine shifted upfield in the ^1H NMR spectrum to δ 0.47 ppm compared to that of free PMe_3 (δ 0.80 ppm). The ^1H NMR spectrum is clean and contains only four resonances (9:2:2:5 ratio) assigned to the methyl groups of PMe_3 , the α - and β -protons on the substituted Cp ring and the unsubstituted Cp ring, respectively. The ^{11}B NMR spectrum reveals a doublet residing at δ -13.5 ppm ($^1J_{\text{BP}} = 46$ Hz), indicative of a B-P bond.⁷¹ ^{19}F NMR spectroscopy shows a single set of resonances for the C_6F_5 rings as they are equivalent. The $\Delta(m,p\text{-F})$ of 5.8 ppm further corroborates the assignment of a four-coordinate boron centre. The phosphorus resonance shifted downfield (δ -12.1 ppm) from that of free PMe_3 (δ -61.9 ppm) in the ^{31}P NMR spectrum. The Lewis acid boron centre, to which the phosphine is coordinated, decreases the

electron density at the phosphorus atom.

An X-ray quality crystal of **3** was isolated from the C₆D₆ NMR sample solution, after standing overnight at room temperature, and submitted for structure determination analysis (Figure 2.8). The solid-state structure confirms the ¹H, ¹¹B and ¹⁹F NMR spectral data. Adduct **3** crystallised from *d*₆-benzene (C₆D₆) as yellow prisms in the space group P2₁/n. Selected bond lengths are collected in Table 2-4. The B-C bond lengths are consistent with literature values.⁵⁷⁻⁶² The B-P bond is within normal the normal for B-P dative bonds when compared to literature values.⁷²⁻⁸² The dihedral angle about C(2)-C(1)-B(1)-P(1) of 10.9° places the phosphorus atom almost in the plane of the Cp ring and perpendicular to the linear Cp-Fe-Cp fragment. The dip angle α was calculated to be -6.3° as the lone pair of the phosphine coordinates through the empty p-orbital of the boron, into which the iron can no longer donate. The negative dip angle α places the boron on the opposite side of the Cp ring from that of the iron, likely a result of steric interactions. The fulvene character observed in **1** has been lost in **3** and all the C-C distance in the Cp ring attached to B are equivalent. The B-C bond has lengthened (d(B(1)-C(1)) = 1.61(1) Å) and indicates single bond character (cf. d(B(1)-C(13)) = 1.501(4) for **1**).⁴⁵

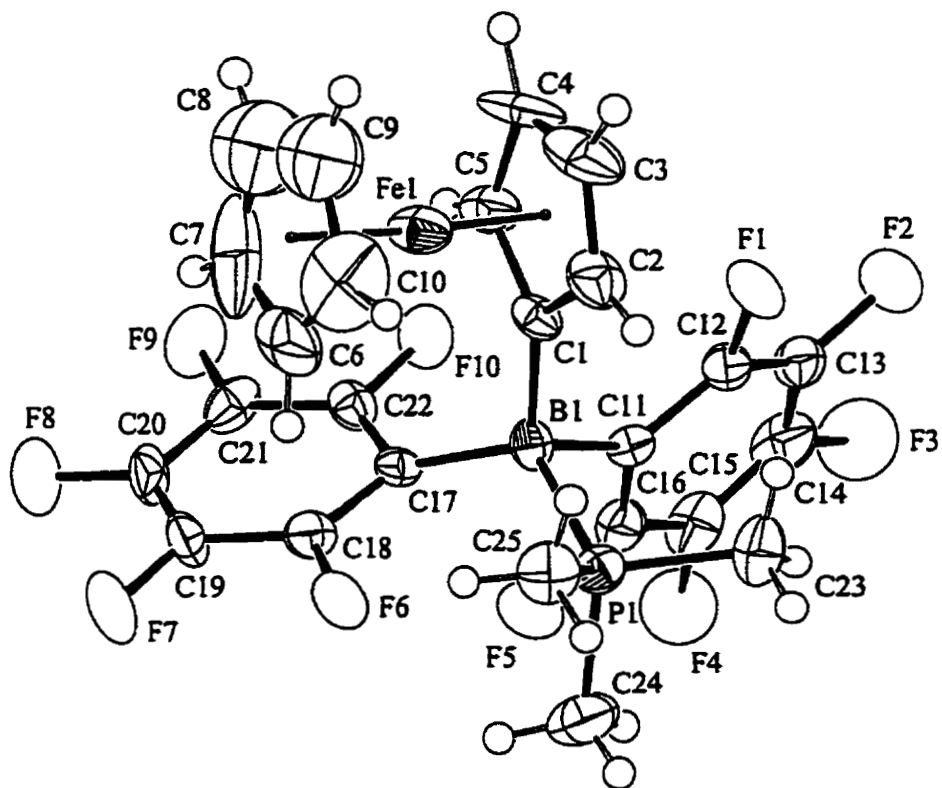


Figure 2.8: ORTEP diagram of 3.

Table 2-4: Selected interatomic distances (\AA) and angles ($^\circ$) for adduct 3.

3			
C(1)-B(1)	1.61(1)	P(1)-B(1)-C(1)	109.3(5)
C(11)-B(1)	1.66(1)	P(1)-B(1)-C(11)	102.1(5)
C(17)-B(1)	1.64(1)	P(1)-B(1)-C(17)	116.0(5)
P(1)-B(1)	1.992(9)	C(1)-B(1)-C(11)	110.6(6)
		C(1)-B(1)-C(17)	109.0(6)
C(1)-C(2)	1.447(9)	C(11)-B(1)-C(17)	109.8(5)
C(1)-C(5)	1.420 (10)		
C(2)-C(3)	1.400(10)		
C(3)-C(4)	1.400(10)		
C(4)-C(5)	1.430(10)		

Phosphine adduct **3** is a light yellow in colour, suggesting nullification of the CT process involving the boron centre in **3**. The UV/visible spectrum of **3** supports the assignment of the CT band in **1** as no CT band is observed for **3** (Figure 2.9). There is no longer an opportunity for an electronic interaction between the iron and boron because phosphine coordinates to the boron in a similar manner that the iron interacts with it in **1**. Electron density is donated into the empty p_z-orbital of the boron by the phosphine in **3** while the iron donates electron density into it in **1**. The CT band assigned to the presence of the Fe...B interaction in **1** is believed to be correct as **3** does not exhibit the same behaviour.

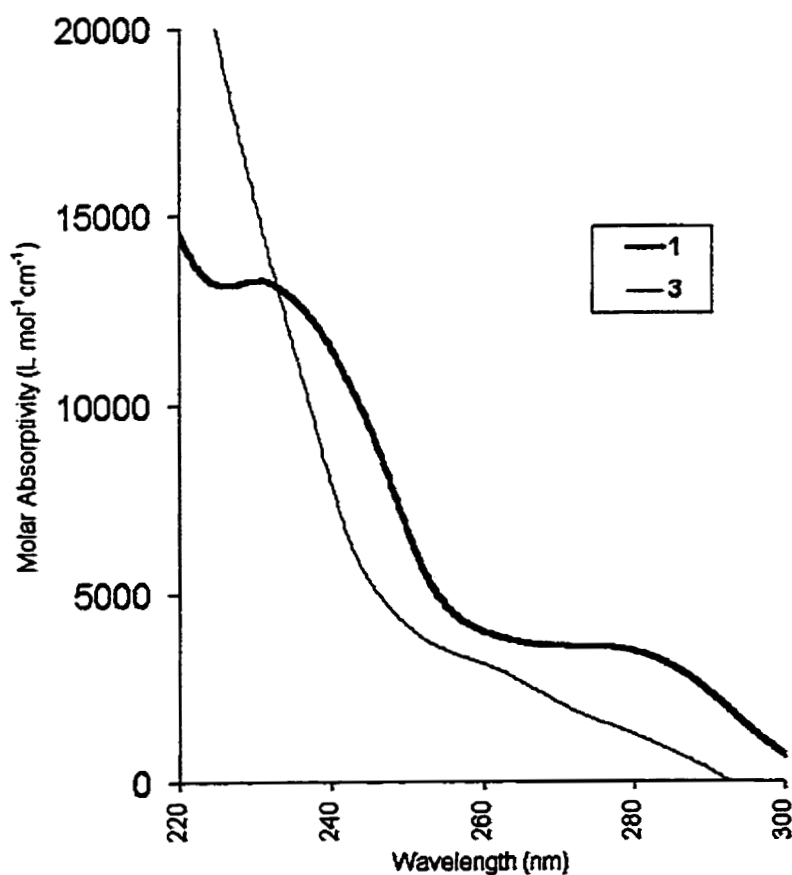
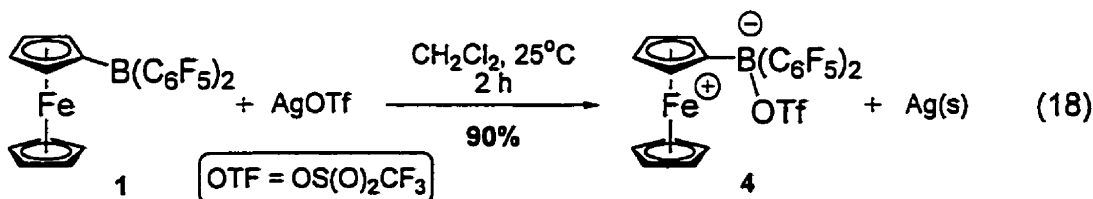


Figure 2.9: UV/Visible spectrum of **1** and **3** in 1,2-dichloroethane. Note charge transfer band at 230 nm present for **1** and lack of CT band for **3**.

2.1.1.1 Oxidation Chemistry of $\text{FcB}(\text{C}_6\text{F}_5)_2$ (1)

With the observance of the CT band for 1 attributed to the $\text{Fe}\cdots\text{B}$ interaction, we became interested in chemistry that could effect disruption of that $\text{Fe}\cdots\text{B}$ interaction. Removal of an electron from the iron was expected to disrupt the electronic communication between iron and boron. Oxidation of the iron(II) centre of 1 should accomplish this task. A one-electron oxidant, such as silver(I) (Ag^+), may be capable of oxidising the iron from Fe(II) to Fe(III) state. Silver trifluoromethanesulfonate (or silver triflate, AgOTf) was mixed with 1 in dry methylene chloride (CH_2Cl_2) (Equation 18). The reaction colour changed from dark maroon to navy blue immediately upon addition of CH_2Cl_2 at low temperature and remained navy blue as the solution was warmed to room temperature.



The navy blue solution was separated from the silver metal powder by filtration. After the solvent was removed the resulting blue powder 4 was collected and fully characterised. ^1H NMR spectroscopy indicated that the reaction proceeds cleanly with no ferrocenylborane 1 observed; there are no signals, other than the NMR solvent, observed in the normal chemical shift window ($-1 < \delta < 10$ ppm) for 4. The absence of signals in this normal ^1H NMR spectral window is attributed to paramagnetic broadening and shifting of the resonances to a region outside that window due to the paramagnetic ferrocenium core. The ^1H NMR spectrum was collected with a widened sweep width and

three broadened signals were observed at δ 42.0, 33.1 and 30.1 ppm. ^{11}B NMR spectroscopy revealed the boron atom resonance in the region typical of a four-coordinate anionic environment (δ -4.75 ppm). This observation is accounted for by triflate coordination to the boron centre to generate an anionic borate. The sharp boron resonance suggests that the boron atom is not strongly interacting with the paramagnetic iron centre to be broadened as was found for the protons of the Cp rings. ^{19}F NMR analysis indicates a single product with four distinct signals; a new signal appearing at δ -89.6 ppm of the coordinated OTf group, a broadened *ortho*-F signal due to the Fe(III) centre and $\Delta(m,p\text{-F}) = 6.2$ ppm indicating a borate, were of note. With this pure material in hand a solid-state structure was sought to confirm this solution data. The X-ray structure confirms the NMR spectroscopic assignments made for zwitterion 4 (Figure 2.10).

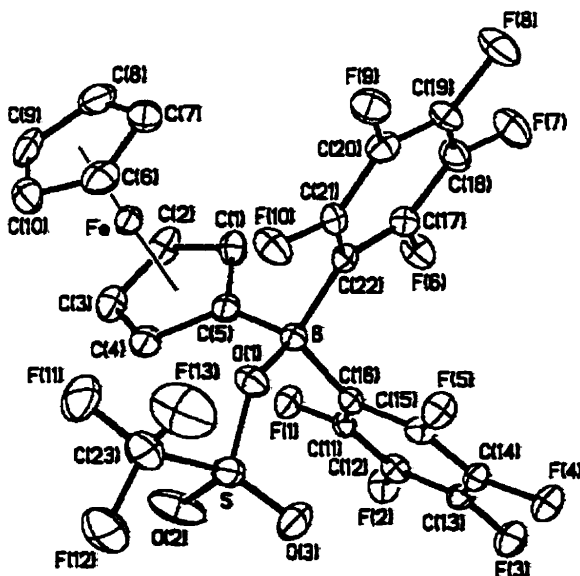


Figure 2.10: ORTEP diagram of 4.

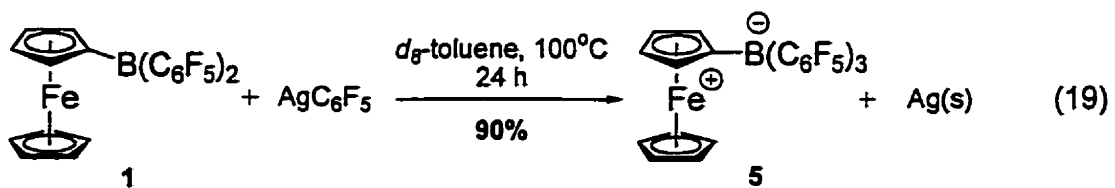
The interesting feature of structure 4 is the bending of the boron away the iron, a negative dip angle ($\alpha = -6.0^\circ$). The triflate is linked directly to the boron where B-O(1) is 1.575(4) Å. Boron resides in a tetrahedral environment where the angles about the central boron atom are close to those of an idealised tetrahedral geometry of 109.5° (Table 2-5). The triflate has a dihedral angle O(1)-B(1)-C(5)-C(4) of 29.3° to the plane of the Cp ring plane. The deviation of Cp and Cp' rings from being in the eclipsed conformer is 22.9° as measured by C(5)-Cp_{centroid}-Cp'_{centroid}-C(6); this is about midway between the eclipsed and staggered conformation. Ferrocenium species generally adopt an eclipsed conformation as observed for pure ferrocenium ions.⁸³⁻⁸⁵ The Fe-C and C-C distances range from 2.062(3) to 2.137(3) Å and from 1.378(5) to 1.440(4) Å, respectively; averages of 2.085 and 1.408 Å, each. These distances are in accord with other reported ferrocenium ion fragments.⁸⁴⁻⁸⁹

Table 2-5: Selected Bond Distances (Å) and Angles (°) and Dihedral Angles (°) for 4.

4			
B(1) – C(5)	1.601(5)	C(1) – C(2)	1.423(3)
B(1) – C(16)	1.624(5)	C(1) – C(5)	1.421(4)
B(1) – C(22)	1.658(4)	C(2) – C(3)	1.417(5)
B(1) – O(1)	1.575(4)	C(3) – C(4)	1.399(5)
Fe(1)-Cp _{centroid}	1.703	C(4) – C(5)	1.440(4)
Fe(1)-Cp' _{centroid}	1.710	Cp _{centroid} -Cp' _{centroid}	3.413
O(1)-B(1)-C(5)	107.7(3)	C(16)-B(1)-C(22)	110.5(3)
O(1)-B(1)-C(16)	109.0(3)	B(1)-C(5)-C(1)	126.7(3)
O(1)-B(1)-C(22)	104.8(2)	B(1)-C(5)-C(4)	127.9(3)
C(5)-B(1)-C(16)	112.7(3)	C(1)-C(5)-C(4)	105.3(2)
C(5)-B(1)-C(22)	111.7(3)		
O(1)-B(1)-C(5)-C(4)	-29.3	B(1)-C(5)-C(1)-C(2)	174.4
C(22)-B(1)-C(5)-C(1)	41.2	B(1)-C(5)-C(4)-C(3)	-174.4
C(16)-B(1)-C(5)-C(1)	91.1	C(16)-B(1)-C(5)-C(4)	-83.9
$\alpha^a = -6.0^\circ$		$\phi^b = 22.9^\circ$	

^a $\alpha = \text{Cp}_{\text{centroid}}-\text{C}_i-\text{B}$. ^b $\phi = \text{deviation from eclipsed conformation of Cp rings}$.

Once it was established that Ag^+ ion could oxidise borane **1**, another silver reagent was prepared to test the generality of the reaction. Pentafluorophenyl silver(I)⁹⁰ reacts with **1** under similar conditions (Equation 19) to those used to generate **4**. It was expected that another zwitterionic molecule would be generated with the coordination of an third C_6F_5 ring to the boron. ^{11}B and ^{19}F NMR spectroscopy suggest only a single anionic boron environment (^{11}B , δ -4.75 ppm; $\Delta(m,p\text{-F})$ = 6.2 ppm) and equivalent C_6F_5 groups, respectively.



Oxidation of Fe(II) to Fe(III) was evidenced by the green solution formed and the absence of the proton signals within the normal ^1H NMR spectral window. When the sweep width of the spectrometer is opened, the proton signals are observed at lower field (Figure 2.11). In the absence of structural confirmation in the solid-state a zwitterionic structure was also proposed in keeping with that found for **4**. Recall from Chapter 1 that zwitterion **5** was one of our initial targets for electron-transfer activation of Cp_2ZrMe_2 . Activation studies of Cp_2ZrMe_2 with this and other borylated ferrocenes will be discussed below.

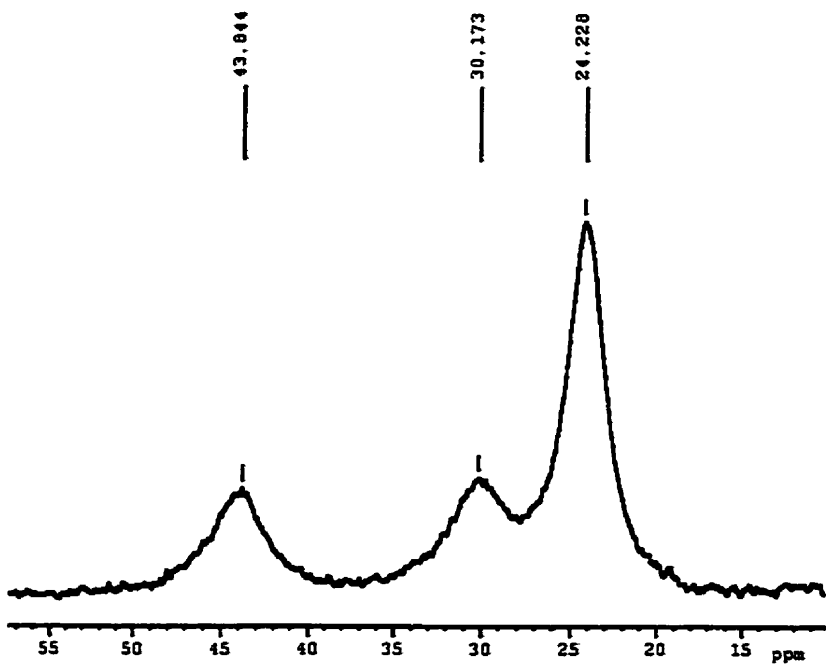
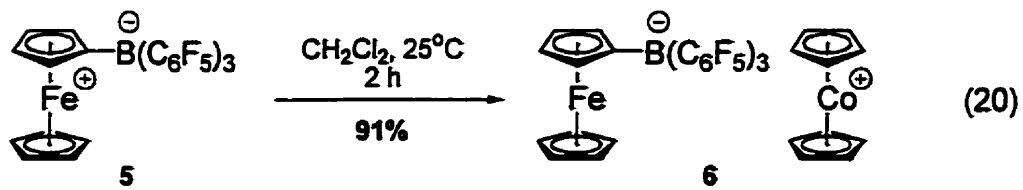


Figure 2.11: ^1H NMR spectrum of **5** in CD_2Cl_2 . Note the paramagnetically shifted and broadened signals (*cf.* ^1H NMR of **1**).

To test the hypothesis that **5** was an iron(III)-based zwitterion we proposed that the reduction of the ferrocenium moiety (Fc^+) to a ferrocenyl group (Fc) with a one-electron reductant should be possible. Cobaltocene (Cp_2Co), a 19-electron metallocene is easily oxidised to the 18-electron species, cobaltocenium (diamagnetic) upon reaction with a one-electron acceptor.⁹¹ Indeed, reaction of Cp_2Co and **5** generated the cobaltocenium ferrocenylborate $[\text{Cp}_2\text{Co}^+][\text{FcB}^-(\text{C}_6\text{F}_5)_3]$ (**6**) (Equation 20).



This class of reaction employing cobaltocene is a general method to establish the presence of a reducible centre in a molecule.^{91,92} Simple observation of Cp₂Co⁺ (diamagnetic) in the normal ¹H NMR spectral window offers support for a paramagnetic ferrocenium as the starting material 5. For the product 6, signals for the ferrocenyl fragment appeared at δ 4.00, 3.94 and 3.67 ppm while Cp₂Co⁺ protons appeared at δ 5.60 ppm in the ¹H NMR spectrum. Characterisation of 6 was further elucidated by ¹¹B (δ -13.2 ppm), ¹³C, ¹⁹F NMR ($\Delta(m,p\text{-F})$ 3.5 ppm) spectroscopy and by combustion analysis. These results advanced excellent evidence of the solution structure of zwitterion borate 5 proposed prior to its solid-state determination. The structure of 5 (Figure 2.12) was confirmed by solid-state structure analysis.

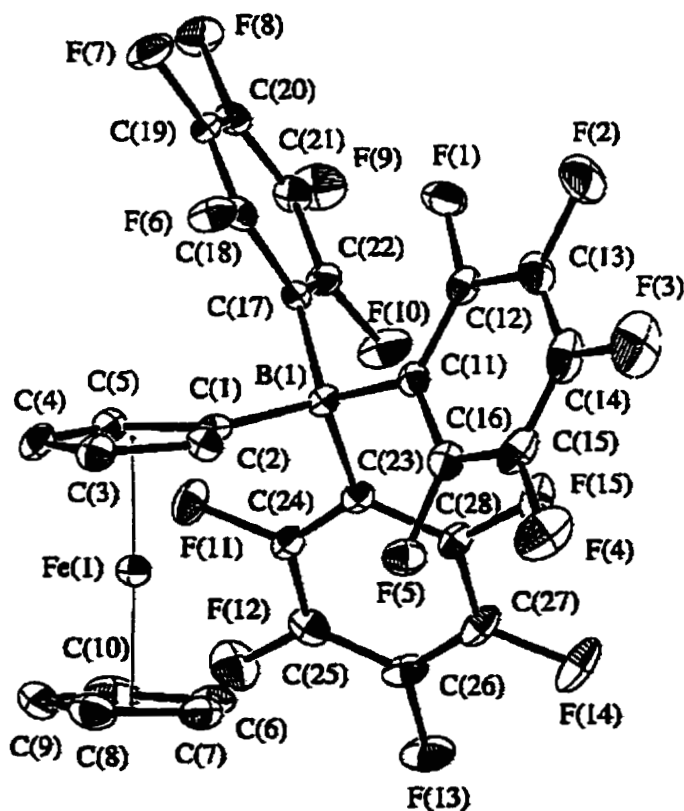


Figure 2.12: ORTEP diagram of 5

Zwitterion **5** crystallises as green irregularly shaped crystals in the monoclinic space group P2₁/n. Selected bond distances and angles are given in Table 2-6. The bonds to carbon about boron are consistent with structure **1**, **3** and **4**, as well as literature.⁵⁷⁻⁶² In this structure, as in **4**, the boron is bent away from the iron with a dip angle α of -5.4° and Fe and B are 3.509 Å apart (*cf.* **1**: α = +16.0°; d(Fe-B) = 2.924 Å). Additional features of note are the tetrahedral environment about the boron atom. Also, the Cp rings are only 2.4° from being eclipsed as was determined in **4**. Ferrocenium ions tend to adopt an eclipsed conformer of their Cp rings.⁸³⁻⁸⁵ The C-C and Fe-C bond distances are also consistent with other reported ferrocenium ion fragments.⁸⁴⁻⁸⁹

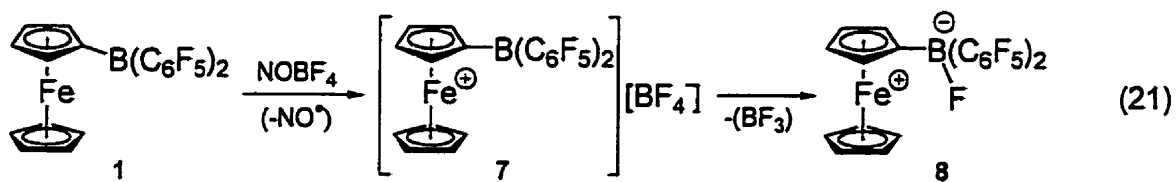
Table 2-6: Selected Bond Distances (Å) and Angles (°) and Dihedral Angles (deg) for **5**.

5			
B(1) – C(1)	1.666(3)	C(1) – C(2)	1.433(3)
B(1) – C(11)	1.648(3)	C(1) – C(5)	1.434(3)
B(1) – C(17)	1.657(3)	C(2) – C(3)	1.428(3)
B(1) – C(23)	1.666(3)	C(3) – C(4)	1.409(3)
Fe(I)-COG	1.712	C(4) – C(5)	1.414(3)
Fe(I)-COG'	1.716	COG-COG'	3.428
C(1)-B(1)-C(11)	106.0(2)	C(17)-B(1)-C(23)	108.9(2)
C(1)-B(1)-C(17)	105.7(2)	B(1)-C(1)-C(2)	127.1(2)
C(1)-B(1)-C(23)	112.0(2)	B(1)-C(1)-C(5)	128.0(2)
C(11)-B(1)-C(17)	113.2(2)	C(2)-C(1)-C(5)	104.4(2)
C(11)-B(1)-C(23)	110.9(2)	Fe(I)-B(1)	3.509
C(11)-B(1)-C(1)-C(2)	-7.8(3)	B(1)-C(1)-C(2)-C(3)	172.9
C(17)-B(1)-C(1)-C(5)	42.4(3)	B(1)-C(1)-C(5)-C(5)	-173.1
$\alpha^a = -5.8^\circ$		$\phi^b = 2.4^\circ$	

^a α = COG-C_i-B. ^b ϕ = deviation from eclipsed conformation of Cp rings.

The formation of zwitterions **4** and **5** show that ferrocene is oxidizable with silver(I) and that the products formed are intramolecular ion pairs. The nature of the anion (A⁻) for these species was of the variety that they coordinate to the boron in the product in anionic borates (Fc⁺B⁻(C₆F₅)₂A). In an effort aimed at avoiding counteranion

coordination reaction with oxidant salts containing weakly coordinating anions were undertaken to probe the Fe···B interaction. In this way, removal of an electron from iron to disrupt the Fe···B interaction of 1 could be accomplished. Nitrosonium tetrafluoroborate (NOBF_4) was chosen as a first candidate as a one-electron oxidant with a weakly coordinating anion (BF_4^-). Reaction of NOBF_4 with borane 1 (Equation 21) generates a gas that bubbles from the dark green solution. The colour change from maroon to green is indirect support for the presence of a ferrocenium ion, based on the colour changes observed for the formation of zwitterions 4 and 5.



The expected result was the ferrocenium-borane tetrafluoroborate (7- BF_4^-). However, the ^{11}B spectrum did not indicate the presence of BF_4^- ($^{11}\text{B}(\text{BF}_4^-)$ δ -1.9 ppm⁷¹). Fortunately, a single crystal was isolated and the X-ray structure was determined and revealed zwitterion 8 (Figure 2.13). The anion BF_4^- was initially chosen to compliment the resulting cation as it is generally a robust anion. However this anion does not always participate as a simple spectator ion in the presence of strong Lewis acids. Fluoride abstraction by perfluorophenyl boranes can occur to release trifluoroborane (BF_3). Examples of this are available in the literature. Norton observed the interactions of the Lewis acid $\text{B}(\text{C}_6\text{F}_5)_3$ with the BF_4^- by ^{19}F NMR.⁹² Williams *et al.* have observed fluoride abstraction from BF_4^- by the highly Lewis acidic 1,2-[$\text{B}(\text{C}_6\text{F}_5)_2$]₂ C_6F_4 .⁹³ The process to afford 8 can be envisioned as oxidation of the ferrocene core, thereby disrupting the Fe···B interaction, followed by fluoride transfer

from BF_4^- to the ferrocenium-borane 7. Therefore, in the present example the Lewis acid strength of the resulting ferrocenium-borane 7 is greater than that of BF_3 , effectively competing for the fluoride ion. There is no reaction when borane 1, possessing a relevant $\text{Fe}\cdots\text{B}$ interaction, is mixed with an excess of tetrabutylammonium tetrafluoroborate $[\text{NBu}_4]\text{[BF}_4]$, a non-oxidizing source of BF_4^- . To overcome the problem of counterion interference in this reaction a more robust, weakly coordinating bulky anion was sought. The *tetrakis-(pentafluorophenyl)borate* anion $\text{B}(\text{C}_6\text{F}_5)_4^-$ was investigated as a suitable counterion support for cation 7. Before this anion could be tried, it was necessary to prepare a reagent that was a single-electron oxidant that contained the bulky $\text{B}(\text{C}_6\text{F}_5)_4^-$ counterion.

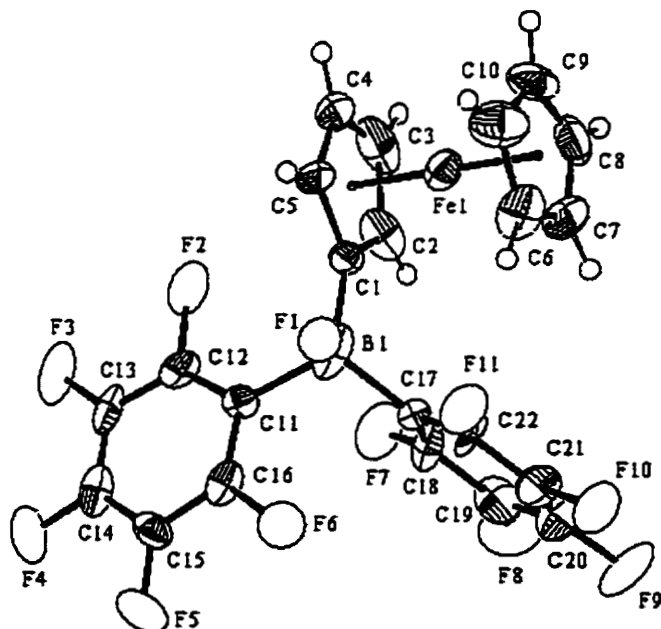


Figure 2.13: ORTEP diagram of 8.

Owing to the success of the silver salt, silver *tetrakis-(pentafluorophenyl)borate* ($\text{AgB}(\text{C}_6\text{F}_5)_4$) was selected as the reagent to pursue, although there are no literature reports regarding its synthesis or indeed existence. The analogous protio-compound,

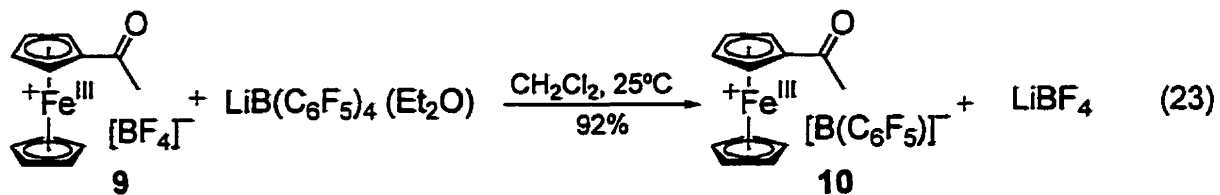
silver tetraphenylborate (AgBPh_4) is known, however.⁹⁴ Using the method to prepare AgBPh_4 , lithium tetrakis(pentafluorophenyl)borate etherate ($\text{LiB}(\text{C}_6\text{F}_5)_4 \cdot \text{Et}_2\text{O}$)⁹⁵ was mixed with silver nitrate and stirred in the dark. A white solid was isolated and it was believed to be lithium nitrate, based solely on its solubility. Unfortunately however, the isolation of $\text{AgB}(\text{C}_6\text{F}_5)_4$ was not possible by this route as it was possibly extremely light-sensitive. It is noteworthy that AgBPh_4 is also light-sensitive but does not decompose as rapidly.⁹⁴ It is unclear as to why the perfluoro silver salt should be unstable when the protio salt is isolable. The fluorine atoms make $\text{B}(\text{C}_6\text{F}_5)_4^-$ less coordinating than $\text{B}(\text{C}_6\text{H}_5)_4^-$ as π -coordination of the phenyl rings to the silver cation is decreased in the case of the perfluoro anion (*cf.* $\text{B}(\text{C}_6\text{F}_5)_4^-$). The decreased π -interaction of $\text{B}(\text{C}_6\text{F}_5)_4^-$ with the silver cation perhaps facilitating a decomposition pathway.

Other oxidising salts were considered due to the lack of success preparing the $\text{AgB}(\text{C}_6\text{F}_5)_4$. Since nitrosonium (NO^+) was an effective oxidant for the generation of 7, work to generate an alternative to NOBF_4 , $\text{NOB}(\text{C}_6\text{F}_5)_4$, was undertaken. Nitrosyl chloride (NOCl),⁹⁶ generated by the solid/gas phase reaction of nitrogen oxide gas over dried and powdered potassium chloride, was condensed onto a frozen (-196°C) solution of $\text{LiB}(\text{C}_6\text{F}_5)_4 \cdot \text{Et}_2\text{O}$ and warmed slowly to room temperature (Equation 22). ^{11}B and ^{19}F NMR spectroscopy both verify the $\text{B}(\text{C}_6\text{F}_5)_4$ anion present in the product, but the ^{15}N NMR spectrum reveals a lack of any kind of nitrogen resonance. The ^1H NMR spectrum contains signals for coordinated diethyl ether. Perhaps all of the lithium-etherate salt did not react. X-ray crystallography of an isolated crystal indicated the complete lack of nitrosonium in the solid. The structure shows that the acid $[\text{Et}_2\text{O} \cdot \text{H} \cdot \text{OEt}_2]^+ [\text{B}(\text{C}_6\text{F}_5)_4]^-$ was the product formed; although an interesting result in its own right, the crystal

structure of this acid will not be discussed. The source of the proton was not known and the quest towards $\text{NOB}(\text{C}_6\text{F}_5)_4$ was abandoned at this point.

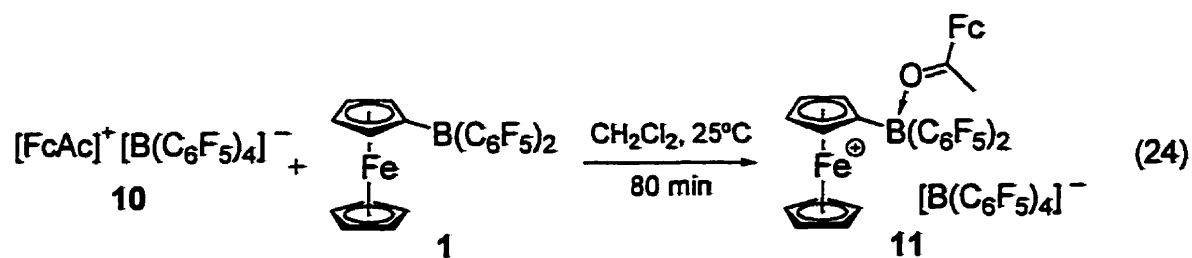


Acetylferrocenium tetrafluoroborate **9** ($[\text{FcAc}]^+[\text{BF}_4]^-$) has been compared to nitrosonium or silver(I) as a one-electron oxidant by Connelly and Geiger.⁹¹ Acetylferrocenium (FcAc^+) was hoped to be sufficiently oxidising to react with **1**. The counterion, though, was a concern as BF_4^- has been shown to lose fluoride in the presence of the strongly Lewis acidic ferrocenium-borane cation **7**, so $\text{B}(\text{C}_6\text{F}_5)_4^-$ was considered as a more robust anion. The oxidant $[\text{FcAc}]^+[\text{B}(\text{C}_6\text{F}_5)_4]^-$ (**10**) is prepared by treatment of acetylferrocene with AgBF_4 ,⁹¹ followed by $\text{LiB}(\text{C}_6\text{F}_5)_4 \cdot \text{Et}_2\text{O}$. LiBF_4 is isolated as a white precipitate from the reaction mixture and the product **10** is a crystalline blue solid (Equation 23). The ^1H NMR spectrum shows the paramagnetically broadened and shifted signals of the acetylferrocenium core, while ^{11}B (δ -16.9 ppm) and ^{19}F NMR ($\Delta(m,p\text{-F}) = 5.0$ ppm) spectra support the presence of the $\text{B}(\text{C}_6\text{F}_5)_4^-$ anion. This was a very clean route to this new reagent **10** which was fully characterised by NMR spectroscopy and elemental analysis.



The oxidation of **1** with the new oxidant **10** proceeds rapidly; the solution changes immediately from a maroon to a violet colour upon mixing (Equation 24). Borane **1** is consumed as noted by the disappearance of its signals in the ^1H NMR spectrum.

Additionally, there is a lack of signals for the expected by-product FcAc (neutral) in the reaction mixture. The violet solid isolated behaves paramagnetically, as there are broadened and shifted resonances at δ 45.2, 31.9, 22.3 ppm and sharper resonances at δ 7.18, 6.85, 3.88, and 2.15 ppm in the ^1H spectrum. The spectrum seems to indicate two different ferrocene moieties in the product. The ^{11}B NMR spectrum shows clearly a resonance for the borate $\text{B}(\text{C}_6\text{F}_5)_4^-$ anion, but the boron attached to the Cp ring is not observed. The infrared spectrum of the violet solid indicates a lower energy C=O stretch at 1644 cm^{-1} than that of free FcAc (1662 and 1655 cm^{-1}). Carbonyls coordinated to Lewis acids possess slightly weaker C=O bonds than they do in their free form. The mass balance of the product isolated and the non-observance of signals for the neutral FcAc by-product in the ^1H NMR spectrum suggest that the acetyl group is binding to the boron following oxidation of the ferrocene core (*cf.* the formation of zwitterion **8**) to form the violet product **11**. In an attempt to dislodge the bound FcAc from **11**, a solution of the **11** was exposed to an excess of PMe_3 but there was no sign of a reaction as monitored by ^1H and ^{19}F NMR spectroscopy. Complex **11** strongly supports the premise of an increased Lewis acid strength of the boron by oxidation of the iron, and disrupting the Fe...B stabilization (*cf.* **1**). Moreover, borane **1** does not react with FcAc, established by an independent experiment. Attempts to grow crystals for X-ray analysis of complex **11** have been unsuccessful.



To date, the separated ion pair $[Fc^+B(C_6F_5)_2][A^-]$ is yet unrealised. The displacement experiment of FcAc from **11** proved fruitless with $PM\bar{e}_3$. In an attempt to further assess the increased Lewis acidity of the boron centre, oxidation of the phosphine adduct **3** was carried out. The B-P bond length was hoped to decrease upon oxidation of the ferrocene core. This was not observed in the crystal structure of ion pair **12**, isolated from the reaction of $AgBF_4$ with **3**. The B-P bond length (2.044(15) Å) of **12** is slightly longer than that seen in the Fe(II) phosphine adduct **3** (1.992(9)), but statistically insignificant. The lengthening observed suggests that the ferrocenium core is electron-withdrawing, compared to the electron-rich ferrocene core of **3**. The anion, BF_4^- , remained intact and is well separated from the ferrocenium-phosphinoborane cation. The X-ray crystal structure (Figure 2.14), and the immediate colour change of the CH_2Cl_2 solution from yellow to navy blue, support the oxidation of Fe(II) to Fe(III). The geometric parameters of **12** are consistent with those of **3** and other structures discussed herein. Some selected bond lengths and angles are shown in Table 2-7.

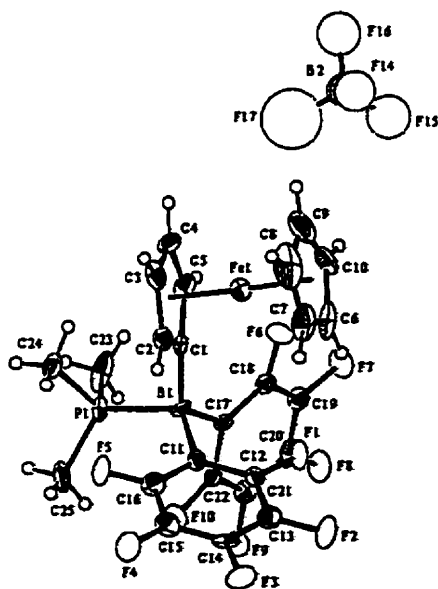


Figure 2.14: ORTEP diagram of **12**.

Table 2-7: Selected Bond Distances (\AA) and Angles ($^\circ$) for 12.

12			
P(1)-B(1)	2.044(15)	C(1)-B(1)-C(17)	122.8(10)
B(1)-C(1)	1.579(18)	C(1)-B(1)-C(11)	109.3(10)
B(1)-C(17)	1.691(15)	C(17)-B(1)-C(11)	107.0(8)
B(1)-C(11)	1.698(15)	C(1)-B(1)-P(1)	98.0(7)
Fe(1)-B(1)	3.480	C(17)-B(1)-P(1)	105.0(8)
		C(11)-B(1)-P(1)	114.9(8)
$\alpha^a = -10.5^\circ$		$\phi^b = 9.2^\circ$	

^a $\alpha = \text{Cp}_{\text{centroid}}-\text{C}_i-\text{B}$. ^b ϕ = deviation from eclipsed conformation of Cp rings.

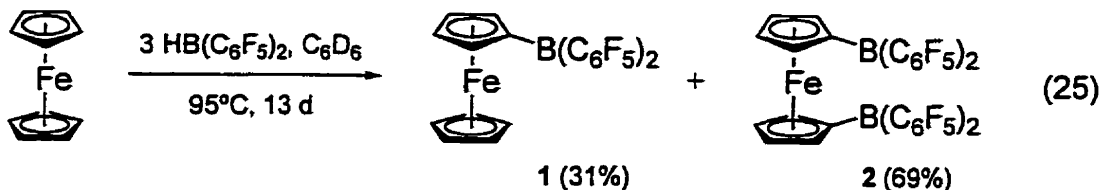
In summary, while we have been unable to prepare $[\text{Fc}^+\text{B}(\text{C}_6\text{F}_5)_2]\text{[B}(\text{C}_6\text{F}_5)_4^-]$, the results we have up to this point regarding 1 and its derivatives are as follows. The Fe...B interaction is involved in the stabilisation of the electrophilic borane present in 1. The interaction is between electrons in the atomic orbital on Fe (either of the d_{z^2} or $d_{x^2-y^2}$ orbitals) and the empty p_z -atomic orbital of the boron. The observed CT band is a result of this metal to ligand interaction. The stabilisation by iron donation decreases the Lewis acidity of 1 as PMe_3 , the strongest Lewis base used, forms a stable adduct with 1 at room temperature while the others do not. When Fe...B interaction is disrupted by the removal of an electron from the iron centre, the formed cation 7 becomes very reactive at the boron centre. The Lewis acid strength increases substantially over that of 1 as zwitterions form (recall 4, 5) and fluoride abstraction occurs from BF_4^- occurs (zwitterion 8). The ferrocenium-borane cation 7 is significantly more reactive than 1 and BF_3 . Borane 1 is less Lewis acidic than BF_3 . The direct observation of cation 7 in any of these reactions has not yet occurred by spectroscopic analysis, but it must be formed and consumed very quickly to explain these results.

2.3 1,1'-*Bis*-(bis-(pentafluorophenyl)boryl) ferrocene (2)

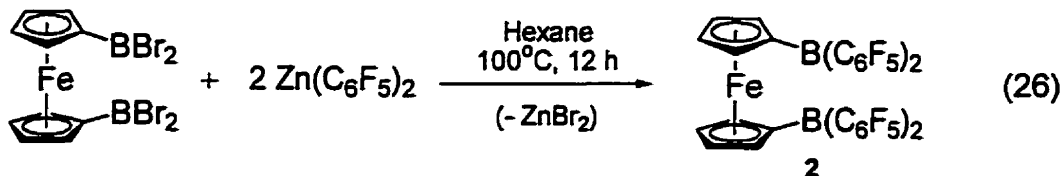
2.3.1 Synthesis and characterisation of $\text{Fc}[\text{B}(\text{C}_6\text{F}_5)_2]_2$ (2)

Utilising the same methodology for preparing borane 1 by the direct borylation of FcH with $\text{HB}(\text{C}_6\text{F}_5)_2$, an attempt to generate 1,1'-*bis*-(bis-(pentafluorophenyl)boryl)-ferrocene(2) was carried out. The *bis*-borylferrocene 2 can be formed, though not completely, by increasing the equivalency of $\text{HB}(\text{C}_6\text{F}_5)_2$ but requires more aggressive reaction conditions. The conversion of mono-borylferrocene 1, formed initially, to 2 is only 69% completed after 13 days at 95°C when an excess of $\text{HB}(\text{C}_6\text{F}_5)_2$ is used (Equation 25). Increasing the reaction temperature further does not increase the amount of 2 produced relative to 1. The electron-withdrawing nature of the boryl group must remove the necessary electron density for the unsubstituted Cp ring to undergo complete diborylation in this manner. This suggests that direct borylation occurs by the iron-mediated mechanism Route A (Scheme 4), to add both the first and second boryl group $\text{B}(\text{C}_6\text{F}_5)_2$.

Separation of 1 and 2 is difficult to carry out as they are both highly soluble in many organic solvents and sensitive to hydrolysis. Conventional chromatography and fractional recrystallization are therefore not useful separation techniques for this mixture of products. There are also no 1,3-substituted ferrocenes observed by ^1H NMR spectroscopy as $\text{B}(\text{C}_6\text{F}_5)_2$ deactivates the substituted Cp ring from being further borylated. In contrast, borylation of FcH with an excess of BI_3 produces 1,1'-*bis*- as well as 1,3-*bis*-(diiodoboryl) ferrocene.²⁷ Another route into 2 using more selective conditions was sought as separation of these products is difficult.



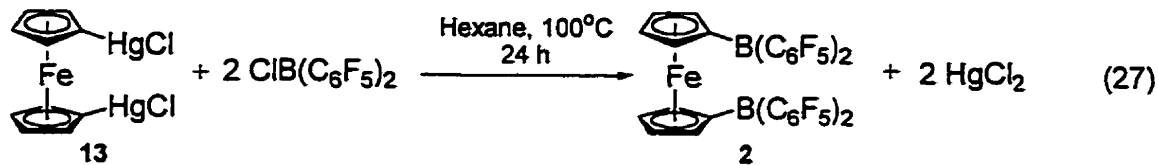
One possibility for borylating ferrocene is by formation of the known 1,1'-bis(dibromoboryl)ferrocene ($\text{Fc}(\text{BBr}_2)_2$).^{24,27} The literature preparation of this compound proceeded cleanly as observed by ^1H and ^{11}B NMR spectroscopy. The NMR tube scale reaction (Equation 26) of $\text{Fc}(\text{BBr}_2)_2$ with bis-(pentafluorophenyl)zinc ($\text{Zn}(\text{C}_6\text{F}_5)_2$)⁹⁷ generates **2**, cleanly by ^1H and ^{19}F NMR spectral analyses. However, when the reaction is scaled up there are small amounts of by-products formed. These by-products are attributed to the lesser ring substituted *bis*-borylated ferrocenes ($\text{Fc}[\text{B}(\text{C}_6\text{F}_5)\text{Br}][\text{B}(\text{C}_6\text{F}_5)_2]$, $\text{Fc}[\text{B}(\text{C}_6\text{F}_5)\text{Br}]_2$, or $\text{Fc}[\text{BBr}_2][\text{B}(\text{C}_6\text{F}_5)\text{Br}]$). Increasing the amount of zinc reagent used compared to that of $\text{Fc}(\text{BBr}_2)_2$ or increasing the reaction time did not mitigate the by-products formation.



Purification of the maroon solid mixture by recrystallization from hexamethyldisiloxane, a solvent found useful for this purpose in the past, also did not afford **2** cleanly. The by-products have similar solubility properties as that of **2**. As the by-products were not easily removed another method was pursued.

Metathetical processes that form insoluble salts of the by-products are highly effective. Borane **2** can be prepared in high crude yield by mercury salt metathesis from 1,1'-di(chloromercuric)ferrocene (**13**) and $\text{ClB}(\text{C}_6\text{F}_5)_2$ (Equation 27). Dimercurated ferrocene **13** was isolated as a by-product from the preparation of FcHgCl .⁵¹ Inspection

of the ^1H spectrum of **2** shows a trace amount of **1** which is not easily removed by fractional recrystallisation. A trace amount of FcHgCl must have been present in mercurial ferrocene **13** used.



The mercury salt metathesis route is good, though, the amount of FcHgCl present in the *bis*-mercurated ferrocene **13** prepared according to the literature method⁵¹ is not satisfactory. A different route to **13** avoiding the potential contamination by FcHgCl was sought. Dilithioferrocene ($\text{FcLi}_2\cdot\text{TMEDA}$) is readily prepared but there have been no reports of generating **13** from it. Simply mixing $\text{FcLi}_2\cdot\text{TMEDA}$ with HgCl_2 in THF at room temperature leads cleanly to **13**. With pure **13** in hand the reaction with $\text{ClB}(\text{C}_6\text{F}_5)_2$ was carried out again (Equation 27). Borane **2** is isolated as a dark maroon oily solid that is purified by recrystallization from hexamethyldisiloxane in 25% isolated yield. The product **2** was analytically pure as determined by combustion analysis. The low isolated yield is due to the high solubility of **2** in hexamethyldisiloxane and organic solvents, similar to that of **1**.

The physical properties of **2** are very similar to those of **1** with regards to solubility, moisture sensitivity and appearance. Both materials are intensely maroon microcrystalline solids. A satisfactory X-ray structure of **2** was unable to be determined, as there was significant disorder in the crystal lattice analysed at low temperature.⁹⁸ The cyclopentadienyl rings are stacked up parallel in a column throughout the structure with uniform spacing between them. The iron atoms lie in alternating positions with 80:20% disorder. There maybe a superposition of two structures which are disordered. The light

atoms, especially fluorine atoms, are highly distorted, likely covering disordered sites. The refinement of the structure was not satisfactory ($R = 20\%$), but confirms the chemical identity of 2.

^1H NMR spectrum of purified *bis*-borane 2 is shown in Figure 2.15. Note the apparent triplet for the β -protons, consistent with a *mono*-substituted metallocene (*vide infra*)²³ and the broadened resonance for the α -protons. Both Cp rings are equivalent as there are only two proton resonances observed.

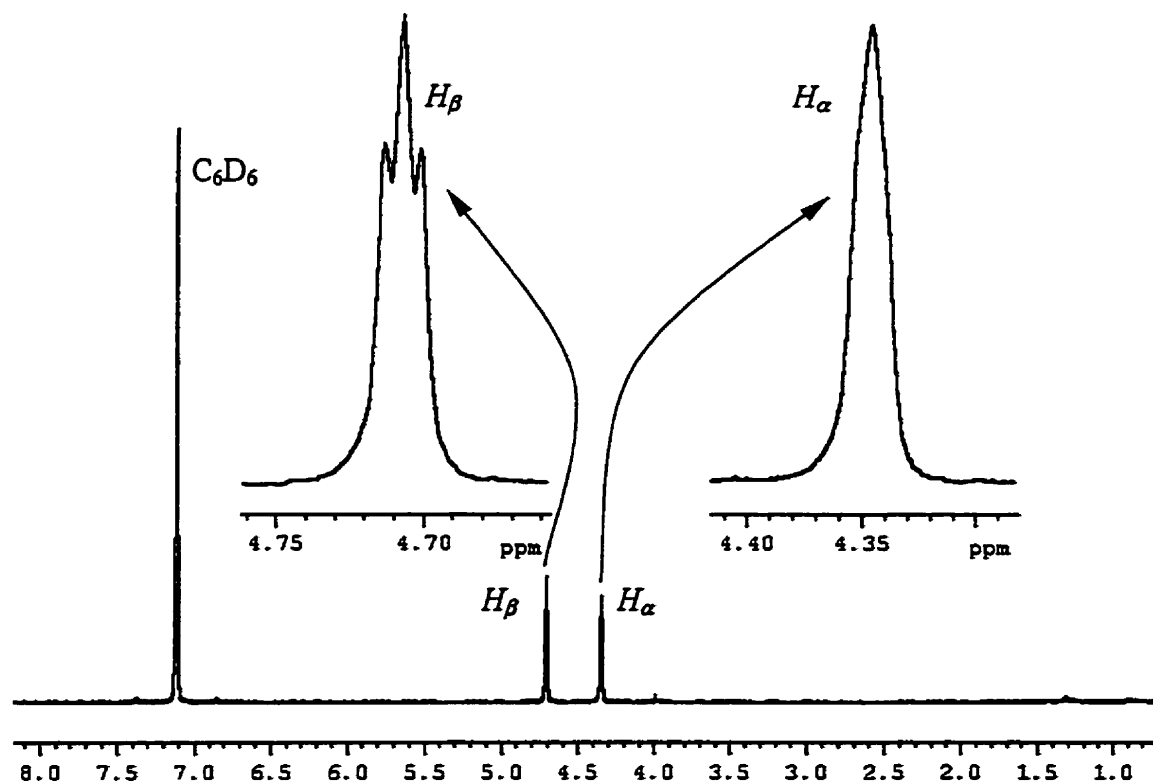


Figure 2.15: ^1H NMR spectrum of 2 in C_6D_6 . Note the apparent triplet for H_β .

The ^{19}F NMR spectrum of 2 is quite similar to that of 1. Three multiplets corresponding to the *ortho*-, *para*- and *meta*-fluorines at δ -129.8, -150.0 and -160.7 ppm are observed, respectively. The $\Delta(m,p\text{-F}) = 10.7$ ppm indicates weak Fe···B interaction of

the two boron atoms with the ferrocene core, but weaker than that of 1. Note that $\Delta(m,p\text{-}F)$ for 1 is smaller by 1.4 ppm. The weaker Fe···B interaction is supported by the calculations and observations Wagner *et al.* made, as the number of boryl groups attached to a ferrocene increases, the dip angle α decreases.⁵⁶ Correspondingly the strength of Fe···B interaction decreases as the number of borons increase. The iron centre must share its electron density with a greater number of electron-deficient borons.

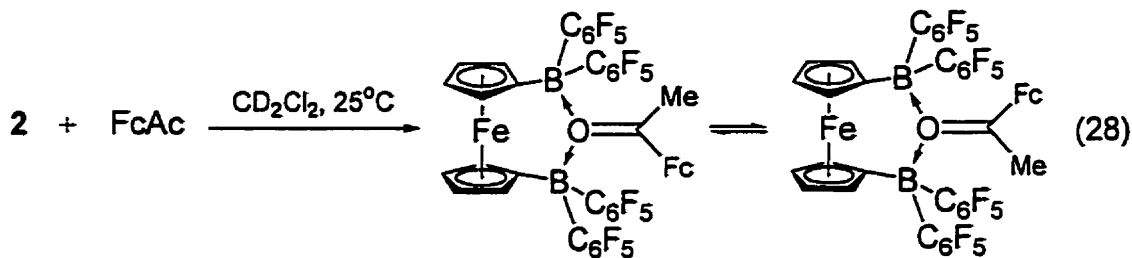
The ^{11}B NMR spectrum of 2 is less than informative as there are no observable resonances. The presence of two *bis*-OBoryl groups may cause the lack of a signal due to quadrupolar broadening of the boron atoms due to a through bond broadening interaction between the boron atoms. This has been observed by Williams *et al.* in the bidentate Lewis acid 1,2-[B(C₆F₅)₂]C₆F₄ as a through bond coupling of the borons to one another.⁹⁹ The ^{11}B NMR signal of Fc(BBr₂)₂ is seen at δ 50.8 ppm as compared to the upfield shifted *mono*-borylated ferrocene FcBBr₂ at δ 46.7 ppm.²⁴ The expected shift of the 2 would likely be *ca.* δ 57 ppm compared to that of 1 (δ 53.0 ppm).

2.3.2 Reaction Behaviour of Fc[B(C₆F₅)₂]₂ (2)

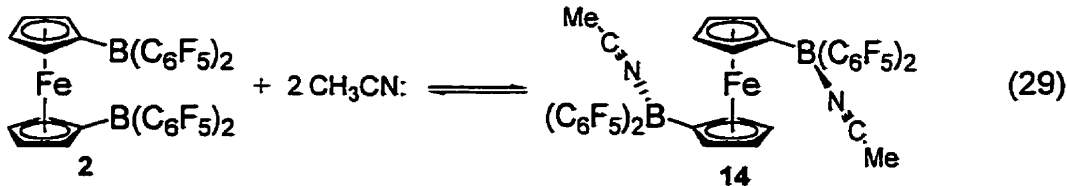
2.3.2.1 Lewis Base reactions with Fc[B(C₆F₅)₂]₂ (2)

In a similar manner used to probe the Lewis acidity of borane 1, borane 2 was exposed to a number of different Lewis bases. Benzophenone, acetophenone, acetylferrocene, acetonitrile and trimethylphosphine were individually mixed with 2 in a 1:1 stoichiometry and monitored by ^1H and ^{19}F NMR spectroscopy. *Bis*-borane 2 reacts with a greater number of Lewis bases than did 1 as expected, suggesting greater Lewis acid character. There is no apparent change in the ^1H or ^{19}F NMR signals of 2 for the reactions of it with acetophenone and benzophenone.

Acetylferrocene reacts with **2** (Equation 28). The ^1H NMR spectrum of **14** shows an upfield shift of the proton signals (*cf.* **2**), while the acetylferrocene protons have all shifted downfield due to complexation. In the ^{19}F NMR the $\Delta(m,p\text{-F}) = 8.7$ ppm is smaller due to upfield shift of the F_p towards the F_m indicating greater anionic character of the boron atoms compared to that of **2** ($\Delta(m,p\text{-F}) = 10.7$ ppm). It appears that FcAc has coordinates in a “symmetric manner” between the boron atoms as the ^1H and ^{19}F NMR spectra simply indicate only two types of protons and one set of C_6F_5 rings. An equilibrium may be in operation that averages out the diastereotopic protons, but at room temperature this is not clear.



Acetonitrile reacts with **2** at room temperature, forming a yellow solution and precipitate. In the case of **1**, CH_3CN coordinates at low temperature, whereas it binds to **2** at room temperature. The reaction of **2** with CH_3CN in various noncoordinating, deuterated solvents all generated a yellow precipitate rendering the solution nonhomogeneous. CD_2Cl_2 does not solubilise the product formed, completely. As a result it appears by ^1H and ^{19}F NMR spectroscopy that a single product persists in solutions along with some starting borane. An equilibrium between **2** and **14** may exist, but as the product exhibits poor solubility it is likely that the equilibrium lies towards the right, *i.e.*, adduct **14** (Equation 29).



Trimethylphosphine also reacts with **2** at room temperature to form an adduct comparable to that of **3**. The reaction is driven to completion by strong B-P bond formations. The yellow crystalline product **15** was isolated and characterised, including an X-ray crystal structure determination (Figure 2.16). ^1H , ^{11}B and ^{19}F NMR spectroscopy support the diphosphinated adduct a conclusion confirmed by the X-ray structure. The geometric parameters of **15** are similar to those of **3**. The B-P bond lengths (1.996(4) and 2.036 (4) Å) are consistent with literature reports⁷²⁻⁸² and similar to those of **3** and **12**. An interesting feature is the eclipsing of the Cp rings in the solid state. The eclipsing causes the PMe_3 -boryl substituents to be nearer to each other, than if the ferrocene core was in the *anti*-conformation. This observation is likely due to the solid-state packing arrangement of the molecules in the crystal lattice, rather than any electronic bonding considerations

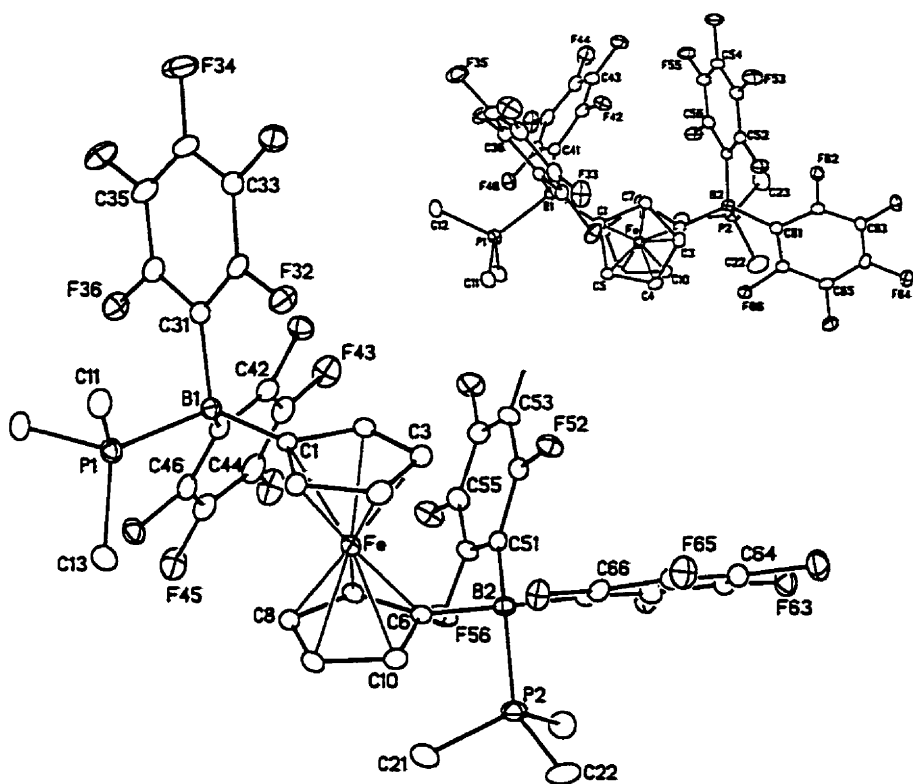


Figure 2.16: ORTEP diagrams of 15.

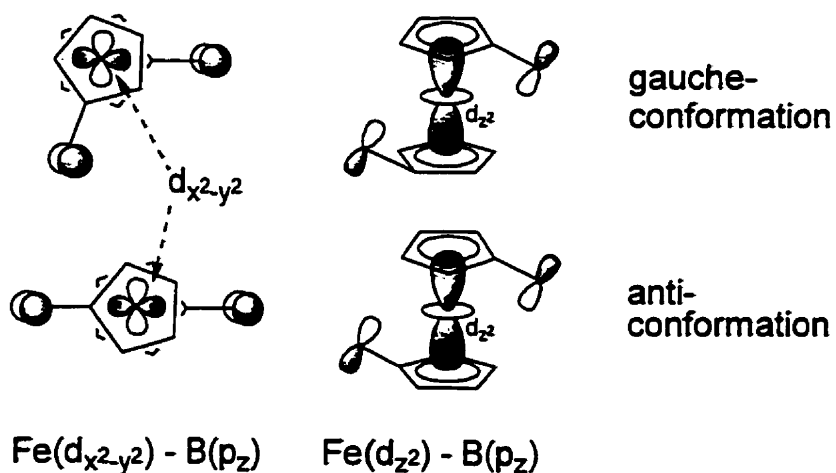
Table 2-8: Selected Bond Distances (\AA) and Angles ($^\circ$) for 15

15			
B(1) – C(1)	1.615(5)	B(2) – C(6)	1.617(4)
B(1) – C(31)	1.666(5)	B(2) – C(41)	1.645(5)
B(1) – C(41)	1.639(5)	B(2) – C(51)	1.648(4)
B(1) – P(1)	1.996 (4)	B(2) – P(2)	2.036(4)
Fe(1) – B(1)	3.405	Fe(1) – B(2)	3.416
P(1)-B(1)-C(1)	108.3(2)	P(2)-B(2)-C(6)	99.39(19)
P(1)-B(1)-C(31)	101.4(2)	P(2)-B(2)-C(51)	114.2(2)
P(1)-B(1)-C(41)	115.7(2)	P(2)-B(2)-C(61)	103.0(2)
C(1)-B(1)-C(31)	111.8(2)	C(6)-B(2)-C(51)	108.1(3)
C(1)-B(1)-C(41)	109.4(3)	C(6)-B(2)-C(61)	122.0(3)
C(31)-B(1)-C(41)	110.1(3)	C(51)-B(2)-C(61)	109.8(2)
$\alpha(B1)^a = -7.0$		$\alpha(B2) = -10.5$	
$\phi^b = 12.5$			

^a $\alpha = \text{Cp}_{\text{centroid}}-\text{C}_i-\text{B}$. ^b ϕ = deviation from eclipsed conformation of Cp rings.

From the above results it is apparent that borane 2 behaves as a stronger Lewis acid than does 1. This can be attributed to the weaker Fe...B interaction as there are two

electrophilic boron atoms competing for the free electrons in the ferrocene core. Wagner *et al.*⁵⁶ describes one of the important molecular orbitals for diborylated ferrocene as the d_{z^2} (or $d_{x^2-y^2}$) atomic orbital of the iron interacting with the empty p_z -atomic orbitals of the boron atoms.



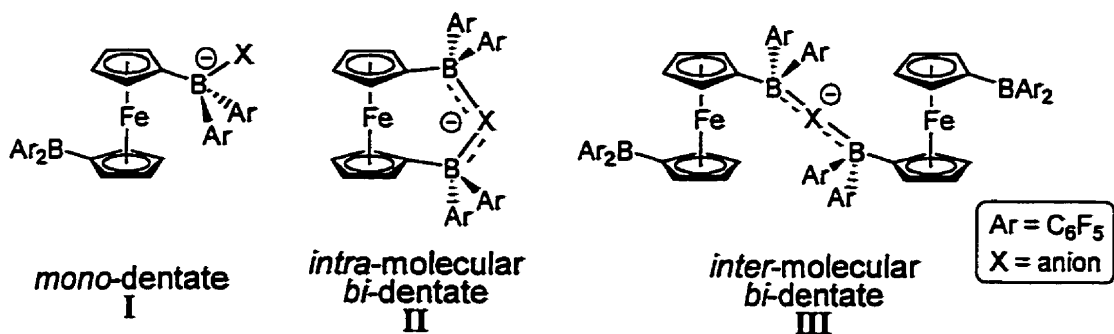
Scheme 6: Schematic orbital plot of *anti*- and *gauche*-conformations of 2.

The *gauche*- and *anti*-conformations are the preferred geometries of the diborylated system. From a bonding perspective these are the two conformers that offer the most stability to the system. There is essentially a “2-electron, 3-centre” bonding mechanism operating between the iron and the two boron atoms. The decrease in bond order of 2 from that of 1 (2 electron, 2 centre) decreases the amount of Fe···B interaction occurring in 2, which is consistent with the increased Lewis acidity observed for 2. In conclusion, from the results presented it is clear that the Fe···B interaction plays a significant role in the behaviour of the borane(s) attached.

2.3.2.2 Reactions of $\text{Fc}[\text{B}(\text{C}_6\text{F}_5)_2]_2$ (2) with anions.

Recently, Williams *et al.* published results on the anion binding of F^- and OH^- by 1,2-bis(bis(pentafluorophenyl)boryl)tetrafluorobenzene.⁹⁹ The proximity of the Lewis acid centres, and the flexibility of the backbone to which they are attached, affects the aperture within which anions of different sizes can coordinate. Bidentate molecular pincers and anion-binding moieties have been of interest in our laboratory for some time. Use of bidentate Lewis acids may allow for methide abstraction and formation of a weakly coordinating anion, more so than $\text{MeB}(\text{C}_6\text{F}_5)_3$ (Equation 2), as the negative charge is more delocalized over more atoms, thereby decreasing the coulombic interaction between the active cationic catalyst and the counteranion.^{99,100}

Recall from Chapter 1, Herberich's work with $\text{Co}(\text{C}_5\text{H}_4\text{B}(i\text{Pr})_2)_2^+$,⁴⁴ isoelectronic to 2, as a molecular pincer to bind small anions (Cl^- and OH^-). As borane 2 contains two Lewis acidic boron centres, it may be possible to accommodate a small anion by chelation of the borons to that anion. There are three possible modes of binding of an anion to bidentate pincers (Scheme 7): as a monodentate borane/borate (I); a bidentate molecular pincer (II) (symmetric binding) or bidentate intermolecular species (III) (bridging). To evaluate the effectiveness of 2 in this regard, a number of anions were reacted with 2 in a 1:1 ratio. Of those tested, trityl methoxide (Ph_3COCH_3), trityl pentafluorophenoxyde ($\text{Ph}_3\text{COC}_6\text{F}_5$) and trityl pentafluorophenylmethoxide ($\text{Ph}_3\text{COCH}_2\text{C}_6\text{F}_5$) show no affinity to react with 2.



Scheme 7: Modes of anion binding to $\text{Fc}[\text{B}(\text{C}_6\text{F}_5)_2]_2$ (2)

Trityl hydroxide (Ph_3COH) reacts with 2, but not cleanly as the ^1H and ^{19}F NMR spectrum indicate a complex mixture. There is no indication whether the hydroxide anion is coordinated to one boron or bridging between both borons in an *intra-* or *inter-*molecular fashion. Copper(II) methoxide ($\text{Cu}(\text{OMe})_2$) delivers a methoxide to 2. After 3 days at 60°C there is an apparent mixture of two products formed observed by ^1H NMR spectroscopy. These products were not isolated but examined *in situ* by ^1H and ^{19}F NMR. There is support for a bridging methoxide (type II) as a signal is observed upfield at δ 1.33 ppm (s, OCH_3)⁴⁴ and a pair of resonances at 3.40 (t, H_β) and 3.35 (s, H_α) integrating in a 3:4:4 ratio, respectively. Herberich *et al.* observed a bridging methoxide between the two boron centres of $\text{Co}(\text{C}_5\text{H}_4\text{B}(i\text{Pr})_2)_2^+$ at 3.32 ppm by ^1H NMR spectroscopy.⁴⁴ The other signals are complicated and may be attributable to a borane/borate compound. The ^{19}F NMR shows a complex spectrum and there is no clear indication of a major product.

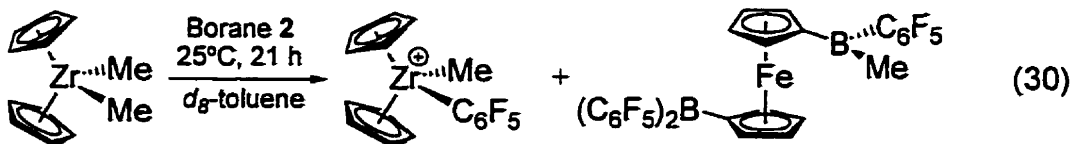
Borane **2** reacts with tetraphenylphosphonium chloride to form a mixture of two products. The ^{19}F NMR spectrum suggests an equilibrium is occurring where a chloride can be either bridging between the two boron centres (type II) or coordinated to a single boron atom (type I). ^1H NMR is less than informative as there is a deficiency of signals for the two anion species mentioned but the phosphonium cation is clearly visible.

This is an area of work that requires investigation in greater depth to understand the full potential of **2** as bidentate molecular pincer. The anion not discussed in this section is a methide anion from a precatalyst such as Cp_2ZrMe_2 . This will be discussed in the next section.

2.4 Activation studies of dimethylzirconocene

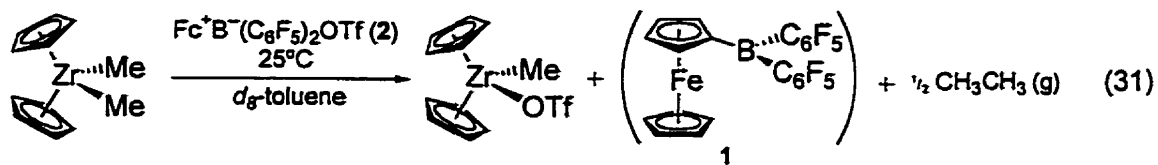
Marks *et al.* have shown that *tris*-(pentafluorophenyl)borane is able to abstract methide (CH_3^-) from dimethylzirconocene rendering a zirconium cation and methylborate counterion.¹⁶ In the hope of using boranes **1** and **2** as cocatalysts, each was reacted with Cp_2ZrMe_2 . Over a long period of time **1** does not effect methide abstraction as no change occurs in the ^1H NMR spectrum. Warming the mixture did not render **1** reactive toward activation of the Zr-Me bond. The depressed Lewis acidity of **1** can in all likelihood, be attributed to the Fe...B interaction. Bis-borane **2** is, however, active towards Zr-Me bond cleavage but it is not able to bind the methide in a symmetric fashion (Equation 30). C_6F_5 -ring transfer occurs from one of the boron centres to zirconium cationic centre as noted by the methyl resonance in the ^1H NMR spectrum. Two products were formed, $\text{Cp}_2\text{ZrMe}(\text{C}_6\text{F}_5)$ ¹⁰¹ and $[(\text{C}_6\text{F}_5)_2\text{B}]^+\text{Fc}[\text{B}(\text{C}_6\text{F}_5)\text{Me}]$. ^1H NMR spectroscopy indicates the lack of symmetry in the molecule, as four distinct signals are observed for each of the pairs of protons on the Cp rings. The decreased interaction of

$\text{Fe}\cdots\text{B}$ allows **2** to exhibits greater Lewis acidity compared to that of **1**. This is consistent with the results of the Lewis base experiments reported herein.



Recall that the two methods of catalyst activation mentioned in Chapter 1 were Lewis acid abstraction of a methide (or alkide) group and the other was by electron-transfer oxidation of the Zr-Me bond by the use of a oxidising agent like ferrocenium or silver cation. The former was just discussed above for **1** and **2**.

Moving from Lewis acid activation to electron-transfer activation, zwitterions **4** and **5** were mixed with Cp_2ZrMe_2 . The triflate zwitterion demonstrates the ability to oxidise the Zr-Me bond to afford a methyl radical that dimerises and bubbles as ethane gas (Equation 31). The triflate ligand of the borate species $[\text{FcB}(\text{C}_6\text{F}_5)_2\text{OTf}]^-$ transfers from the boron centre to the more Lewis acidic zirconium cation. ^{19}F NMR spectroscopy shows the downfield shift of the CF_3 resonance ($\delta = -78.1$ ppm) from that of the zwitterion **4** ($\delta = -89.6$ ppm). ^1H NMR spectroscopy supports the assignment of the product $\text{Cp}_2\text{ZrMe}(\text{OTf})^{102}$ as a 10:3 ratio was observed corresponding to the $\text{Cp}:\text{Me}$ protons. The other portion of the product mixture, the neutral borane **1**, for some reason was not observed in the ^1H NMR spectrum.



The initial zwitterionic target **5** does not oxidise Cp_2ZrMe_2 . There is no reaction observed by ^1H and ^{19}F NMR, nor is there bubbling from the green solution as had been observed above (Equation 31). Zwitterion **5** is apparently a weaker oxidant than ferrocenium, and the electrochemical behaviour of **5** may reveal something of its reluctance as an oxidative activator.

To summarise, these activation results indicate that **1** is a weaker Lewis acid than **2** which was substantiated by the Lewis base experiments described above. *Bis*-borane **2** is able to abstract a methide from zirconium, but a ring transfer occurs from the anion formed, $\text{Fc}[\text{B}(\text{C}_6\text{F}_5)_2][\text{B}(\text{C}_6\text{F}_5)_2(\text{Me})]^-$. The triflate zwitterion **4** is able to oxidise $\text{Zr}-\text{Me}$ while **5** cannot.

2.5 Electrochemical studies

The redox properties of the ferrocene compounds and derivatives are of interest as the electrochemical behaviour of each can have an impact on their behaviour in reactions. Electrochemistry can be used to probe the metal/ligand relationship present in a molecule. Neutral ferrocene substrates (**1**, **2**, **3**, **15**) and the zwitterion **5** were examined to determine their oxidation potentials for the purpose of assessing their behaviour in redox and other reactions. Due to the air-sensitive nature of these compounds a silver wire *quasi*-reference electrode (QRE) was employed in the sealed electrochemical cell. The cyclic voltammetry (CV) experiments were carried out in tetrabutylammonium

tetrakis-(pentafluorophenyl)borate (16) solutions (*ca.* 100 mM) in α,α,α -trifluorotoluene (TFT). This more specialized electrolyte **16** was chosen as BF_4^- has been shown to dissociate into BF_3 and F^- in the presence of intermediate **7**. The cyclic voltammograms of each substrates **1**, **2**, **3** and **5** show a one step, one-electron reversible oxidation wave in the potential range between -472 mV and $+450$ mV, referenced to the ferrocene/ferrocenium (FcH/FcH^+) redox couple (Table 2-9). Borane **2** shows an irreversible oxidation wave at $E_{1/2} = +820$ mV (*cf.* FcH/FcH^+).

Table 2-9: Electrochemical data observed for **1**, **2**, **3**, **5**, **15**

Substrate	$E_{1/2}(\text{substrate})$ (mV) ^a
$\text{FcB}(\text{C}_6\text{F}_5)_2$ (1)	+450
$\text{Fc}[\text{B}(\text{C}_6\text{F}_5)_2]_2$ (2)	+820
$\text{FcB}(\text{C}_6\text{F}_5)_2\text{PMe}_3$ (3)	-100
$\text{Fc}[\text{B}(\text{C}_6\text{F}_5)_2 \text{PMe}_3]_2$ (15)	-201
$\text{FcB}(\text{C}_6\text{F}_5)_3$ (5)	-472

^a Compared to $E_{1/2}(\text{Fc}/\text{Fc}^+)$ set to 0 mV; internal reference.

Borane **1** (Figure 2.17) shows a half-wave potential ($E_{1/2}$) of +450 mV while **2** (Figure 2.18) is almost double that value at +820 mV. Again, the additive effect of the second boryl group to the ferrocene core has a doubling affect observed in the redox nature of **2** (*cf.* **1**).⁵⁶ This implies that reagents that can oxidise **1** may not be able to effect the oxidation of **2** due to the 370 mV gap between them. This was observed when **2** is stirred for a long period with freshly prepared AgC_6F_5 and no reaction occurs. Borane **2** is not converted to the desired zwitterion ($\text{Fc}^+(\text{B}(\text{C}_6\text{F}_5)_2)(\text{B}(\text{C}_6\text{F}_5)_3^-)$) as compared to the near instantaneous reaction of **1** with the same reagent (*i.e.* zwitterion **5**).

The greater the half-wave potential $E_{1/2}$, the more difficult the oxidation process of the metal centre.

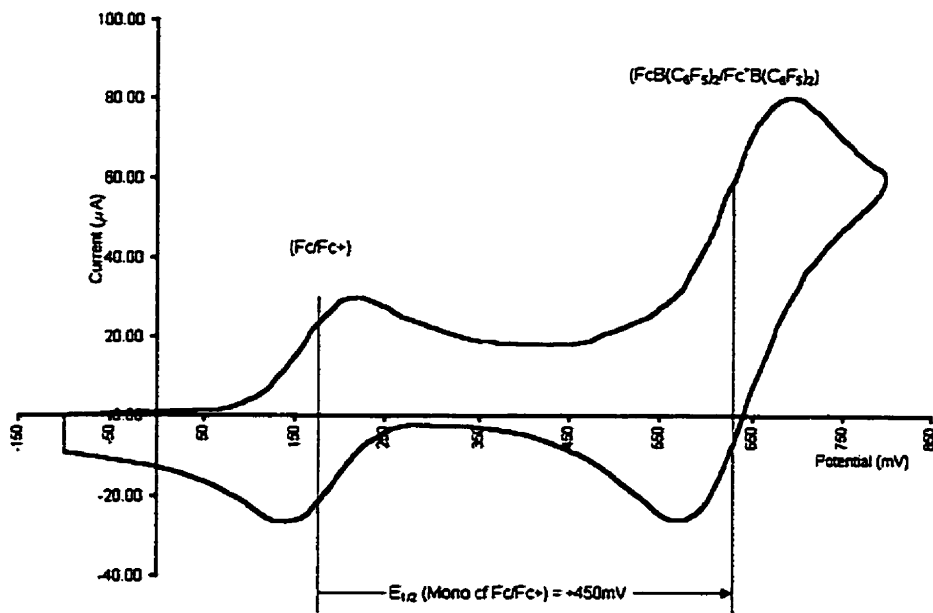


Figure 2.17: CV of 1 (1 mM) in TFT. Electrolyte 16 $[\text{Bu}_4\text{N}][\text{B}(\text{C}_6\text{F}_5)_4]$ at 100 mM.
 $E_{1/2}(1) = +450 \text{ mV}$ (cf. FcH/FcH^+).

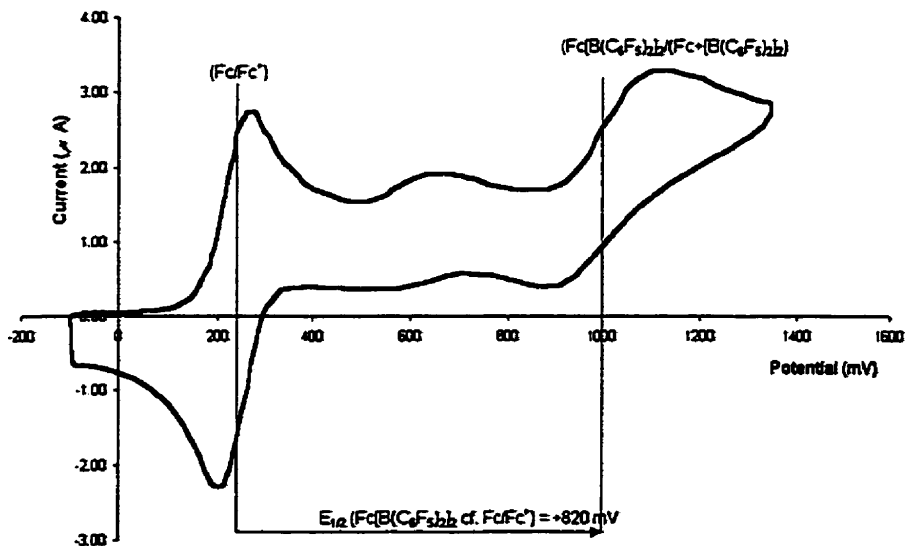
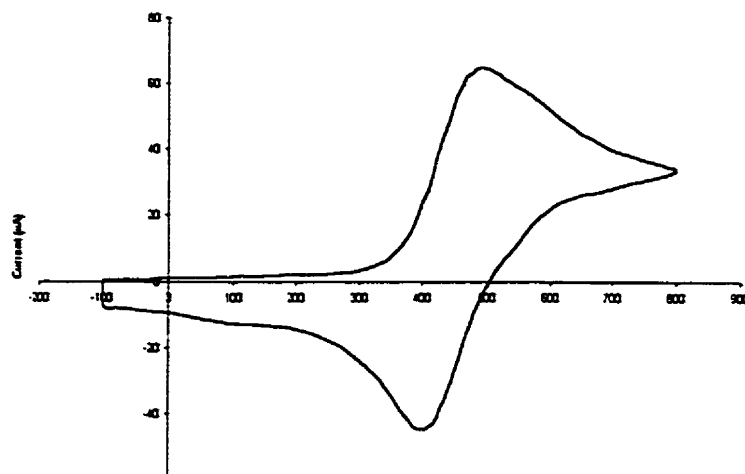
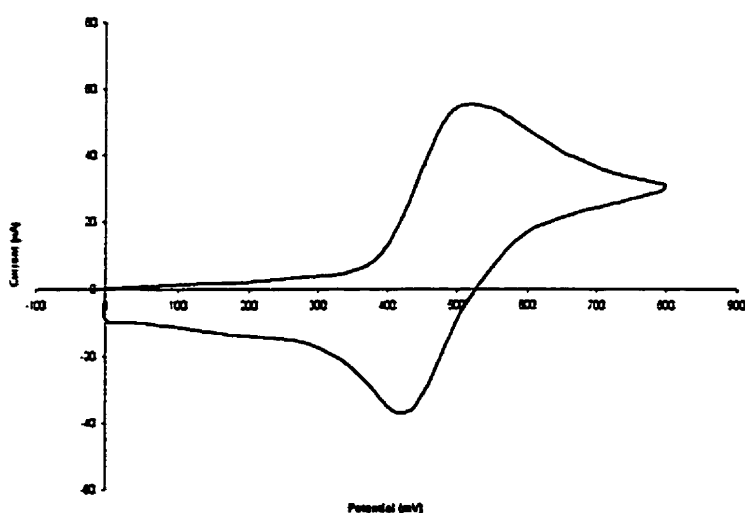


Figure 2.18: CV of 2 (1 mM) in TFT. Electrolyte 16 $[\text{Bu}_4\text{N}][\text{B}(\text{C}_6\text{F}_5)_4]$ at 100 mM.
 $E_{1/2}(2) = +420 \text{ mV}$ (cf. Fc/Fc^+).

The redox couples observed for the phosphine adducts **3** and **15** are -100 mV and -200 mV, respectively (Figure 2.19 (a) and (b)). Again, we see a two-fold increase of the $E_{\text{1/2}}$ (**15**) over that of $E_{\text{1/2}}$ (**3**) resulting from the increased number of phosphinated-boryl groups ($\text{B}(\text{C}_6\text{F}_5)_2\text{PMe}_3$) present in **15**. The electron donation of the phosphines into the boranes increases the electron density at iron (II) centre, therefore, the iron becomes more easily oxidised. The internal reference shifted significantly from that of *ca.* 200 mV for substrates examined (**1** and **2**) to $+545$ and $+670$ mV (vs. Ag-wire QRE) for **3** and **15**, respectively. The change in the position of the ferrocene redox couple vs. Ag-wire QRE is likely due to an interaction of the phosphine with the silver electrode, thereby changing the surface of the silver electrode. For reasons identified here, it is important to use an internal standard, like ferrocene, to allow correlation of electrochemical results. The QRE was exchanged for a platinum-wire and the CVs of **1** and **3** were collected under the same solvent and electrolyte concentrations. For **3**, the value of $E_{\text{1/2}}(\text{FcH/FcH}^+)$ did not change significantly and $E_{\text{1/2}}$ (**3**) was of the same magnitude at -137 mV confirming the likelihood of phosphine interference with both the silver (Ag) and platinum (Pt) reference electrodes. For the neutral borane **1** the $E_{\text{1/2}}$ is $+400$ mV (vs. FcH/FcH^+). Swapping the QRE from Ag to Pt shows that the surface change occurring in both cases does not obscure the results. Therefore, the value observed for **3** and **1** are independent of the QRE used.



(a)



(b)

Figure 2.19: (a) CV of **3** and (b) **15** in TFT at 1 mM.
Electrolyte **16** $[\text{Bu}_4\text{N}] [\text{B}(\text{C}_6\text{F}_5)_4]$ at $c = 100$ mM.
Ag-wire QRE.

The curious result of these electrochemical studies is the E_{h} of zwitterion **5** being quite negative (-472 mV vs FcH/FcH⁺). The electron-withdrawing effect of the three

C_6F_5 rings should make the boron more electron-deficient in the case of the borate, but inductively the $B(C_6F_5)_3$ group is overall σ -donating into the Cp ring to which it is attached. The net result is electron donation into the iron centre affording the negative $E_{1/2}$ value for zwitterion 5. This most likely is the reason for the observed lack of electron transfer activation of Cp_2ZrMe_2 by 5. Electronic tuning of this system is necessary to move it from the realm of an “inactive” to that of an “active” cocatalyst for Cp_2ZrMe_2 .

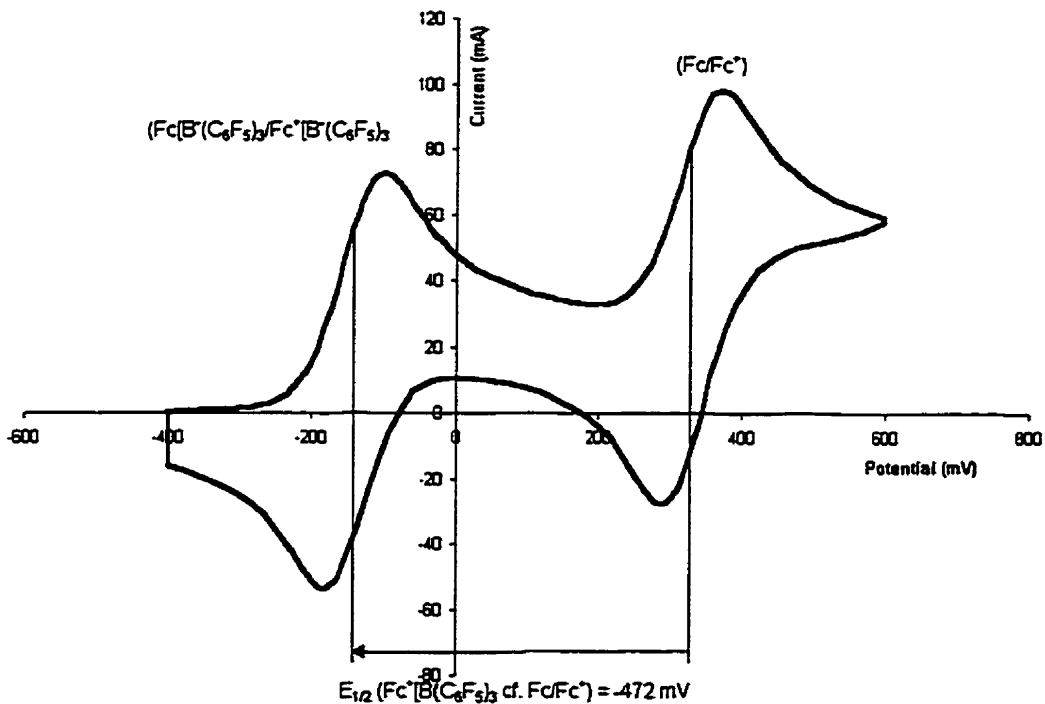


Figure 2.20: CV of 5 (1 mM) in TFT. Electrolyte 16 $[Bu_4N][B(C_6F_5)_4]$.

2.6 Quantitative assessment of the Lewis acid strength of 1 and 2.

Lewis acid (A) strength can be assessed quantitatively by the use a spectroscopic method developed by Childs.¹⁴ The 1H chemical shift differences of the protons

(particularly the H₃ proton) of crotonaldehyde (CH₃CHCHCHO) are sensitive to slight variations in the electronic nature of the carbonyl fragment upon coordination to a Lewis acid centre (Equation 32). The other proton signals (H₁, H₂ and H₄) do not show such a linear relationship as does the response of H₃. The relative scale is believed to be insensitive to steric factors and is consistent with thermodynamic data.¹⁴ The samples were prepared according to the description by Childs. Results were obtained for boranes 1 and 2, BBr₃, AlCl₃ and SnCl₄; the results for the latter three are consistent with those reported.¹⁴

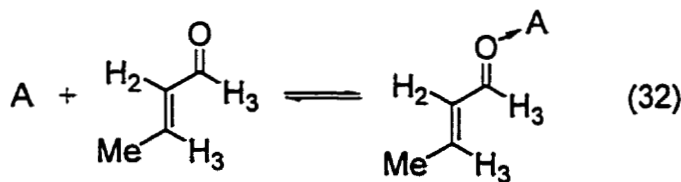


Table 2-10: ¹H NMR chemical shift differences ($\Delta\delta$) of crotonaldehyde on complexation with various Lewis acids.^a

Lewis Acid	$\Delta\delta_{\text{H}1}$	$\Delta\delta_{\text{H}2}$	$\Delta\delta_{\text{H}3}$	$\Delta\delta_{\text{H}4}$
BBr ₃	0.11	0.93	1.47	0.50
AlCl ₃	-0.22	0.79	1.30	0.45
Fc[B(C ₆ F ₅) ₂] ^b	-0.37	0.81	1.03	0.39
SnCl ₄	-0.06	0.57	0.83	0.26
FcB(C ₆ F ₅) ₂	-0.01	0.37	0.54	0.33

^aIn ppm. Chemical shifts of uncomplexed crotonaldehyde protons are: 9.45 (d, ¹H, H₁); 6.88 (m, 1H, H₃); 6.08 (dq, 1H, H₂); 2.00 (dd, 3H, H₄). Approximately 0.3 M solution in CD₂Cl₂ at -20°C, unless otherwise stated.

^b0.14 M solution in CD₂Cl₂ at -20°C.

The relative Lewis acid strength scale by Childs was calculated from normalising the results obtained for $\Delta\delta_{\text{H}3}$ of the aldehyde compared to that of the strongest Lewis acid adduct, BBr₃ ($\Delta\delta_{\text{H}3}(\text{A})/\Delta\delta_{\text{H}3}(\text{BBr}_3)$) (Table 2-11). These results confirms the qualitative

assessment of the relative Lewis acidity of the boranes **1** and **2**. Borane **2** (0.70) is of comparable Lewis acid strength to that of $B(C_6F_5)_3$ (0.77), whereas borane **1** (0.37) is a much weaker Lewis acid; the Fe...B interaction significantly decreases the Lewis acidity of the boron centre in **1**.

Table 2-11: Lewis acid scale based on $\Delta\delta_{H3}$ resonances of crotonaldehyde.

Lewis Acid	Relative Acidity Observed ^a	Relative Acidity Reported ^b
BBr_3	1.00	1.00 ± 0.005
BCl_3		0.93 ± 0.02
$SbCl_5$		0.85 ± 0.03
$AlCl_3$	0.88	0.82^a
$B(C_6F_5)_3$		0.77 ^c
BF_3		0.77 ± 0.02
$EtAlCl_2$		0.77^a
$Fc[B(C_6F_5)_2]_2$ 2	0.70	
$TiCl_4$		0.66 ± 0.03
Et_2AlCl		0.59 ± 0.03
$SnCl_4$	0.56	0.52 ± 0.04
Et_3Al		0.44 ± 0.02
$FcB(C_6F_5)_2$ 1	0.37	

^(a)Determined using crotonaldehyde, only. ^(b)Relative acidity determined using a number of different Lewis bases. See Childs *et al.* for more details.¹⁴ ^(c)Luo, L.; Marks, T. J. *Topic in Catalysis* 1999, 7, 97-106.

2.7 Conclusions

Ferrocenylboranes **1** and **2** are novel Lewis acids with interesting reaction behaviours. The interaction of the iron centre with the boryl substituents strongly affects the type of chemistry possible with each. The electron donation from the iron to the boron is much stronger in **1** and decreases as a second boryl group is introduced, as in borane **2**. The Lewis acid strength of **1** was determined to be lower than that of **2**, as borane **2** reacts with a greater number of weak Lewis bases than does **1** at room temperature. The additive effect of one and two boryl groups attached to ferrocene has been manifested by the observed results in reactions that probe the Lewis acid strengths, activation of Cp_2ZrMe_2 and a study of these species electrochemically. Placing a second $\text{B}(\text{C}_6\text{F}_5)_2$ group onto **1** effects the half reaction potential ($E_{\text{h.s.}}$) of **2** by a positive increase of about 400 mV; the iron centre of **2** is appreciably more difficult to oxidise than the iron centre of **1**. The amount of $\text{Fe}\cdots\text{B}$ interaction therefore appears inversely related to the Lewis acid strength of the borane centres.

The intermediate cation **7**, formed upon oxidation of **1**, has not been directly observed or isolated but is believed to be a very reactive species due to the formation of **8** by fluoride abstraction from BF_4^- . Therefore, on the basis of these observations it is not unreasonable to suggest that intermediate **7** is a stronger Lewis acid than BF_3 . Complex **11** and zwitterion **8** provide the best support for the ferrocenium-borane **7**. Isolation of a compound containing cation **7** would be very desirable allowing the direct observation of the decreased $\text{Fe}\cdots\text{B}$ interaction, however attempts focused at realising this goal have failed.

Bis-borane **2** shows a propensity to be much more difficult to work with as purification is tedious as it exhibits high solubility in many non-polar solvents. The preparation of **2** on a large scale is necessary, as the purified yield is moderate at best. Anion binding and recognition is possible using **2** but finding the most suitable choice of anion remains a challenge. Comparable anions were briefly investigated, however the work is preliminary and requires further examination.

The relative Lewis acid strengths for some of the compounds studied were established as follow: $\text{FcB}(\text{C}_6\text{F}_5)_2 \ 1 < \text{Fc}[\text{B}(\text{C}_6\text{F}_5)_2]_2 \ 2 < \text{B}(\text{C}_6\text{F}_5)_3$. Also, $\text{FcB}(\text{C}_6\text{F}_5)_2 \ 1 < \text{BF}_3 <$ cation $\text{Fc}^+ \text{B}(\text{C}_6\text{F}_5)_2 \ 7$. Electrochemical experiments showed the ordering of compounds by increasing half-wave potentials as: $\text{Fc}^+ \text{B}^-(\text{C}_6\text{F}_5)_3 \ 5 < \text{Fc}[\text{B}(\text{C}_6\text{F}_5)_2 \text{PMe}_3]_2 \ 15 < \text{FcB}(\text{C}_6\text{F}_5)_2 \text{PMe}_3 \ 3 < \text{FcB}(\text{C}_6\text{F}_5)_2 \ 1 < \text{Fc}[\text{B}(\text{C}_6\text{F}_5)_2]_2 \ 2$.

Many of the compounds mentioned are easily stored and handled under inert gas conditions. The industrial importance of **1** and **2** and their derivatives has yet to be developed, but academically we can learn a great deal from these systems. Moreover, these boranes have shed some light on plausible directions for future study of highly Lewis acidic molecules.

2.8 Future Considerations

Experiments to isolate an ionic compound containing the reactive cation **7** should be continued. A one-electron oxidant with a weakly coordinating anion is required to reach this goal.

Work should be continued in the area of anion binding for borane **2**. A better understanding of the size and type of anion that can be accommodated and the structures that can be formed would prove informative in addressing some still unanswered questions.

Generation of a zwitterionic one-electron oxidant for the activation of Cp_2ZrMe_2 by cleavage of a Zr-Me bond with electron withdrawing groups should be investigated. The σ -donation of electron density into the attached Cp ring from the $\text{B}(\text{C}_6\text{F}_5)_3$ group decreases the ability of **5** to oxidise a Zr-Me bond. Attachment of electron withdrawing groups (C_6F_5) to the Cp rings should aid the oxidising ability of the iron(III) centre to effect activation with a zwitterionic compounds. Deck reports the preparation of 1,1'-bis(pentafluorophenyl)ferrocene.¹⁰³ Borylation of this ferrocene and then formation of a zwitterion similar to **5** should afford the desired activation. Electronic tuning of ferrocenes can allow for new and exciting chemistry to occur with this well-known metallocene framework.

3 Chapter 3: Experimental Methods

3.1 General Considerations

All reactions were carried out under an argon atmosphere either on a double manifold high vacuum line or in an Innovative Technology System One dry box. Air sensitive materials were stored and manipulated in the dry box. Argon gas was purified by passage through an Oxisorb-W scrubber purchased from Matheson Gas Products. Standard inert atmosphere, Schlenk, vacuum line and glove box techniques were used throughout, under prepurified argon.¹⁰⁴ The most common specialty glassware used was the thick-wall glass bomb, needle valve and the swivel frit assembly. The thick-walled glass bomb refers to a thick walled Pyrex tube closed at one end with a rounded bottom and joined to a 5mm Kontes Teflon stopcock at the other end; a female joint (24/40) was fused to the stopcock which allowed simple manipulations on a high vacuum line. Various size bombs were available in different diameters and lengths to accommodate different reaction scales. Glassware used in anhydrous reactions was stored in a drying oven at 75°C overnight prior to transfer into the glove box antechamber and evacuation or assembled warm and evacuated on the high vacuum line prior to use. NMR tube scale reactions were routinely accomplished by placing measured amounts of the reagents into an dry NMR tube in the dry box to which was added a small amount of the deuterate solvent of choice.

Nuclear magnetic resonance (NMR) spectra were obtained from solutions in either *d*₂-methylene chloride (CD₂Cl₂), *d*₆-benzene or *d*₈-toluene on either a Bruker AMX400 (¹H 400.132 MHz, ¹³C{¹H} 100.623 MHz), Bruker AMX300 (¹H 300.138

MHz, ^{11}B 96.293 MHz, ^{19}F 282.371 MHz), Varian XL200 (^{13}C 50.310 MHz, ^{11}B 64.184 MHz, ^{31}P 80.988 MHz), Bruker ACE-200 (^1H 200.134 MHz) spectrometer. All ^1H NMR spectra, ^{13}C NMR spectra, ^{11}B NMR spectra, ^{19}F NMR spectra and ^{31}P NMR spectra were collected in d_2 -methylene chloride (CD_2Cl_2) at 200.134 MHz, 100.623 MHz, 64.184 MHz, 282.371 MHz and 80.988 MHz, respectively, unless otherwise stated. ^1H NMR spectra were referenced to the tetramethylsilane (SiMe_4) through the residual ^1H residual signal of CH_2Cl_2 (δ 5.32 ppm), benzene (δ 7.15 ppm), and the methyl group of toluene (δ 2.09 ppm). ^{13}C NMR spectra were referenced to SiMe_4 through the deuterium coupled signal of CD_2Cl_2 (δ 54.00 ppm), d_6 -benzene (δ 128.39 ppm), and the methyl group of d_8 -toluene (δ 20.4 ppm). ^{11}B NMR spectra were externally referenced to borane trifluoride diethyl etherate (δ 0.0 ppm), prior to acquisition of the first spectrum. ^{19}F NMR spectra were externally referenced to CFCl_3 (δ 0.00 ppm) through the an external standard of hexafluorobenzene (δ -163.0 ppm)¹⁰⁵ in d_6 -benzene prior to the acquisition of the first spectrum. ^{31}P NMR spectra were reference to the external standard H_3PO_4 in deuterium oxide (δ 0.00 ppm) prior to the acquisition of the first spectrum. ^1H NMR spectra are listed according to the following format: δ chemical shift (ppm) (multiplicity, number of protons, J = coupling constant (Hz), assignment). ^{13}C NMR spectra are listed according to the following format: chemical shift (ppm) (multiplicity, J = coupling constant (Hz), assignment). ^{11}B NMR are listed according to the following format: chemical shift (ppm) (multiplicity, WHM = width at half maximum (Hz) or J = coupling constant (Hz)). ^{31}P NMR spectra are listed according to the following format: chemical shift (ppm) (multiplicity, WHM = width at half maximum (Hz) or J = coupling constant (Hz)).

Elemental analyses were performed by Mrs. Dorothy Fox (University of Calgary) on a Control Equipment Corporation 440 Elemental Analyzer. X-ray crystallographic structures were determined by Dr. Masood Parvez (University of Calgary), Dr. Bob MacDonald (University of Alberta) and Dr. Glen Yap (University of Ottawa).

Cooling baths consisting of dry ice/acetone (-78°C) were used routinely for cooling receiving vessels to collect solvents transferred under vacuum or to maintain to cool reaction temperatures for a short period of time.

Solvents and reagents were purified according to standard methods.¹⁰⁶ Toluene, tetrahydrofuran (THF) and hexanes were purified using the Grubbs purification system¹⁰⁷ and stored in solvent pots over an appropriate drying agent (titanocene¹⁰⁸ for hexanes and toluene, sodium/benzophenone ketyl for THF) under vacuum. Benzene and *d*₆-benzene (C₆D₆) were dried over sodium/benzophenone ketyl in a glass bomb under vacuum. Methylene chloride (CH₂Cl₂), *d*₂-methylene chloride (CD₂Cl₂), *d*₈-toluene, hexamethyldisiloxane, and acetonitrile (CH₃CN) were dried and stored in a glass bombs over calcium hydride (CaH₂) under vacuum. Diethyl ether (Et₂O) was predried over lithium aluminum hydride then stored over sodium/benzophenone ketyl in a glass bomb under vacuum. α, α, α -Trifluorotoluene (TFT) was predried over phosphorus pentoxide (P₂O₅) and stored over CaH₂ in a glass bomb under vacuum. 1,2-Dichloroethane (ClCH₂CH₂Cl) was purified over P₂O₅ and dried over basic alumina, and stored over CaH₂, in that order. Deuterated solvents were purchase from Cambridge Isotopes Laboratories and dried appropriately.

All chemicals were purchased from the Aldrich Chemical Company unless otherwise stated. Tris(pentafluorophenyl)borane (B(C₆F₅)₃),¹¹ purchased from Boulder

Scientific Company, was dried by stirring the solid with chlorodimethylsilane (Me_2SiHCl) under argon for 1 hour, then the volatiles were removed *in vacuo*. The dried $\text{B}(\text{C}_6\text{F}_5)_3$ was then sublimed under dynamic vacuum at an oil bath temperature of 50-60°C. Ferrocene (FcH) was prepared by a literature procedure⁴ or purchased from Boulder Scientific Company; purification of ferrocene was achieved by sublimation under dynamic vacuum at 55°C. Literature procedures were used to prepare the following reagents: *bis*-(pentafluorophenyl)chloroborane ($\text{ClB}(\text{C}_6\text{F}_5)_2$),⁵⁰ *bis*-(pentafluorophenyl)borane ($\text{HB}(\text{C}_6\text{F}_5)_2$),⁴⁸ lithium *tetrakis*-(pentafluorophenyl)borate etherate ($\text{LiB}(\text{C}_6\text{F}_5)_4 \cdot \text{Et}_2\text{O}$),⁹⁵ pentafluorophenyl silver(I) (AgC_6F_5),⁹⁰ chloromericuricferrocene (FcHgCl),⁵¹ 1,1'-*bis*-(chloromericuric)ferrocene ($\text{Fc}[\text{HgCl}]_2$),⁵¹ 1,1'-*bis*-(dibromoboryl)ferrocene ($\text{Fc}[\text{BBr}_2]_2$),^{24,27} 1,1'-dilithioferrocene(TMEDA) ($\text{FcLi}_2 \cdot \text{TMEDA}$),¹⁰⁹ and acetylferrocenium tetrafluoroborate ($[\text{FcAc}]^+[\text{BF}_4]^-$).⁹¹ Base free *bis*-(pentafluorophenyl)zinc ($\text{Zn}(\text{C}_6\text{F}_5)_2$) was prepared⁹⁷ and used a C_6F_5 ring transfer reagent.¹¹⁰

Electrochemical measurements were made by cyclic voltammetry of TFT solutions under argon at 25°C, using a three electrode air tight cell attached to a Hitek Instruments of England Potentiostat Type DT2101 and Waveform Generator PPRI system. The electrolyte:substrate concentrations were approximately 100:1. The electrolyte, tetrabutylammonium *tetrakis*(pentafluorophenyl)borate [$n\text{-Bu}_4\text{N}^+[\text{B}(\text{C}_6\text{F}_5)_4]$] was not commercially available but prepared by an unpublished procedure provided to us by Dr. W. Geiger (University of Vermont). An airtight electrochemical cell consisting of a thick-walled glass bulb, Kontes Teflon tap, a set of platinum wire electrodes (working and secondary) and a silver wire (Ag-wire) quasi-reference electrode, was used. Each

experiment consisted of collecting the data for the substrate alone, then referenced to the ferrocene/ferrocenium couple in this medium.

The ultraviolet/visible spectra were obtained from dilute sample (typically $\sim 2.0 \times 10^{-4}$ M) in dry $\text{ClCH}_2\text{CH}_2\text{Cl}$ using a Cary 5E UV/Visible and Infrared Spectrometer. The samples were prepared in volumetric flasks in the dry box and transferred to a 1 mm pathlength air tight cell fused to a Kontes Teflon tap. A background spectrum of the solvent was collected and automatically subtracted from the spectrum collected of the substrate. The solvent used for all UV/Vis spectra was from the same dried batch. Conversion of the absorptivity (A) to the molar absorptivity (ϵ) was by the relation $\epsilon = A/lc$ where l is the pathlength of the cell ($l = 1\text{mm}$) and c is the concentration of the sample (mol/L or M).

Degassing of solvents occurred by the freeze-pump-thaw technique (repeated three times): cooling of the solvent pot to freeze the solvent within; any gas in the headspace was removed by evacuation from the frozen vessel; warming to allow the solid to melt and dissolved gas to escape into the headspace of the vessel.

3.2 Preparation of Mono-borylated Ferrocene and Related Compounds

3.2.1 Preparation of *Bis*-(pentafluorophenyl)borylferrocene $\text{FcB}(\text{C}_6\text{F}_5)_2$ (1).

3.2.1.1 Method A - Direct Borylation of Ferrocene

Ferrocene (FcH) (1.90 g, 10.2 mmol) and $\text{HB}(\text{C}_6\text{F}_5)_2$ (3.45 g, 9.98 mmol) were placed into a dry 100 mL round bottomed flask (RBF) which was fitted with a frit assembly, in the dry box. The flask was cooled to -78°C and dry toluene (60 mL) was condensed into it under vacuum transfer conditions. Upon warming slowly to 80°C

under argon the reaction was stirred for an additional 22.5 h under argon opened to a mercury bubbler. The reaction mixture was cooled and the toluene was removed under vacuum to afford a dark maroon solid. Dry hexanes were condensed in to extract 1 from any unreacted $\text{HB}(\text{C}_6\text{F}_5)_2$ by filtration. The hexanes were removed under vacuum to afford a crimson red crystalline solid. Excess ferrocene was removed from the product by sublimation (55°C under full vacuum). Yield of 1: 4.39 g (8.28 mmol, 91%). X-ray quality crystals were grown from a saturated solution of 1 in dry hexamethyldisiloxane cooled to -35°C on standing or two days. ^1H NMR (C_6D_6): 4.51 (t, 2H, $J = 1.8$ Hz, H_β); 4.03 (s, 5H, C_5H_5); 3.95 (bs, 2H, H_α). $^{13}\text{C}\{\text{H}\}$ NMR (50 MHz, C_6D_6): 145.9 (d, $^1J_{\text{CF}} = 242$ Hz); 141.9 (d, $^1J_{\text{CF}} = 242$ Hz); 137.7 (d, $^1J_{\text{CF}} = 251$ Hz); 115.0 (bs, WHM = 87 Hz, $\text{C}_{ipso}(\text{C}_6\text{F}_5)$); 79.5 (s, WHM = 7.4 Hz, C_β); 77.7 (s, WHM = 8 Hz, C_α); 70.5 (s, WHM = 7.4 Hz, C_5H_5). $^{11}\text{B}\{\text{H}\}$ NMR (96 MHz, C_6D_6): 53.7 (bs, WHM = 650 Hz). $^{19}\text{F}\{\text{H}\}$ NMR (282 MHz, C_6D_6): -129.3 (dd, 4F, F_o); -152.5 (t, 2F, F_p); -161.7 (dt, 4F, F_m). UV (TFT) λ_{max} , nm (ϵ): 231 (1.33×10^4). Anal. Calcd for $\text{C}_{22}\text{H}_9\text{BF}_{10}\text{Fe}$: C, 49.86; H, 1.71. Found: 49.69; H, 1.90.

3.2.1.2 Method B - Mercury Salt Metathesis Route

I-(Chloromericuric)ferrocene FcHgCl (2.403 g, 5.32 mmol) and $\text{ClB}(\text{C}_6\text{F}_5)_2$ (1.987 g, 5.23 mmol) were placed into a 100 mL bomb. Dry hexanes (80 mL) were condensed under vacuum transfer conditions, back filled with argon and sealed. The mixture was slowly warmed to room temperature and stirred for an additional 22 h. The orange chalky suspension changed to a dark maroon solution with a green/grey precipitate (HgCl_2). The suspension was cannula-transferred under argon flow into a 100 mL RBF and filtered to extracted 1 from the mercury chloride (HgCl_2) solid. The HgCl_2

was washed with hexanes until the washings were colourless. The solvent was removed *in vacuo* to afford the maroon solid 1. Yield: 2.461 g (4.64 mmol, 87%). The crude 1 was subjected to sublimation to remove any residual ClB(C₆F₅)₂.

3.2.1.3 Method C – “Friedel-Crafts” Type Borylation

Into a 25 mL RBF, fitted with a frit assembly, was loaded FcH (109 mg, 0.586 mmol), ClB(C₆F₅)₂ (222 mg, 0.583 mmol) and aluminum trichloride (AlCl₃) (90 mg, 0.675 mmol) in the dry box. The flask was cooled to -78°C and evacuated. Dry CH₂Cl₂ (10 mL) was added by vacuum transfer and the flask was warmed slowly to room temperature under argon, opened to a mercury bubbler. The mixture was stirred for an additional 75 min at which time the solvent was removed *in vacuo*. Dry hexanes (15 mL) were condensed into the flask and the mixture was sonicated and filtered. The solids collected were washed with hexanes until the washings were colourless. Removal of hexanes afforded a viscous oily residue that was taken up into C₆D₆ for NMR analysis. 1 was present by ¹H NMR in the complex mixture formed.

3.2.2 Preparation of Ferrocenium Bis-(pentafluorophenyl)(trifluoromethane-sulfonyl)borate (Fc⁺B⁻(C₆F₅)₂OTf) (4)

Silver trifluoromethanesulfonate (245 mg, 0.953 mmol) and 1 (505 mg, 0.953 mmol) were placed into a 50 mL RBF fitted with a frit assembly. The flask was evacuated and cooled to -78°C. Dry CH₂Cl₂ (25 mL) was condensed under vacuum transfer conditions. The flask was then backfilled with argon, warmed to room temperature and stirred under argon for two hours. The solution changed from maroon to navy blue immediately. The reaction mixture was filtered with a grey residue remaining on the frit (silver metal) and the solvent was removed under vacuum to afford 585 mg

(0.858 mmol, 90%) of a paramagnetic dark blue solid of high purity by ^{19}F NMR. Crystals of **4** were grown at 25°C when dissolved into a minimum amount of dry CH_2Cl_2 onto which was placed a layer of dry hexane. A single crystal was selected for X-ray diffraction structure determination. ^1H NMR: 42.0 (bs, WHM = 2780 Hz), 33.1 (bs, WHM = 2500 Hz), 30.1 (bs, WHM = 1050 Hz). $^{13}\text{C}\{^1\text{H}\}$ NMR: 142.9 (d, $^1J_{\text{CF}} = 245$ Hz); 137.7 (d, $^1J_{\text{CF}} = 257$ Hz); 133.0 (d, $^1J_{\text{CF}} = 241$ Hz); 92.1 (bs, C_{ipso}). $^{11}\text{B}\{^1\text{H}\}$ NMR: -4.75 (bs, WHM = 394 Hz). $^{19}\text{F}\{^1\text{H}\}$ NMR: -89.6 (s, 3F, CF_3); -155.8 (bs, 4F, F_o); -159.6 (s, 2F, F_p); -165.8 (s, 4F, F_m). UV (TFT) λ_{max} , nm (ϵ): 256 (1.42 x 10⁴). Anal. Calcd for $\text{C}_{23}\text{H}_9\text{BF}_{13}\text{FeO}_3\text{S}$: C, 40.68; H, 1.34. Found: C, 40.51; H, 1.13.

3.2.3 Preparation of Ferrocenium Tris(pentafluorophenyl)borate ($\text{Fc}^+\text{B}^-(\text{C}_6\text{F}_5)_3$)

(5)

Pentafluorophenyl silver(I) (AgC_6F_5) (614 mg, 2.23 mmol) and **1** (1.183 g, 2.23 mmol) were placed into a 100 mL bomb to which was added 50 mL of dry toluene. The vessel was sealed and warmed to 100°C in an oil bath for 23.5 h. The flask was cooled to room temperature and the green solution was cannula-transferred to a two neck RBF with a frit assembly under an argon flow. The toluene was removed under vacuum and CH_2Cl_2 was condensed in at -78°C. The green solution was extracted from the silver powder by filtration and washed until the extracts were colourless. The solvent was removed *in vacuo* to afford a dark green solid. Yield: 1.397 g (2.00 mmol, 90%). Crystals of **5** were grown at 25°C when dissolved into a minimum amount of dry CH_2Cl_2 onto which was placed a layer of dry hexane. A single crystal was selected for X-ray diffraction structure determination. ^1H NMR (300 MHz, d_6 -toluene): 43.8 (bs, WHM = 1150 Hz); 30.2 (bs, WHM = 1400 Hz); 24.2 (bs, WHM = 780 Hz). $^{13}\text{C}\{^1\text{H}\}$ NMR:

142.7 (d, 4C, $^1J_{CF} = 225$ Hz); 139.3 (d, 2C, $^1J_{CF} = 246$ Hz, C_p); 133.6 (d, 4C, $^1J_{CF} = 246$ Hz). $^{11}\text{B}\{\text{H}\}$ NMR: -23.7 (bs, 55 Hz). $^{19}\text{F}\{\text{H}\}$ NMR: -139.6 (bs, 6F, F_o); -161.0 (s, 3F, F_p); -167.8 (d, 6F, F_m). UV (TFT) λ_{max} , nm (ϵ): 258 (1.33 $\times 10^4$). Anal. Calcd for $\text{C}_{28}\text{H}_9\text{BF}_{15}\text{Fe}$: C, 48.24; H, 1.30. Found: C, 48.25; H, 1.30.

3.2.4 Preparation of Cobaltocenium Ferrocenyl Tris(pentafluorophenyl)borate (6)

Zwitterion **5** (420 mg, 0.619 mmol) and cobaltocene CoCp_2 (117 mg, 0.619 mmol) were placed into a 25 mL RBF fitted with a frit assembly in the dry box. The system was evacuated and dry CH_2Cl_2 (12 mL) was condensed in at -78°C. The solution was warmed slowly under argon and stirred at room temperature for 130 min. Filtration and washing of the residue on the frit afforded, after removal of the solvent *in vacuo*, a shiny/brown crystalline foam. Yield: 490 mg (0.564 mmol, 91%). ^1H NMR: 5.60 (s, 10H, $\text{Co}(\text{C}_5\text{H}_5)$); 4.00 (t, 2H, $J = 1.68$ Hz, H_β); 3.94 (bs, 2H, H_α); 3.67 (s, 5H, $\text{Fe}(\text{C}_5\text{H}_5)$). $^{13}\text{C}\{\text{H}\}$ NMR: 149.3 (d, $^1J_{CF} = 246$ Hz); 138.4 (d, $^1J_{CF} = 245$ Hz, C_p); 137.0 (d, $^1J_{CF} = 258$ Hz); 85.2 (s, $\text{Co}(\text{C}_5\text{H}_5)$); 75.9 (s, C_α); 68.3 (s, $\text{Fe}(\text{C}_5\text{H}_5)$); 67.0 (s, C_β). $^{11}\text{B}\{\text{H}\}$ NMR: -13.19 (bs, WHM = 39 Hz). $^{19}\text{F}\{\text{H}\}$ NMR: -128.3 (d, 6F, F_o); -164.5 (dt, 3F, F_p); -168.0 (t, 6F, F_m). Anal. Calcd for $\text{C}_{38}\text{H}_{19}\text{BCoF}_{15}\text{Fe}$: C, 51.51; H, 2.16. Found: C, 51.30; H, 2.34.

3.2.5 Preparation of Bis-(pentafluorophenyl)borylferrocene Trimethylphosphine adduct $\text{FcB}(\text{C}_6\text{F}_5)_2\cdot\text{PMe}_3$ (3)

Borane **1** (394 mg, 0.743 mmol) was placed into a 25 mL RBF, cooled to -196°C and dry trimethylphosphine PMe_3 (>15 cmHg in a 115 cm³ bulb, excess) was condensed into the flask under vacuum conditions. The reaction was warmed to -78°C and then to room temperature and stirred for 1 h. The maroon solution changed colour to light

yellow on warming to -78°C. The solvent was removed *in vacuo* to afford a yellow powder. Yield: 443 mg (0.731 mmol, 98%). A single crystal was isolated from the NMR tube solution in *d*₈-toluene and the X-ray structure was determined. ¹H NMR (*d*₈-toluene): 4.15 (t, 2H, *J* = 1.80 Hz, *H*_β); 3.99 (s, 5H, Fe(C₅H₅)); 3.62 (bs, 2H, *H*_α); 0.47 (d, 9H, ²*J*_{PH} = 10.7 Hz, P(CH₃)₃). ¹³C{¹H} NMR (*d*₈-toluene): 148.1 (d, ¹*J*_{CF} = 234 Hz); 139.7 (d, ¹*J*_{CF} = 263 Hz, *C*_p); 137.7 (d, ¹*J*_{CF} = 246 Hz); 120.3 (bs, *C*_{ipso}(C₆F₅)); 80.2 (bs, *C*_{ipso}(C₅H₄)); 73.7 (s, *C*_α); 69.9 (s, *C*_β); 68.8 (s, Fe(C₅H₅)); 9.5 (d, ¹*J*_{CP} = 37 Hz, P(CH₃)₃). ¹¹B{¹H} NMR (*d*₈-toluene): -13.5 (d, ¹*J*_{BP} = 46 Hz). ¹⁹F NMR (*d*₈-toluene): -127.6 (d, 4F, *F*_o); -157.6 (t, 2F, *F*_p); -163.2 (dt, 4F, *F*_m). ³¹P NMR (*d*₈-toluene): -12.1 (d, ¹*J*_{PB} = 64 Hz).

3.2.6 Preparation of Fe⁺B⁻(C₆F₅)₂F (8)

Borane 1 (306 mg, 0.577 mmol) and nitrosonium tetrafluoroborate (NOBF₄) (65 mg, 0.557 mmol) were placed into a dry 50 mL bomb. The bomb was evacuated and cooled to -78°C dry CH₂Cl₂ (20 mL) was condensed in under vacuum transfer conditions. The solution was warmed slowly to room temperature under argon and sealed. The bomb was placed into a 60°C oil bath and stirred for 18 min. The heat was removed and the solution was degassed, after cooling it to room temperature. The solution was taken into the dry box where it was transferred to a 50 mL flask which was fitted with a frit assembly. The solvent was removed *in vacuo* and dry CH₂Cl₂ was condensed on top of the solid. Sonication and filtration afforded a dark blue solid on the frit, after solvent removal. Yield: 250 mg (0.405 mmol, 72%). Recrystallization was achieved by layering hexanes over a solution in CH₂Cl₂ and standing for 24 h. A single crystal was isolated and the structure was determined by X-ray crystallography. ¹H NMR: 33.1 (bs,

WHM = 1360 Hz, 2H); 28.0 (bs, WHM = 700 Hz, 5H, Fe(C₅H₅)); 30.1 (bs, WHM = 2150 Hz, 2H). ¹⁹F NMR: -157.1 (bs, 4F, F_o); -162.4 (t, 2F, F_p); -166.8 (bs, 4F, F_m).

3.2.7 Preparation of [FcB(C₆F₅)₂·PMe₃]⁺[BF₄]⁻ (12)

The borane adduct FcB(C₆F₅)₂·PMe₃ (208 mg, 0.343 mmol) and silver tetrafluoroborate (AgBF₄) (64 mg, 0.329 mmol) were placed into a 25 mL RBF fitted with a frit assembly in the dry box. The flask was cool to -78°C and dry CH₂Cl₂ (10 mL) was condensed in under vacuum transfer conditions. The solution turned dark green with a grey precipitate at low temperature. The flask was opened to argon and warmed slowly to room temperature and stirred for 75 min. The solid silver was filtered off and washed thoroughly. The solvent was removed from the green filtrate to afford a dark blue solid. Yield: 197 mg (0.283 mmol, 86%). The product was subjected to recrystallization by layering hexanes over a TFT solution and allowing to stand for 24 h. A single crystal was isolated for X-ray structure determination. ¹H NMR: 40.1 (bs, WHM = 1820 Hz); 27.9 (bs, WHM = 690 Hz); 1.29 (d, ²J_{PH} = 15 Hz, P(CH₃)₃). ¹¹B{¹H} NMR: -7.73 (s, WHM = 10.1 Hz, BF₄); -10.7 (bs, WHM 262 Hz, BPMe₃).

3.2.8 Reaction of 1 with Acetylferrocenium Tetrakis(pentafluorophenyl)borate

Borane 1 (262 mg, 0.494 mmol) and [FcAc]⁺[B(C₆F₅)₄]⁻ (440 mg, 0.485 mmol) were loaded into a dry 25 mL RBF fitted with a frit assembly in the dry box. The flask was cooled to -78°C and dry CH₂Cl₂ (15 mL) was condensed onto the solids under vacuum transfer conditions. The solution was warmed to room temperature under argon and stirred for an additional 80 min. The solvent was removed *in vacuo* to afford a violet solid which was triturated with dry hexanes, to remove any excess borane present, and filtered to collect the violet solid on the frit. The solid was washed with hexanes three

times. Yield of violet solid: 683 mg (0.475 mmol, 98%). ^1H NMR (300 MHz): 45.2 (bs, 2H, WHM = 1630 Hz, $\text{H}_{\alpha/\beta}$); 31.9 (bs, 5H, WHM = 900 Hz, BCpFe(C_5H_5)); 22.3 (bs, 2H, WHM = 1900 Hz, $\text{H}_{\alpha/\beta}$); 7.21 (s, 2H); 6.85 (s, 5H, AcCpFe(C_5H_5)); 2.15 (s, 3H, CH_3). ^{11}B NMR: -17.0 (s, WHM = 17.4 Hz, $B(\text{C}_6\text{F}_5)_4$). ^{19}F NMR: -149.8 (s, 1F); -151.2 (s, 2F); -153.4 (s, 1F); -158.9 (s, 1F); 164.8 (s, 1F); -133.2 (s, F_{α} , 8F); -162.4 (s, F_p , 4F); -167.2 (s, F_m , 8F). IR (cm^{-1}): 3123, 1644 (C=O), 1516, 1464, 1277, 1089, 979.

3.2.9 Reaction of 1 with Tetrabutylammonium Tetrafluoroborate $[\text{NBu}_4]^+[\text{BF}_4]^-$

Borane **1** (7 mg, 0.0132 mmol) and $[\text{NBu}_4]^+[\text{BF}_4]^-$ (48 mg, 0.146 mmol, 11.0 equiv) were loaded into a dry NMR tube and dissolved in dry CD_2Cl_2 (ca. 0.5 mL). The NMR tube was sealed and shaken. The ^1H NMR spectrum was collected and indicated that no reaction occurred; the proton signals for borane **1** remained unchanged.

3.3 Preparation of Bis-borylated Ferrocene and Related Compounds

3.3.1 Preparation of 1,1'-*Bis*-(*bis*-(pentafluorophenyl)boryl)ferrocene $\text{Fc}[\text{B}(\text{C}_6\text{F}_5)_2]_2$ (2)

3.3.1.1 Method A - Mercury Salt Metathesis Route

1,1-*Bis*-(chloromercuric)ferrocene **13** (1.47 g, 2.24 mmol) and $\text{ClB}(\text{C}_6\text{F}_5)_2$ (1.70 g, 4.48 mmol, 2.0 equiv) were placed into a 100 mL bomb under argon. The bomb was evacuated and cooled to -78°C to which was added dry hexanes (50 mL) under vacuum transfer conditions. The bomb was backfilled with argon, sealed and warmed slowly to 60°C in an oil bath and stirred for 72 h. The orange suspension of **13** was consumed and a dark maroon solution with a grey precipitate (HgCl_2) resulted. The warm product mixture was cannula-transferred to a 100 mL 2-neck RBF fitted with a frit assembly under argon. Filtration of the solution afforded a red/grey solid on the frit and a clear

maroon filtrate. The solid was washed with hexanes until the washings were colourless. The solvent was removed under vacuum and the resulting oily maroon solid was recrystallized from a minimum amount of hot hexamethyldisiloxane which was cooled in the freezer to -35°C. Yield: 537 mg (0.605 mmol, 27 %). ¹H NMR (300 MHz, C₆D₆): 4.75 (t, 4H, ³J_{HH} = 1.6 Hz, H_β); 4.39 (bs, 4H, WHM = 5.4 Hz, H_α). ¹³C{¹H} NMR (C₆D₆): 145.7 (d, ¹J_{CF} = 244 Hz); 142.5 (d, ¹J_{CF} = 256 Hz, C_p); 137.8 (d, ¹J_{CF} = 253 Hz); 114.1 (bs, C_{ipso}(C₆F₅)); 80.0 (s, C_β); 79.1 (s, C_α); 75.1 (bs, C_{ipso}(C₅H₅)). ¹¹B{¹H} NMR (C₆D₆): not observable. ¹⁹F NMR (C₆D₆): -129.8 (d, 8F, F_o); -150.0 (t, 4F, F_p), -160.7 (dt, 8F, F_m). Anal. Calcd for C₃₄H₈B₂F₂₀Fe: C, 46.73; H, 0.92. Found: C, 46.35; H, 0.61. UV (TFT) λ_{max}, nm (ε): 233 (1.64 × 10⁴).

3.3.1.2 Method B - Zinc Salt Metathesis Route

1,1'-*Bis*-(dibromoboryl)ferrocene (909 mg, 1.731 mmol) and Zn(C₆F₅)₂ (1.432 g, 3.584 mmol, 2.07 equiv) were placed into a 100 mL bomb to which was added, at -78°C under vacuum transfer condition, dry hexanes (70 mL). The vessel was sealed, after being backfilled with argon, and warmed to 100°C in an oil bath for 12 h. The colour changed from red to maroon with a grey precipitate. The mixture was transferred via cannula into a 100 mL RBF fitted with a frit assembly. Filtration and washing, until colourless, of the grey solid afforded a maroon solution. Removal of the solvent afforded a dark maroon solid. Yield 1.400 g (92%). Subjected to sublimation to remove any residual Zn(C₆F₅)₂. The product (containing four C₆F₅ rings) was difficult to purify from lesser ring-substituted boranes by recrystallization or sublimation.

3.3.2 Preparation of 1,1'-*Bis*-(trimethylphosphino-*bis*-(pentafluorophenyl)boryl)-ferrocene $\text{Fc}[\text{B}(\text{C}_6\text{F}_5)_2\text{PMe}_3]_2$ (15)

A solution of **2** (100 mg, 0.114 mmol) in hexanes was cooled to -78°C and an excess of trimethylphosphine (150 mmHg in a 35.1 cm³ bulb, 0.285 mmol, 2.5 equiv) was vacuum transferred into the vessel. Upon warming to room temperature, the maroon solution quickly turned colour to a yellow suspension; stirring continued for an additional 60 min. The solvent was removed along with the unreacted PMe₃ under vacuum to afford 107 mg (85%) of a yellow powder. A d₈-toluene solution was prepared for NMR analysis from which was isolated a single crystal for X-ray diffraction analysis. ¹H NMR (400 MHz, d₈-toluene): 4.29 (s, 4H, H _{β}); 3.62 (s, 4H, H _{α}); 0.41 (d, 18H, ²J_{PH} = 10.6 Hz, CH₃). ¹³C{¹H} NMR (d₈-toluene): 147.9 (d, ¹J_{CF} = 239 Hz); 139.6 (d, ¹J_{CF} = 246 Hz, C _{ρ}); 137.6 (d, ¹J_{CF} = 264 Hz); 120.1 (bs, C_{ipso}(C₆F₅)); 73.9 (s, C _{α}); 72.2 (s, C _{β}); 9.1 (d, ¹J_{CP} = 37 Hz, CH₃). ¹¹B{¹H} NMR (d₈-toluene): -13.4 (d, WHM = 190 Hz). ¹⁹F NMR (d₈-toluene): -127.5 (d, 8F, F _{σ}); -157.3 (t, 4F, F _{ρ}); -163.3 (dt, 8F, F _{m}). ³¹P NMR (d₈-toluene): -14.5 (bs).

3.3.3 Preparation of 1,1'-*Bis*-(chloromercuric)ferrocene ($\text{Fc}[\text{HgCl}]_2$) (13)

To a solution of $\text{FcLi}_2\bullet\text{TMEDA}$ (1.60 g, 5.90 mmol) dissolved in dry THF (50 mL) in a 100 mL RBF, fitted with a needle valve, was added a solution of mercuric chloride (3.53 g, 13.0 mmol, 2.2 equiv) in dry THF (15 mL) via cannula under argon. The clear orange solution immediately turned chalky orange upon addition of mercuric chloride. The orange suspension was stirred for 24h under argon. The 100 mL RBF was attached to an argon-flushed frit assembly. The orange solid was collected by filtration and washed with dry THF until washings were colourless. Removal of the solvent under

vacuum afforded an insoluble orange product overnight. Yield: 3.23 g (4.90 mmol, 83%). $\text{Fc}[\text{HgCl}]_2$ is insoluble in most solvents which is in accordance with literature.⁵¹ There was no trace of FcHgCl by $^1\text{H-NMR}$. NMR data not available due to the high insolubility of the $\text{Fc}[\text{HgCl}]_2$.

3.4 Preparation of other reagents

3.4.1 Preparation of Tetrabutylammonium Tetrakis(pentafluorophenyl)borate (16)[†]

A solution of lithium etherate tetrakis(pentafluorophenyl)borate $\text{Li}(\text{Et}_2\text{O})_{2.3}\text{B}(\text{C}_6\text{F}_5)_4$ (8.623 g, 10.01 mmol) dissolved in water (150 mL) was added dropwise by syringe to a solution of tetrabutylammonium bromide Bu_4NBr (3.165 g, 9.817 mmol) in wet methanol (50 mL) with stirring. A white precipitate formed as the lithium salt was added. The mixture was stirred at ambient temperature for an additional 60 minutes and filtered to collect the white solid. The solid was air dried overnight and then taken up into a minimum amount of methylene chloride; diethyl ether was added to encourage recrystallisation. Colourless cubic crystals were collected after two days at -5°C. The mother liquor was concentrated again and subjected to the same recrystallisation regime. The purified product was crushed to afford a white powder and dried by *in vacuo* at 70°C. Yield: 7.024 g (7.65 mmol, 78 %). ^1H (400 MHz): 3.04 (m, 2H, $\text{NCH}_2\text{CH}_2\text{CH}_2\text{CH}_3$); 1.59 (m, 2H, $\text{NCH}_2\text{CH}_2\text{CH}_2\text{CH}_3$); 1.39 (m, 2H, $\text{NCH}_2\text{CH}_2\text{CH}_2\text{CH}_3$); 0.99 (t, 3H, $^3J_{\text{HH}} = 7.3$ Hz, $\text{NCH}_2\text{CH}_2\text{CH}_2\text{CH}_3$). $^{13}\text{C}\{^1\text{H}\}$ NMR:

[†] We would like to thank Dr. W. Gieger at the University of Vermont for sharing this unpublished result with us.

59.7 (s, NCH₂CH₂CH₂CH₃); 24.3 (s, NCH₂CH₂CH₂CH₃); 20.2 (s, NCH₂CH₂CH₂CH₃); 13.7 (s, NCH₂CH₂CH₂CH₃). ¹⁹F NMR: -133.1 (t, 8F, *F_o*); -163.6 (t, 4F, *F_p*); -167.5 (t, 8F, *F_m*). Anal. Calcd for C₄₀H₃₆BF₂₀N: C, 52.14; H, 3.94; N, 1.52. Found: C, 51.95; H, 4.01; N, 1.59.

3.4.2 Preparation of Acetylferrocenium Tetrakis(pentafluorophenyl)borate (10)

Acetylferrocenium tetrafluoroborate **9** (298 mg, 0.946 mmol) and lithium tetrakis(pentafluorophenyl)borate etherate (843 mg, 0.947 mmol) were placed into a 50 mL RBF fitted with a frit assembly. Dry CH₂Cl₂ was added by vacuum transfer at -78°C, warmed to room temperature under argon and the solution was stirred for 12 h. Filtration removed the silver metal from the filtrate; the silver was washed with CH₂Cl₂ three times and the solvent was removed *in vacuo* to afford a fluffy blue solid. Yield: 794 mg (0.875 mmol, 92 %). ¹H NMR: 35.8 (bs, WHM = 750 Hz); 30.4 (bs, WHM = 1800 Hz); 0.89 (s, CH₃); -12.1 (bs, WHM = 120 Hz); 0.90 (s, 3H, COOCH₃). ¹³C{¹H} NMR: 147.5 (d, ¹J_{CF} = 242 Hz); 138.2 (d, ¹J_{CF} = 232 Hz); 135.9 (d, ¹J_{CF} = 232 Hz); 126.3 (bs, C_{ipso}(C₆F₅)). ¹¹B NMR: -16.9 (s, WHM = 28 Hz). ¹⁹F NMR: -135.6 (s, 8F, *F_o*); -164.4 (s, 4F, *F_p*); -169.4 (s, 8H, *F_m*). Anal. Calcd for C₃₆H₁₂BF₂₀FeO: C, 47.66; H, 1.33. Found: C, 46.88; H, 1.53.

3.5 Reactivity studies

3.5.1 Activation Studies with Dimethylzirconocene

3.5.1.1 General Procedure

Activation studies of Cp_2ZrMe_2 with borane or zwitterionic borate substrates were carried out on an NMR tube scale. The solids, Cp_2ZrMe_2 along with the potential activator substrate were placed into a dry NMR tube in the dry box. A deuterated NMR solvent was added and the tube was capped with a rubber septum or flame sealed, as required. The substrates tested were boranes 1 and 2 and zwitterions 4 and 5. The reaction with 1 proved fruitless as there was no change in the chemical shift of the borane or Cp_2ZrMe_2 , by ^1H NMR. There was also no apparent reaction between Cp_2ZrMe_2 and the C_6F_5 -zwitterion 5; Cp_2ZrMe_2 remained intact by ^1H -NMR. The results of 2 and 4 are reported below.

3.5.1.1.1 Borane 1

In the dry box 1 (12 mg, 0.023 mmol) and Cp_2ZrMe_2 (12 mg, 0.048 mmol) were load into a dry NMR tube, dissolved in d_6 -toluene (*ca.* 0.5 mL). The NMR tube was capped and shaken. The ^1H NMR spectrum was collected and there was no change in the signals for the starting materials.

3.5.1.1.2 Borane 2

In the dry box 2 (30 mg, 0.034 mmol, 1.08 equiv) and Cp_2ZrMe_2 (8 mg, 0.032

mmol) were loaded into a dry NMR tube and dissolved in d_6 -toluene (*ca.* 0.5 mL). The NMR tube was flame-sealed and shaken. The ^1H NMR spectrum was collected immediately and again after 21 h. There was a definite change and little starting material was observed after 21 h. ^1H NMR (d_6 -toluene): 5.69 (s, 10H, Zr(C₅H₅)); 4.62 (t, 2H, J = 1.8 Hz); 4.52 (t, 2H, J = 1.8 Hz); 4.37 (m, 2H), 4.14 (m, 2H), 0.82 (s, 3H, ZrCH₃); 0.26 (t, 3H, $^2J_{\text{HB}} = 4.0$ Hz, BC₂H₃).

3.5.1.1.3 Zwitterion 4

In the dry box 4 (45 mg, 0.066 mmol, 1.04 equiv) and Cp₂ZrMe₂ (16 mg, 0.064 mmol) were loaded into a dry NMR tube and dissolved in CD₂Cl₂ (*ca.* 0.5 mL). Bubbling (CH₃CH₃) was observed immediately from the solution, which changed colour from blue to maroon. The NMR tube was capped and shaken. After 2 h the ^1H NMR spectrum was collected and revealed a different Zr-species in solution. ^1H NMR: 6.37 (s, 10H, Zr(C₅H₅)); 0.58 (s, 3H, ZrCH₃). ^{19}F NMR: -78.1 (s, 3F, OSO₂CF₃).

3.5.1.1.4 Zwitterion 5

In the dry box the zwitterion **5** (61 mg, 0.088 mmol, 1.1 equiv) and Cp_2ZrMe_2 (20 mg, 0.080 mmol) were loaded into a dry NMR tube and dissolved in CD_2Cl_2 (*ca.* 0.5 mL). The NMR tube was flame-sealed and shaken. The ^1H NMR spectrum was collected after 2 h. There was no change in the Cp_2ZrMe_2 signals observed by ^1H NMR. Zwitterion **5** remained intact as observed by ^{11}B and ^{19}F NMR.

3.5.2 Borane **1** with Lewis Bases

3.5.2.1 General Procedure

Into an NMR tube was placed solid **1** (15 mg, 0.028 mmol). The Lewis base was added either by microsyringe, by weight or by vacuum transfer using a known volume bulb, as appropriate (1 mol equiv). The NMR solvent, d_6 -benzene (0.5 mL), was added and the tube was capped with a rubber septum or flame-sealed under a slight vacuum, and shaken. The solution remained unchanged, both visually and by ^1H NMR spectroscopy, for all the Lewis bases added (benzophenone, acetophenone, *N,N*-diisopropylbenzamide, FcAc, THF, CH_3CN , PMe_3) except for PMe_3 . CH_3CN reacted with the borane as the temperature was lowered but this binding was reversible.

3.5.2.1.1 Acetonitrile (CH_3CN)

There was no reaction with CH_3CN and **1** at room temperature in d_6 -benzene. There was also no reaction with CH_3CN (1.1 equiv) and **1** (1.0 equiv) at room temperature in d_6 -toluene (*ca.* 0.5 mL), but upon cooling this sample to -78°C the solution colour changed from maroon (uncomplexed **1**) to yellow. The maroon colour was restored as the sample started to warm to room temperature. A variable temperature ^1H NMR study of the toluene solution was carried out. The study qualitatively

demonstrates the binding of CH₃CN to the boron atom. A linear relationship exists between the temperature and δ of the signals monitored (Table 3-1).

Table 3-1: Variable temperature ¹H NMR data for the reaction of 1 and CH₃CN (1:1.1) in *d*₈-toluene.

Temperature (K)	$\delta(\text{CH}_3\text{CN})$ (ppm)	$\delta(\text{H}_\beta)$ (ppm)	$\delta(\text{H}_{\text{C}\beta})$ (ppm)
300	0.675	4.541	4.033
280	0.625	4.511	4.024
260	0.567	4.457	4.000
240	0.498	4.371	3.967
220	0.435	4.261	3.939
200	0.375	4.12	3.926

3.5.2.1.2 Trimethylphosphine (PMe₃)

An immediate reaction occurred as the phosphine condensed onto the *d*₈-toluene solution of 1. The NMR tube was flame-sealed, under a slight vacuum, and the maroon coloured solution turned yellow upon warming and shaking. The NMR data is consistent with that of the isolated product according to Section 3.2.5. Free PMe₃ was observed at δ 0.78 ppm (d, $^2J_{\text{PH}} = 2.4$ Hz) and bound PMe₃ at δ 0.47 ppm (d, $^2J_{\text{PH}} = 10.7$ Hz).

3.5.3 Borane 2 with Lewis Bases

3.5.3.1 General Procedure

Into an NMR tube were placed solid **2** and the Lewis base, either by microsyringe, by weight or by vacuum transfer using a known volume bulb, as appropriate (1 equiv). The NMR solvent, *d*₆-benzene (0.5 mL), was added, unless otherwise stated, and the tube was capped with a rubber septum or flame-sealed under a slight vacuum, and shaken. The solutions changed, both visually or spectrally by ¹H NMR, for all the Lewis bases added except for benzophenone and acetophenone.

3.5.3.1.1 Acetylferrocene

In the dry box **2** (20 mg, 0.023 mmol, 1.04 equiv) and FcAc (5 mg, 0.022 mmol) were loaded into a dry NMR tube and dissolved in CD₂Cl₂ (*ca.* 0.5 mL). The NMR tube was capped and shaken. ¹H NMR (300 MHz): 5.06 (s, 4H, H_β); 5.00 (s, 2H, FcAc(H_β)); 4.96 (s, 2H, FcAc(H_α)); 4.42 (s, 5H, FcAc(C₅H₅)); 4.30 (s, 4H, H_α); 2.29 (s, 3H, CH₃). ¹⁹F NMR: -129.9 (d, 8F, F_o); -158.8 (s, 4F, F_p); -162.5 (s, 8H, F_m).

3.5.3.1.2 Acetonitrile (14)

In the dry box **2** (26 mg, 0.030 mmol) and CH₃CN (1.6 μL, 0.031 mmol) were placed into a dry NMR tube and dissolved in C₆D₆ (*ca.* 0.5 mL). Upon capping and shaking the NMR tube the solution change to a light violet colour and a yellow precipitate slowly formed (*cf.* PMe₃ adduct formation of **1** and **2** in C₆D₆). ¹H NMR: indicated consumption of **2** only. ¹⁹F NMR (C₆D₆): -133.0 (d, 2F, F_o); -150.9 (bs, 1F, F_p); -161.0 (t, 2F, F_m).

3.5.3.1.3 Trimethylphosphine (15)

PMe_3 reacted immediately with **2** according to the procedure described in Section 3.3.1. A small scale NMR tube reaction was not carried out with PMe_3 .

3.5.4 Borane **2** with Anions X^-

3.5.4.1 General Procedure

Into an NMR tube was placed solid **2** (15 mg, 0.028 mmol) and the anion salt by weight as appropriate (1 mol equiv). An NMR solvent was added and the tube was capped with a rubber septum or flame-sealed under a slight vacuum, and shaken. There was no observed reaction of **2** with trityl methoxide, trityl pentafluorophenoxyde or trityl benzyl ether.

3.5.4.1.1 Reaction with Trityl Hydroxide In the dry box an NMR tube was loaded with **2** (22 mg, 0.024 mmol) and trityl hydroxide (6 mg, 0.023 mmol), dissolved in dry CD_2Cl_2 (*ca.* 0.5 mL). The tube was capped with a rubber septum and shaken. The maroon solution immediately turned green/brown upon mixing. A complex mixture was observed by ^1H and ^{19}F NMR with no clear indication of a major product formed.

3.5.4.1.2 Reaction with Tetraphenylphosphonium Chloride $[\text{Ph}_4\text{P}]^+[\text{Cl}]^-$

In the dry box **2** (17 mg, 0.195 mmol, 1.04 equiv) and (7 mg, 0.0187 mmol) were placed into a small vial and dissolved in CD_2Cl_2 . The vial was capped and shaken for 10 min and the colour changed from maroon to orange at room temperature. The solution was transferred to a dry NMR tube by a pipette. ^1H NMR: 7.91 (m, 4H, H_p); 7.75 (m, 8H, H_{m-or-o}); 7.61 (m, 8H, H_{m-or-o}); 4.15 (m, 4H, $H_{\alpha,\beta}$). $^{11}\text{B} \{^1\text{H}\}$ NMR: 3.39 (bs, WHM = XX Hz); 1.07 (bs). ^{19}F NMR: -133.0 (m, 2.03F, F_o); -131.3 (m, 2.03F, F_o); (m, 1.16F,

F_o); -134.6 (m, 1.09F, F_o); -155.3 (m, 1.00F, F_p); -161.5 (m, 0.51F, F_p); -162.0 (m, 0.57F, F_p); -164.3 (m, 2.44F, F_m); -166.5 (m, 1.12F, F_m); -167.0 (m, 1.74F, F_m).

3.5.4.1.3 Reaction with copper(II)methoxide ($\text{Cu}(\text{OMe})_2$)

In the dry box borane **2** (154 mg, 0.176 mmol) and copper(II) methoxide (11 mg, 0.876 mmol) were placed into a dry 25 mL bomb to which was added dry toluene (10 mL). The flask was fitted with a needle valve, sealed and warmed to 60°C over 72 h. The brown solution was cooled and the toluene was removed *in vacuo* to afford an oily solid. Further isolation was not carried out but d_8 -toluene was added to compare the ^1H NMR with that of a previous NMR tube scale reaction. ^1H NMR (300 MHz, d_8 -toluene): 5.80 (m, 2H); 4.68 (s, 2H); 4.32 (s, 2H); 4.21 (s, 2H); 3.40 (s, 4H, H_β); 3.35 (s, 4H, H_α); 1.33 (s, 3H, $\mu\text{-OCH}_3$); -3.66 (s, 3H); -7.02 (s, 3H).

3.6 General reaction of Lewis acids with crotonaldehyde¹⁴

In the dry box a known amount of Lewis acid was placed into a dry NMR tube, dissolved in a known amount of CD_2Cl_2 and capped with a rubber septum. The sample was cooled to -78°C to which dry crotonaldehyde was added *via* syringe to the NMR tube. The tube was quickly shaken to ensure mixing. The ^1H NMR spectrum was collected at -20°C; the crotonaldehyde signals are only reported.

3.6.1 $\text{FcB}(\text{C}_6\text{F}_5)_2$ (**1**) with crotonaldehyde

The above general procedure was followed for the reaction of an excess of **1** (64 mg, 0.121 mmol) with crotonaldehyde (1.0 μL , 0.13 mmol) in CD_2Cl_2 (0.46 mL). ^1H NMR (400 MHz, -20°C): 9.44 (d, 1H, $H1$); 7.42 (m, 1H, $H3$); 6.45 (m, 1H, $H2$); 2.19 (d, 3H, Me).

3.6.2 $\text{Fc}[\text{B}(\text{C}_6\text{F}_5)_2]_2$ (2) with crotonaldehyde

The above general procedure was followed for the reaction of an excess of 2 (57 mg, 0.065 mmol) with crotonaldehyde (0.6 μL , 0.0075 mmol) in CD_2Cl_2 (0.46 mL). ^1H NMR (400 MHz, -20°C): 9.08 (d, 1H, *H1*); 7.91 (m, 1H, *H3*); 6.89 (m, 1H, *H2*); 2.39 (d, 3H, Me).

3.6.3 BBr_3 with crotonaldehyde¹⁴

The above general procedure was followed for the reaction of an excess of BBr_3 (12 μL , 0.127 mmol) with crotonaldehyde (1.0 μL , 0.0125 mmol) in CD_2Cl_2 (0.46 mL). ^1H NMR (400 MHz, -20°C): 9.56 (d, 1H, *H1*); 8.35 (m, 1H, *H3*); 7.01 (m, 1H, *H2*); 2.50 (d, 3H, Me).

3.6.4 AlCl_3 with crotonaldehyde¹⁴

The above general procedure was followed for the reaction of an excess of AlCl_3 (18 mg, 0.135 mmol) with crotonaldehyde (1.0 μL , 0.0125 mmol) in CD_2Cl_2 (0.45 mL). ^1H NMR (400 MHz, -20°C): 9.23 (d, 1H, *H1*); 8.18 (m, 1H, *H3*); 6.87 (m, 1H, *H2*); 2.45 (d, 3H, Me).

3.6.5 SnCl_4 with crotonaldehyde¹⁴

The above general procedure was followed for the reaction of an excess of SnCl_4 (16 μL , 0.137 mmol) with crotonaldehyde (1.0 μL , 0.0125 mmol) in CD_2Cl_2 (0.45 mL). ^1H NMR (400 MHz, -20°C): 9.39 (d, 1H, *H1*); 7.71 (m, 1H, *H3*); 6.54 (m, 1H, *H2*); 2.26 (d, 3H, Me).

3.7 Electrochemical Experiments – Cyclic Voltammetry (CV)

In the dry box a known amount of electrolyte 16 $[n\text{Bu}_4\text{N}]^+[\text{B}(\text{C}_6\text{F}_5)_4]^-$ was dissolved into a minimum amount of dry TFT and added quantitatively to a volumetric

flask. This solution was diluted to a known volume with additional TFT. The electrolyte:substrate ratio was typically 100:1. The solution was mixed thoroughly and transferred to the electrochemical cell under argon. The Teflon tap was closed and an arbitrary amount of dry ferrocene was placed in the side arm. A 24/40 septum was placed into the ground-glass joint. Outside the dry box the electrochemical cell was attached to the potentiostat and the cyclic voltammetry (CV) data were collected appropriately. After the data for the substrate were collected the Teflon tap was opened to allow the ferrocene in the side arm to be added and dissolved by stirring. The stirring was halted and the CV data for the internal reference was collected along with the substrate. The ΔE value refers to the potential difference between the oxidation and reduction waves of the redox couple. The half-wave potential ($E_{1/2}$) of the substrate was referenced to that of the ferrocene/ferrocenium (Fc/Fc^+) redox couple; a silver wire quasi-reference electrode was employed in the airtight cell. The scan rate of the CV scan was 0.1 V s^{-1} at 25°C . The results are presented in Table 3-2.

Table 3-2: CV experiment data.

Substrate	[Substrate] (10^{-3} mol/L) ^a	[Electrolyte 16] (10^{-3} mol/L) ^a	$E_{1/2}(\text{substrate})$ (mV) ^b	$\Delta E(\text{substrate})$ (mV)
1	1.51	99.4	+450	104
2	0.915	99.4	+820	255
3	1.16	99.4	-100	90
15	0.975	99.6	-201	92
5	1.00	99.6	-472	83

^a Diluted to 10 mL in dry α,α,α -trifluorotoluene. ^b Compared to $E_{1/2}(\text{Fc}/\text{Fc}^+)$ set to 0 mV; internal reference. ^c $\Delta E(\text{substrate}) = E_{pc} - E_{pa}$ where E_{pc} and E_{pa} are the peak cathodic and anodic peak potentials, respectively.

3.8 Crystallographic Data Collection and results

The crystallographic data collection experimental details are reported in Appendix I for compounds **1**, **3**, **4**, **5**, **7**, **12** and **15**. The ORTEP diagrams are included in Chapter 2.

4 References

- (1) Kealy, T. J.; Pauson, P. L. *Nature* **1951**, *168*, 1039.
- (2) Miller, S. A.; Tebboth, J. A.; Tremaine, J. F. *J. Chem. Soc.* **1952**, 632.
- (3) Long, N. J. *Metallocenes: An Introduction to Sandwich Complexes*; 1 ed.; Blackwell Science: London, 1998.
- (4) Wilkinson, G. *Org. Synth.* **1956**, *36*, 31-35.
- (5) Rosenblum, M. *Chemistry of the Iron Group Metallocenes: Ferrocene, Ruthenocene, Osmocene*; John Wiley & Sons: New York, 1965; Vol. 1.
- (6) Togni, A.; Hayashi, T. *Ferrocenes: Homogeneous Catalysis, Organic Synthesis, Materials Science*; VCH: Weinheim, 1995.
- (7) Piers, W. E.; Chivers, T. *Chem. Soc. Rev.* **1997**, *26*, 345-354.
- (8) Ishihara, K.; Yamamoto, H. *Eur. J. Org. Chem.* **1999**, 527-538.
- (9) Chambers, R. D.; Chivers, T. *Organometal. Chem. Rev.* **1966**, *1*, 279-304.
- (10) Cohen, S. C.; Massey, A. G. *Adv. Fluorine Chem.* **1970**, *6*, 149.
- (11) Massey, A. G.; Park, A. J. *J. Organomet. Chem.* **1964**, *2*, 245-250.
- (12) Doerrter, L. H.; Green, M. L. H. *J. Chem. Soc. Dalton Trans.* **1999**, 4325-4329.
- (13) Massey, A. G.; Park, A. J. *J. Organomet. Chem.* **1966**, *5*, 218-225.
- (14) Childs, R. F.; Mulholland, D. L.; Nixon, A. *Can. J. Chem.* **1982**, *60*, 801-812.
- (15) Luo, L.; Marks, T. J. *Topic in Catalysis* **1999**, *7*, 97-106.
- (16) Yang, X.; Stern, C. L.; Marks, T. J. *J. Am. Chem. Soc.* **1991**, *113*, 3623-3625.
- (17) Jordan, R. F. *J. Chem. Ed.* **1988**, *65*, 285-289.
- (18) Jordan, R. F.; LaPointe, R. E.; Bajgur, C. S.; Echols, S. F.; Willett, R. *J. Am. Chem. Soc.* **1987**, *109*, 4111-4113.
- (19) Jordan, R. F.; Echols, S. F. *Inorg. Chem.* **1987**, *26*, 383-386.
- (20) Guram, A. S.; Jordan, R. F. *Cationic Organozirconium and Organohafnium Complexes*; Pergamon Press: Oxford, 1995; Vol. 4.
- (21) Herberhold, M. *Ferrocene Compounds Containing Heteroelements*; Togni, A. and Hayashi, T., Ed.; VCH: Weinheim, 1995, pp 219-278.
- (22) Ruf, W.; Fueller, M.; Siebert, W. *J. Organomet. Chem.* **1974**, *64*, C45-C47.
- (23) Renk, T.; Ruf, W.; Siebert, W. *J. Organomet. Chem.* **1976**, *120*, 1-25.
- (24) Ruf, W.; Renk, T.; Siebert, W. *Z. Naturforsch.* **1976**, *31b*, 1028-1034.
- (25) Kotz, J. C.; Post, E. W. *J. Am. Chem. Soc.* **1968**, *90*, 4503-4505.
- (26) Kotz, J. C.; Post, E. W. *Inorg. Chem.* **1970**, *9*, 1661-1669.

- (27) Wrackmeyer, B.; Dörfler, U.; Herberhold, M. *Z. Naturforsch.* **1993**, *48b*, 121-123.
- (28) Post, E. W.; Cooks, R. G.; Kotz, J. C. *Inorg. Chem.* **1970**, *9*, 1670-1677.
- (29) Lopez, T.; Campero, A. *J. Organomet. Chem.* **1989**, *378*, 91-98.
- (30) Wrackmeyer, B.; Dorfler, U.; Milius, W.; Herberhold, M. *Z. Naturforsch.* **1995**, *50b*, 201-204.
- (31) Cowan, D. O.; Shu, P.; Hedberg, F. L.; Rossi, M.; Kistenmacher, T. J. *J. Am. Chem. Soc.* **1979**, *101*, 1304-1306.
- (32) Jäkle, F.; Priermeier, T.; Wagner, M. *Chemische Berichte* **1995**, *128*, 1163-1169.
- (33) Jäkle, F.; Priermeier, T.; Wagner, M. *J. Chem. Soc., Chem. Commun.* **1995**, 1765-1766.
- (34) Herdtweck, E.; Jäkle, F.; Wagner, M. *Organometallics* **1997**, *16*, 4737-4745.
- (35) Knüppel, S.; Erker, G.; Fröhlich, R. *Angew. Chem. Int. Ed. Engl.* **1999**, *38*, 1923-1926.
- (36) Jäkle, F.; Mattner, M.; Priermeier, T.; Wagner, M. *J. Organomet. Chem.* **1995**, *502*, 123-130.
- (37) Jäkle, F.; Priermeier, T.; Wagner, M. *Organometallics* **1996**, *15*, 2033-2040.
- (38) Jäkle, F.; Polborn, K.; Wagner, M. *Chemische Berichte* **1996**, *129*, 603-606.
- (39) deBiani, F. F.; Jäkle, F.; Spiegler, M.; Wagner, M.; Zanello, P. *Inorganic Chemistry* **1997**, *36*, 2103-2111.
- (40) Fontani, M.; Peters, F.; Scherer, W.; Wachter, W.; Wagner, M.; Zanello, P. *Eur. J. Inorg. Chem.* **1998**, 1453-1465.
- (41) de Baini, F. F.; Gmeinwieser, T.; Herbtweck, E.; Jäkle, F.; Laschi, F.; Wagner, M.; Zanello, P. *Organometallics* **1997**, *16*, 4776-4787.
- (42) Wrackmeyer, B.; Dorfler, U.; Milius, W.; Herberhold, M. *Zeitschrift Fur Naturforschung Section B-a Journal of Chemical Sciences* **1996**, *51*, 851-858.
- (43) Foucher, D. A.; Tang, B.-Z.; Manners, I. *J. Am. Chem. Soc.* **1992**, *114*, 6246.
- (44) Herberich, G. E.; Fischer, A.; Wielbelhaus, D. *Organometallics* **1996**, *15*, 3106-3108.
- (45) Herberich, G. E.; Fischer, A. *Organometallics* **1996**, *15*, 58-67.
- (46) Duchateau, R.; Lancaster, S. J.; Thornton-Pett, M.; Bochmann, M. *Organometallics* **1997**, *16*, 4995-5005.
- (47) Herberich, G. E.; Englert, U.; Fischer, A.; Wiebelhaus, D. *Organometallics* **1998**, *17*, 4769-4775.
- (48) Parks, D. J.; Spence, R. E. v. H.; Piers, W. E. *Angew. Chem. Int. Ed. Engl.* **1995**, *34*, 809-811.
- (49) Cerichelli, G.; Floris, B.; Illuminati, G.; Ortaggi, G. *J. Org. Chem.* **1974**, *39*, 3948-3950.

- (50) Chambers, R. D.; Chivers, T. *J. Chem. Soc.* 1965, 3933-3939.
- (51) Fish, R. W.; Rosenblum, M. *J. Org. Chem.* 1965, 30, 1253-1254.
- (52) Slocum, D. W.; Ernst, C. R. *J. Org. Chem.* 1973, 38, 1620-1621.
- (53) Lupan, S.; Kapon, M.; Cais, M.; Herbstein, F. H. *Angew. Chem. Int. Ed. Engl.* 1972, 11, 1025-1027.
- (54) Horton, A. D.; de With, J. *Organometallics* 1997, 16, 5424-5436.
- (55) Deck, P. A.; Beswick, C. L.; Marks, T. J. *J. Am. Chem. Soc.* 1998, 120, 1771-1784.
- (56) Appel, A.; Jäkle, F.; Priermeier, T.; Schmid, R.; Wagner, M. *Organometallics* 1996, 15, 1188-1194.
- (57) Burtich, J. M.; Burk, J. H.; Leonowicz, M. E.; Hughes, R. E. *Inorg. Chem.* 1979, 18, 1702.
- (58) Appel, A.; Nöth, H.; Schmidt, M. *Chem. Ber.* 1995, 128, 621-626.
- (59) Herberhold, M.; Dörfler, U.; Milius, W.; Wrackmeyer, B. *J. Organomet. Chem.* 1995, 492, 59.
- (60) Wrackmeyer, B.; Dörfler, U.; Milius, W.; Herberhold, M. *Polyhedron* 1995, 14, 1425-1431.
- (61) Wrackmeyer, B.; Dörfler, U.; Milius, W.; Herberhold, M. *Z. Naturforsch., Teil B* 1995, 50, 201.
- (62) Allen, F. H.; Kennard, O. *Chemical Design Automation News* 1983, 8, 131-137.
- (63) Behrens, U. *Journal of Organometallic Chem.* 1979, 182, 89-98.
- (64) Olmstead, M. M.; Power, P. P.; Weese, K. J.; Doedens, R. J. *J. Am. Chem. Soc.* 1987, 109, 2541.
- (65) Zettler, F.; Hausen, H. D.; Hess, H. J. *J. Organomet. Chem.* 1974, 72, 157.
- (66) Blount, J. F.; Finocchiaro, P. *J. Am. Chem. Soc.* 1973, 95, 7019.
- (67) Atkins, P. W. *Physical Chemistry*; 4 ed.; W. H. Freeman and Company: New York, 1990.
- (68) Parks, D. J.; Piers, W. E.; Parvez, M.; Atencio, R.; Zaworotko, M. J. *Organometallics* 1008, 17, 1369-1377.
- (69) Parks, D. J.; Piers, W. E. *J. Am. Chem. Soc.* 1996, 118, 9440-9441.
- (70) Jacobsen, H.; Berke, H.; Doring, S.; Kehr, G.; Erker, G.; Frohlich, R.; Meyer, O. *Organometallics* 1999, 18, 1724-1735.
- (71) Nöth, H.; Wrackmeyer, B. *Nuclear Magnetic Resonance Spectroscopy of Boron Compounds*; Diehl, P., Flück, E. and Kosfeld, R., Ed.; Springer: Berlin, 1978; Vol. 14.
- (72) Barton, L.; Bould, J.; Fang, H.; Kupp, K.; Rath, N. P.; Gloeckner, C. *J. Am. Chem. Soc.* 1997, 119, 631.

- (73) Gonaghy, K. J.; Carroll, P. J.; Sneddon, L. G. *Inorg. Chem.* **1997**, *36*, 547.
- (74) Binger, P.; Sandmeyer, F.; Kruger, C.; Kuhnigk, J.; Goddard, R.; Erker, G. *Angew. Chem. Int. Ed. Engl.* **1994**, *33*, 197.
- (75) Makhaev, V. D.; Dzhafarov, M. K.; Baranetskaya, N. K.; Vil'chevskaya, V. D.; Batsanov, A. S.; Yanovsky, A. I.; Struchkov, Y. T. *Koord. Khim.* **1994**, *20*, 838.
- (76) Katoh, K.; Shimoi, M.; Ogino, H. *Inorg. Chem.* **1992**, *31*, 670.
- (77) Allcock, H. R.; Coggio, W. D.; Manners, I.; Parvez, M. *Organometallics* **1991**, *10*, 3090.
- (78) Shimoi, M.; Katoh, K.; Ogino, H. *J. Chem. Soc., Chem. Commun.* **1990**, 811.
- (79) Manners, I.; Coggio, W. D.; Mang, M. N.; Parvez, M.; Allcock, H. R. *J. Am. Chem. Soc.* **1989**, *111*, 3481.
- (80) MacNamara, W. F.; Duesler, E. N.; Paine, R. T.; Ortiz, J. V.; Kolle, P.; Noth, H. *Organometallics* **1986**, *5*, 380.
- (81) Angerer, W.; Sheldrick, W. S.; Malisch, W. *Chem. Ber.* **1985**, *118*, 1261.
- (82) Snow, S. A.; Shimoi, M.; Ostler, C. D.; Thompson, B. K.; Kodama, G.; Parry, R. W. *Inorg. Chem.* **1984**, *24*, 511.
- (83) Rheingold, A. L.; Landers, A. G. *J. Chem. Soc., Chem. Commun.* **1979**, 143-144.
- (84) Mammano, N. J.; Zalkin, A.; Landers, A.; Rheingold, A. L. *Inorg. Chem.* **1977**, *16*, 297-300.
- (85) Churchill, M. R.; Landers, A. G.; Reingold, A. L. *Inorg. Chem.* **1981**, *20*, 849-853.
- (86) Paulus, E. F.; Schafer, L. *J. Organomet. Chem.* **1987**, 205.
- (87) Reis Jr., A. H.; Preston, L. D.; Williams, J. M.; Peterson, S. W.; Candela, G. A.; Schwartzendruber, L. T.; J. S. Miller 1979, 2756. *J. Am. Chem. Soc.* **1979**, *101*, 2756.
- (88) Miller, J. S.; Reis Jr., A. H.; Gebert, E.; Ritsko, J. J.; Salaneck, W. R.; Kovnat, L.; Cape, T. W.; Duyne, R. P. V. *J. Am. Chem. Soc.* **1979**, 7111.
- (89) Bats, J. W.; de Boer, J. J.; Bright, D. *Inorg. Chem.* **1971**, *5*, 605.
- (90) Sun, K. K.; Miller, W. T. *J. Am. Chem. Soc.* **1970**, *92*, 6985-6987.
- (91) Connelly, N. G.; Geiger, W. E. *Chem. Rev.* **1996**, *96*, 877-910.
- (92) Harlan, C. J.; Hascall, T.; Fujita, E.; Norton, J. R. *J. Am. Chem. Soc.* **1999**, *121*, 7274-7275.
- (93) Irvine, G.; Williams, V. C.; Piers, W. E., manuscript in progress for *J. Am. Chem. Soc.*
- (94) Witting, G.; Raff, P. *Liebigs Ann. Chem.* **1951**, 573, 195-209.
- (95) Lambert, J. B.; Zhang, S.; Ciro, S. M. *Organometallics* **1994**, *13*, 2430-2443.

- (96) Ratcliffe, C. T.; Shreeve, J. n. M. *Inorg. Synth.* **1968**, *II*, 194-200.
- (97) Sartori, P.; Weidenbruch, M. *Chem. Ber.* **1967**, *100*, 3016.
- (98) Clegg, W., personal communication by email.
- (99) Williams, V. C.; Piers, W. E.; Clegg, W.; Elsegood, M. R. J.; Collins, S.; Marder, T. B. *J. Am. Chem. Soc.* **1999**, *121*, 3244-3245.
- (100) Köhler, K.; Piers, W. E.; Jarvis, A. P.; S. Xin; Feng, T.; Bravakis, A. M.; Collins, S.; Clegg, W.; Yap, G. P. A.; Marder, T. B. *Organometallics* **1998**, *17*, 3557-3566.
- (101) Dormond, A.; Dachour, A. *J. Organomet. Chem.* **1980**, *193*, 321-3.
- (102) Jaquith, J. B.; Guan, J.; Wang, S.; Collins, S. *Organometallics* **1995**, *14*, 1079-1081.
- (103) Deck, P. A.; Jackson, W. F.; Fronczek, F. R. *Organometallics* **1996**, *15*, 5287-5291.
- (104) Burger, B. J.; Bercaw, J. E. *Experimental Organometallic Chemistry*; Wayda, A. L. and Daresbourg, M. Y., Ed.; American Chemical Society: Washington, DC, 1987.
- (105) Harris, R. K.; Mann, B. E. *NMR and the Periodic Table*; Academic Press: New York, 1978, pp 99.
- (106) Perrin, D. D.; Armarego, W. L. F. *Purification of Laboratory Chemicals*; 3 ed.; Pergamon Press: Toronto, 1998.
- (107) Pangborn, A. B.; Giardello, M. A.; Grubbs, R. H.; Rosen, R. K.; Timmers, F. J. *Organometallics* **1996**, *15*, 1518.
- (108) Marvich, R. H.; Brintzinger, H. H. *J. Am. Chem. Soc.* **1971**, *93*, 2046.
- (109) Rausch, M. D.; Ciappinelli, D. J. *J. Organomet. Chem.* **1967**, *10*, 127-136.
- (110) Sun, Y.; Spence, R. E. v. H.; Piers, W. E.; Parvez, M.; Yap, G. P. A. *J. Am. Chem. Soc.* **1997**, *119*, 5132-5143.

5 Appendix I: Crystal Structure Data

5.1 Table 5-1: Crystal Data Collection and Refinement Parameters for 1, 3, 4 and 5.

	1	3	4	5
formula	C ₂₂ H ₉ BF ₁₀ Fe	C ₂₅ H ₁₈ BF ₁₀ FeP	C ₂₃ H ₉ BF ₁₃ FeO ₃ S	C ₂₈ H ₉ BF ₁₅ Fe
fw	529.95	606.03	679.01	697.01
cryst system	orthorhombic	monoclinic	monoclinic	monoclinic
a, (Å)	9.758(1)	10.899(3)	10.909(3)	15.9529(13)
b, (Å)	11.994(1)	12.953(2)	12.896(4)	10.0171(7)
c, (Å)	33.255(4)	17.012(3)	17.017(5)	16.5882(3)
α, °	90	90	90	90
β, °	90	92.95(2)	95.177(6)	111.1394(5)
γ, °	90	90	90	90
V, Å ³	3892.2(7)	2398.5(8)	2384(1)	2472.4(2)
space group	P2 ₁ 2 ₁ 2 ₁	P2 ₁ /n	P2 ₁ /c	P2 ₁ /n
Z	8	4	4	4
F(000)	2096	1216	1340	1372
d _{calc} , mg m ⁻³	1.809	1.678	1.892	1.872
μ, mm ⁻¹	0.878	7.86	0.85	7.43
R		0.055		0.035
R _w		0.053		0.032
R1	0.0373		0.0327	
wR2	0.0616		0.0621	
gof	1.008	2.07	1.082	1.26

5.2 Table 5-2: Crystal Data Collection and Refinement Parameters for 7, 13 and 15.

	7	12	15
formula	C ₂₂ H ₉ BF ₁₁ Fe	C ₃₈ H ₃₇ F ₁₇ B ₂ PFe	C ₄₀ H ₂₆ B ₂ F ₂₀ FeP ₂
fw	548.95	808.97	1026.02
cryst system	triclinic	triclinic	monoclinic
a, (Å)	12.226(2)	11.349(5)	11.1605(9)
b, (Å)	13.1790(10)	16.823(5)	20.7099(18)
c, (Å)	14.123(4)	10.064(6)	16.7151(12)
α, °	109.40(2)	96.56(4)	90
β, °	108.87(2)	114.46(4)	102.0813(16)
γ, °	93.150(9)	99.80(3)	90
V, Å ³	1997.1(9)	1686.7(13)	3960.3(5)
space group	<i>P</i> 1	<i>P</i> - <i>I</i>	P2 ₁ /c (No. 14)
Z	4	2	4
F(000)	1084	814	
d _{calc} , mg m ⁻³	1.826	1.593	1.721
μ, mm ⁻¹	7.113	0.604	0.589
R	0.063		
R _w	0.033		
R1		0.1221	0.0439
wR2		0.3233	0.0890
gof	2.73	1.186	0.852

5.3 Crystal Data Obtained for 1

Table 5-3: Atomic Parameters x, y, z and U(eq) for 1.

	<u>x</u>	<u>y</u>	<u>z</u>	<u>U(eq)</u>
Fe1	0.42711(4)	0.68915(3)	0.877212(10)	0.02700(9)
Fe2	1.13226(4)	0.19225(3)	0.869653(10)	0.02807(9)
B1	0.6932(3)	0.8008(2)	0.87351(8)	0.0259(6)
B2	0.8647(3)	0.3037(2)	0.87494(8)	0.0268(6)
C1	0.8514(3)	0.8446(2)	0.81581(7)	0.0298(6)
C2	0.8930(3)	0.8862(2)	0.77913(8)	0.0373(7)
C3	0.8079(3)	0.9592(2)	0.75942(8)	0.0360(7)
C4	0.6855(3)	0.9882(2)	0.77563(8)	0.0359(7)
C5	0.6466(3)	0.9434(2)	0.81248(7)	0.0312(6)
C6	0.7272(3)	0.86877(19)	0.83321(7)	0.0253(6)
C7	0.8512(3)	0.7927(2)	0.93592(7)	0.0348(7)
C8	0.9079(3)	0.8342(2)	0.97109(8)	0.0440(8)
C9	0.8588(4)	0.9319(3)	0.98679(8)	0.0462(8)
C10	0.7563(3)	0.9888(2)	0.96757(9)	0.0435(8)
C11	0.7054(3)	0.9474(2)	0.93202(8)	0.0343(7)
C12	0.7491(3)	0.8475(2)	0.91494(7)	0.0290(6)
C13	0.6347(2)	0.6856(2)	0.86933(7)	0.0245(5)
C14	0.5637(3)	0.6444(2)	0.83423(8)	0.0294(6)
C15	0.4853(3)	0.5500(2)	0.84515(8)	0.0336(7)
C16	0.5039(3)	0.5313(2)	0.88689(8)	0.0311(6)
C17	0.5935(3)	0.6132(2)	0.90199(8)	0.0308(6)
C18	0.3505(3)	0.8468(2)	0.88851(9)	0.0404(7)
C19	0.3196(3)	0.7743(2)	0.92060(9)	0.0453(8)
C20	0.2415(3)	0.6856(3)	0.90544(11)	0.0546(9)
C21	0.2231(3)	0.7024(3)	0.86425(10)	0.0516(8)
C22	0.2920(3)	0.8012(3)	0.85333(9)	0.0433(7)
C23	0.9032(3)	0.4298(2)	0.94097(7)	0.0320(6)
C24	0.8590(3)	0.4671(2)	0.97802(8)	0.0413(7)
C25	0.7376(4)	0.4300(2)	0.99317(9)	0.0461(8)
C26	0.6599(3)	0.3538(2)	0.97241(9)	0.0452(8)
C27	0.7070(3)	0.3193(2)	0.93535(8)	0.0348(6)
C28	0.8290(3)	0.35407(19)	0.91813(7)	0.0277(6)
C29	0.8602(3)	0.4709(2)	0.82362(7)	0.0309(6)
C30	0.8191(3)	0.5205(2)	0.78833(8)	0.0365(7)
C31	0.7238(3)	0.4687(2)	0.76480(8)	0.0385(7)
C32	0.6689(3)	0.3681(2)	0.77632(9)	0.0376(7)
C33	0.7153(3)	0.3200(2)	0.81126(8)	0.0325(6)

C34	0.8130(3)	0.3677(2)	0.83616(7)	0.0276(6)
C35	0.9228(2)	0.1883(2)	0.87128(7)	0.0276(5)
C36	0.9814(3)	0.1236(2)	0.90378(8)	0.0308(6)
C37	1.0625(3)	0.0372(2)	0.88729(8)	0.0353(7)
C38	1.0594(3)	0.0476(2)	0.84476(8)	0.0351(7)
C39	0.9752(3)	0.1382(2)	0.83455(8)	0.0302(6)
C40	1.2498(3)	0.2976(3)	0.90377(9)	0.0461(8)
C41	1.3255(3)	0.2007(3)	0.89332(10)	0.0498(8)
C42	1.3323(3)	0.1949(3)	0.85132(10)	0.0531(8)
C43	1.2620(3)	0.2873(2)	0.83526(9)	0.0469(8)
C44	1.2124(3)	0.3507(2)	0.86751(9)	0.0413(7)
F1	0.93847(16)	0.77622(13)	0.83536(5)	0.0442(4)
F3	0.84704(19)	1.00217(14)	0.72344(5)	0.0583(5)
F4	0.6026(2)	1.05914(15)	0.75584(5)	0.0566(5)
F5	0.52372(16)	0.97407(14)	0.82711(5)	0.0500(5)
F6	0.90182(16)	0.69636(14)	0.92175(4)	0.0479(4)
F7	1.0117(2)	0.78013(16)	0.98915(5)	0.0663(6)
F8	0.9113(2)	0.97170(15)	1.02123(5)	0.0705(6)
F9	0.7087(2)	1.08488(14)	0.98319(5)	0.0648(6)
F10	0.60775(18)	1.00729(12)	0.91305(5)	0.0498(5)
F11	1.02377(17)	0.46858(13)	0.92737(5)	0.0465(4)
F12	0.9351(2)	0.54166(14)	0.99891(5)	0.0638(5)
F13	0.6935(2)	0.46863(16)	1.02905(5)	0.0748(6)
F14	0.54246(19)	0.31568(17)	0.98775(5)	0.0681(5)
F15	0.62745(17)	0.24736(13)	0.91489(5)	0.0494(4)
F16	0.95263(16)	0.52525(12)	0.84626(5)	0.0434(4)
F17	0.8717(2)	0.61811(13)	0.77618(5)	0.0547(5)
F18	0.68427(18)	0.51611(15)	0.72998(5)	0.0577(5)
F19	0.57277(18)	0.31918(17)	0.75357(5)	0.0618(5)
F2	1.01500(19)	0.85722(16)	0.76345(5)	0.0611(5)
F20	0.65981(17)	0.22024(13)	0.82138(5)	0.0498(5)

Table 5-4: Hydrogen Parameters x, y, z and U(eq) for 1.

	<u>x</u>	<u>y</u>	<u>z</u>	<u>U(eq)</u>
H14	0.5695	0.6768	0.8069	0.035
H15	0.4259	0.5059	0.827	0.04
H16	0.4592	0.4719	0.9029	0.037
H17	0.6233	0.6202	0.9303	0.037
H18	0.4045	0.9165	0.8902	0.048
H19	0.348	0.7844	0.9489	0.054
H20	0.2044	0.6227	0.9213	0.066

H21	0.1708	0.6533	0.8459	0.062
H22	0.2963	0.8339	0.826	0.052
H36	0.9668	0.1374	0.9328	0.037
H37	1.1152	-0.0188	0.9027	0.042
H38	1.1095	-0.0005	0.8255	0.042
H39	0.9552	0.1641	0.8069	0.036
H40	1.2289	0.3238	0.9313	0.055
H41	1.3666	0.1468	0.9124	0.06
H42	1.3789	0.136	0.8356	0.064
H43	1.2506	0.3048	0.8064	0.056
H44	1.1588	0.4205	0.8652	0.05

Table 5-5: Interatomic Distances (Å) and Angles (°) for 1.**Distances:**

Fe(1)-C(14)	2.027(3)	B(2)-C(28)	1.596(3)
Fe(1)-C(17)	2.036(3)	C(1)-C(6)	1.374(3)
Fe(1)-C(20)	2.040(3)	C(1)-C(2)	1.378(3)
Fe(1)-C(21)	2.043(3)	C(2)-C(3)	1.373(4)
Fe(1)-C(13)	2.043(2)	C(3)-C(4)	1.356(4)
Fe(1)-C(22)	2.043(3)	C(4)-C(5)	1.391(3)
Fe(1)-C(19)	2.056(3)	C(5)-C(6)	1.376(3)
Fe(1)-C(15)	2.060(2)	C(7)-C(12)	1.382(4)
Fe(1)-C(16)	2.062(2)	C(7)-C(8)	1.386(4)
Fe(1)-C(18)	2.067(3)	C(8)-C(9)	1.370(4)
Fe(2)-C(39)	2.033(3)	C(9)-C(10)	1.369(4)
Fe(2)-C(36)	2.033(3)	C(10)-C(11)	1.375(4)
Fe(2)-C(35)	2.045(2)	C(11)-C(12)	1.393(3)
Fe(2)-C(41)	2.045(3)	C(13)-C(14)	1.444(3)
Fe(2)-C(42)	2.046(3)	C(13)-C(17)	1.448(3)
Fe(2)-C(40)	2.049(3)	C(14)-C(15)	1.414(3)
Fe(2)-C(43)	2.052(3)	C(15)-C(16)	1.418(3)
Fe(2)-C(38)	2.050(2)	C(16)-C(17)	1.407(4)
Fe(2)-C(44)	2.057(2)	C(18)-C(19)	1.409(4)
Fe(2)-C(37)	2.065(3)	C(18)-C(22)	1.412(4)
F(1)-C(1)	1.348(3)	C(19)-C(20)	1.402(4)
F(2)-C(2)	1.345(3)	C(20)-C(21)	1.396(4)
F(3)-C(3)	1.358(3)	C(21)-C(22)	1.411(4)
F(4)-C(4)	1.346(3)	C(23)-C(24)	1.380(3)
F(5)-C(5)	1.346(3)	C(23)-C(28)	1.388(3)
F(6)-C(7)	1.343(3)	C(24)-C(25)	1.362(4)

F(7)-C(8)	1.344(3)	C(25)-C(26)	1.374(4)
F(8)-C(9)	1.343(3)	C(26)-C(27)	1.379(4)
F(9)-C(10)	1.347(3)	C(27)-C(28)	1.386(4)
F(10)-C(11)	1.350(3)	C(29)-C(30)	1.375(3)
F(11)-C(23)	1.344(3)	C(29)-C(34)	1.385(3)
F(12)-C(24)	1.354(3)	C(30)-C(31)	1.366(4)
F(13)-C(25)	1.351(3)	C(31)-C(32)	1.374(4)
F(14)-C(26)	1.335(3)	C(32)-C(33)	1.374(4)
F(15)-C(27)	1.345(3)	C(33)-C(34)	1.386(3)
F(16)-C(29)	1.343(3)	C(35)-C(36)	1.448(3)
F(17)-C(30)	1.341(3)	C(35)-C(39)	1.454(3)
F(18)-C(31)	1.346(3)	C(36)-C(37)	1.414(3)
F(19)-C(32)	1.340(3)	C(37)-C(38)	1.420(3)
F(20)-C(33)	1.356(3)	C(38)-C(39)	1.405(3)
B(1)-C(13)	1.501(4)	C(40)-C(44)	1.411(4)
B(1)-C(12)	1.584(4)	C(40)-C(41)	1.420(4)
B(1)-C(6)	1.604(4)	C(41)-C(42)	1.400(4)
B(2)-C(35)	1.501(4)	C(42)-C(43)	1.409(4)
B(2)-C(34)	1.583(4)	C(43)-C(44)	1.401(4)

Angles:

C(14)-Fe(1)-C(17)	69.05(10)	F(7)-C(8)-C(9)	120.4(3)
C(14)-Fe(1)-C(20)	154.53(13)	F(7)-C(8)-C(7)	120.3(3)
C(17)-Fe(1)-C(20)	120.81(12)	C(9)-C(8)-C(7)	119.3(3)
C(14)-Fe(1)-C(21)	120.84(12)	F(8)-C(9)-C(10)	120.0(3)
C(17)-Fe(1)-C(21)	153.77(12)	F(8)-C(9)-C(8)	119.7(3)
C(20)-Fe(1)-C(21)	39.99(12)	C(10)-C(9)-C(8)	120.3(3)
C(14)-Fe(1)-C(13)	41.56(9)	F(9)-C(10)-C(9)	119.9(3)
C(17)-Fe(1)-C(13)	41.58(9)	F(9)-C(10)-C(11)	121.1(3)
C(20)-Fe(1)-C(13)	159.83(12)	C(9)-C(10)-C(11)	119.0(3)
C(21)-Fe(1)-C(13)	160.17(11)	F(10)-C(11)-C(10)	117.7(2)
C(14)-Fe(1)-C(22)	108.93(11)	F(10)-C(11)-C(12)	118.9(2)
C(17)-Fe(1)-C(22)	165.07(12)	C(10)-C(11)-C(12)	123.4(3)
C(20)-Fe(1)-C(22)	67.65(13)	C(7)-C(12)-C(11)	115.1(2)
C(21)-Fe(1)-C(22)	40.38(12)	C(7)-C(12)-B(1)	121.3(2)
C(13)-Fe(1)-C(22)	127.14(11)	C(11)-C(12)-B(1)	123.6(2)
C(14)-Fe(1)-C(19)	164.18(12)	C(14)-C(13)-C(17)	105.6(2)
C(17)-Fe(1)-C(19)	110.20(12)	C(14)-C(13)-B(1)	124.9(2)
C(20)-Fe(1)-C(19)	40.05(12)	C(17)-C(13)-B(1)	126.0(2)
C(21)-Fe(1)-C(19)	67.19(13)	C(14)-C(13)-Fe(1)	68.61(14)
C(13)-Fe(1)-C(19)	127.34(12)	C(17)-C(13)-Fe(1)	68.94(14)

C(22)-Fe(1)-C(19)	67.46(12)	B(1)-C(13)-Fe(1)	110.20(17)
C(14)-Fe(1)-C(15)	40.48(10)	C(15)-C(14)-C(13)	109.0(2)
C(17)-Fe(1)-C(15)	68.11(11)	C(15)-C(14)-Fe(1)	71.02(15)
C(20)-Fe(1)-C(15)	117.76(13)	C(13)-C(14)-Fe(1)	69.83(13)
C(21)-Fe(1)-C(15)	102.83(12)	C(14)-C(15)-C(16)	108.0(2)
C(13)-Fe(1)-C(15)	69.10(10)	C(14)-C(15)-Fe(1)	68.50(14)
C(22)-Fe(1)-C(15)	120.62(11)	C(16)-C(15)-Fe(1)	69.96(14)
C(19)-Fe(1)-C(15)	155.02(11)	C(17)-C(16)-C(15)	108.6(2)
C(14)-Fe(1)-C(16)	68.15(10)	C(17)-C(16)-Fe(1)	68.92(14)
C(17)-Fe(1)-C(16)	40.16(10)	C(15)-C(16)-Fe(1)	69.80(14)
C(20)-Fe(1)-C(16)	103.40(12)	C(16)-C(17)-C(13)	108.9(2)
C(21)-Fe(1)-C(16)	117.28(12)	C(16)-C(17)-Fe(1)	70.92(15)
C(13)-Fe(1)-C(16)	68.91(10)	C(13)-C(17)-Fe(1)	69.48(13)
C(22)-Fe(1)-C(16)	154.07(12)	C(19)-C(18)-C(22)	107.6(3)
C(19)-Fe(1)-C(16)	122.17(11)	C(19)-C(18)-Fe(1)	69.57(15)
C(15)-Fe(1)-C(16)	40.24(10)	C(22)-C(18)-Fe(1)	69.00(15)
C(14)-Fe(1)-C(18)	127.44(11)	C(20)-C(19)-C(18)	108.2(3)
C(17)-Fe(1)-C(18)	128.61(11)	C(20)-C(19)-Fe(1)	69.39(17)
C(20)-Fe(1)-C(18)	67.33(12)	C(18)-C(19)-Fe(1)	70.47(15)
C(21)-Fe(1)-C(18)	67.37(12)	C(21)-C(20)-C(19)	108.3(3)
C(13)-Fe(1)-C(18)	113.64(11)	C(21)-C(20)-Fe(1)	70.12(17)
C(22)-Fe(1)-C(18)	40.17(11)	C(19)-C(20)-Fe(1)	70.57(17)
C(19)-Fe(1)-C(18)	39.96(11)	C(20)-C(21)-C(22)	108.2(3)
C(15)-Fe(1)-C(18)	159.14(11)	C(20)-C(21)-Fe(1)	69.89(17)
C(16)-Fe(1)-C(18)	160.55(11)	C(22)-C(21)-Fe(1)	69.82(15)
C(39)-Fe(2)-C(36)	69.25(10)	C(21)-C(22)-C(18)	107.8(3)
C(39)-Fe(2)-C(35)	41.77(9)	C(21)-C(22)-Fe(1)	70.83(15)
C(36)-Fe(2)-C(35)	41.60(10)	C(18)-C(22)-Fe(1)	70.83(15)
C(39)-Fe(2)-C(41)	158.71(11)	F(11)-C(23)-C(24)	117.5(2)
C(36)-Fe(2)-C(41)	118.20(12)	F(11)-C(23)-C(28)	119.9(2)
C(35)-Fe(2)-C(41)	155.79(12)	C(24)-C(23)-C(28)	122.5(3)
C(39)-Fe(2)-C(42)	123.61(12)	F(12)-C(24)-C(25)	120.2(3)
C(36)-Fe(2)-C(42)	149.74(12)	F(12)-C(24)-C(23)	120.0(3)
C(35)-Fe(2)-C(42)	164.17(12)	C(25)-C(24)-C(23)	119.7(3)
C(41)-Fe(2)-C(42)	40.02(11)	F(13)-C(25)-C(24)	119.5(3)
C(39)-Fe(2)-C(40)	159.47(11)	F(13)-C(25)-C(26)	119.8(3)
C(36)-Fe(2)-C(40)	110.22(11)	C(24)-C(25)-C(26)	120.8(3)
C(35)-Fe(2)-C(40)	123.98(11)	F(14)-C(26)-C(25)	120.6(3)
C(41)-Fe(2)-C(40)	40.60(12)	F(14)-C(26)-C(27)	121.7(3)
C(42)-Fe(2)-C(40)	67.75(13)	C(25)-C(26)-C(27)	117.7(3)
C(39)-Fe(2)-C(43)	108.80(11)	F(15)-C(27)-C(26)	116.9(3)
C(36)-Fe(2)-C(43)	169.39(11)	F(15)-C(27)-C(28)	118.7(2)
C(35)-Fe(2)-C(43)	130.11(11)	C(26)-C(27)-C(28)	124.4(3)

C(41)-Fe(2)-C(43)	67.56(13)	C(27)-C(28)-C(23)	114.8(2)
C(42)-Fe(2)-C(43)	40.22(12)	C(27)-C(28)-B(2)	116.5(2)
C(40)-Fe(2)-C(43)	67.71(12)	C(23)-C(28)-B(2)	128.8(2)
C(39)-Fe(2)-C(38)	40.26(10)	F(16)-C(29)-C(30)	117.6(2)
C(36)-Fe(2)-C(38)	68.39(11)	F(16)-C(29)-C(34)	119.2(2)
C(35)-Fe(2)-C(38)	69.18(10)	C(30)-C(29)-C(34)	123.1(3)
C(41)-Fe(2)-C(38)	121.11(12)	F(17)-C(30)-C(31)	119.1(3)
C(42)-Fe(2)-C(38)	102.92(12)	F(17)-C(30)-C(29)	121.6(3)
C(40)-Fe(2)-C(38)	159.99(12)	C(31)-C(30)-C(29)	119.4(3)
C(43)-Fe(2)-C(38)	117.34(12)	F(18)-C(31)-C(30)	119.7(3)
C(39)-Fe(2)-C(44)	124.15(11)	F(18)-C(31)-C(32)	120.0(3)
C(36)-Fe(2)-C(44)	131.98(11)	C(30)-C(31)-C(32)	120.3(3)
C(35)-Fe(2)-C(44)	113.73(11)	F(19)-C(32)-C(31)	120.0(3)
C(41)-Fe(2)-C(44)	67.48(13)	F(19)-C(32)-C(33)	121.6(3)
C(42)-Fe(2)-C(44)	67.19(12)	C(31)-C(32)-C(33)	118.4(3)
C(40)-Fe(2)-C(44)	40.22(11)	F(20)-C(33)-C(32)	116.7(2)
C(43)-Fe(2)-C(44)	39.87(11)	F(20)-C(33)-C(34)	119.4(2)
C(38)-Fe(2)-C(44)	154.20(12)	C(32)-C(33)-C(34)	123.9(3)
C(39)-Fe(2)-C(37)	68.14(11)	C(29)-C(34)-C(33)	114.7(2)
C(36)-Fe(2)-C(37)	40.37(10)	C(29)-C(34)-B(2)	124.9(2)
C(35)-Fe(2)-C(37)	69.03(11)	C(33)-C(34)-B(2)	120.4(2)
C(41)-Fe(2)-C(37)	103.83(12)	C(36)-C(35)-C(39)	105.5(2)
C(42)-Fe(2)-C(37)	114.41(13)	C(36)-C(35)-B(2)	125.6(2)
C(40)-Fe(2)-C(37)	125.62(12)	C(39)-C(35)-B(2)	125.6(2)
C(43)-Fe(2)-C(37)	149.54(11)	C(36)-C(35)-Fe(2)	68.74(14)
C(38)-Fe(2)-C(37)	40.37(10)	C(39)-C(35)-Fe(2)	68.67(14)
C(44)-Fe(2)-C(37)	165.31(11)	B(2)-C(35)-Fe(2)	110.99(17)
C(13)-B(1)-C(12)	122.5(2)	C(37)-C(36)-C(35)	108.9(2)
C(13)-B(1)-C(6)	118.0(2)	C(37)-C(36)-Fe(2)	71.06(15)
C(12)-B(1)-C(6)	118.4(2)	C(35)-C(36)-Fe(2)	69.66(14)
C(35)-B(2)-C(34)	120.1(2)	C(36)-C(37)-C(38)	108.1(2)
C(35)-B(2)-C(28)	120.3(2)	C(36)-C(37)-Fe(2)	68.56(14)
C(34)-B(2)-C(28)	118.7(2)	C(38)-C(37)-Fe(2)	69.22(15)
F(1)-C(1)-C(6)	118.7(2)	C(39)-C(38)-C(37)	108.7(2)
F(1)-C(1)-C(2)	117.5(2)	C(39)-C(38)-Fe(2)	69.22(14)
C(6)-C(1)-C(2)	123.8(2)	C(37)-C(38)-Fe(2)	70.41(15)
F(2)-C(2)-C(3)	121.0(3)	C(38)-C(39)-C(35)	108.8(2)
F(2)-C(2)-C(1)	120.7(3)	C(38)-C(39)-Fe(2)	70.52(15)
C(3)-C(2)-C(1)	118.4(3)	C(35)-C(39)-Fe(2)	69.56(13)
F(3)-C(3)-C(4)	120.1(3)	C(44)-C(40)-C(41)	107.1(3)
F(3)-C(3)-C(2)	119.5(3)	C(44)-C(40)-Fe(2)	70.19(16)
C(4)-C(3)-C(2)	120.4(3)	C(41)-C(40)-Fe(2)	69.58(16)
F(4)-C(4)-C(3)	119.8(3)	C(42)-C(41)-C(40)	108.0(3)

F(4)-C(4)-C(5)	120.7(3)	C(42)-C(41)-Fe(2)	69.99(17)
C(3)-C(4)-C(5)	119.5(3)	C(40)-C(41)-Fe(2)	69.83(16)
F(5)-C(5)-C(6)	120.4(2)	C(41)-C(42)-C(43)	108.4(3)
F(5)-C(5)-C(4)	117.1(2)	C(41)-C(42)-Fe(2)	69.98(17)
C(6)-C(5)-C(4)	122.5(3)	C(43)-C(42)-Fe(2)	70.14(16)
C(1)-C(6)-C(5)	115.5(2)	C(44)-C(43)-C(42)	107.8(3)
C(1)-C(6)-B(1)	115.3(2)	C(44)-C(43)-Fe(2)	70.24(16)
C(5)-C(6)-B(1)	129.1(2)	C(42)-C(43)-Fe(2)	69.64(17)
F(6)-C(7)-C(12)	119.8(2)	C(43)-C(44)-C(40)	108.6(3)
F(6)-C(7)-C(8)	117.3(2)	C(43)-C(44)-Fe(2)	69.89(15)
C(12)-C(7)-C(8)	122.9(3)	C(40)-C(44)-Fe(2)	69.59(16)

5.4 Crystal Data Obtained for 3

Table 5-6: Atomic Parameters x, y, z and U(eq) for 3.

	<u>x</u>	<u>y</u>	<u>z</u>	<u>U(eq)</u>
Fe(1)	0.52548(12)	0.30104(9)	0.07772(7)	3.33(3)
P(1)	0.38206(18)	0.05277(17)	0.22296(12)	2.57(5)
F(1)	0.3975(4)	0.3244(3)	0.3274(2)	3.74(12)
F(2)	0.4205(5)	0.3657(4)	0.4786(3)	4.78(14)
F(3)	0.5372(5)	0.2332(4)	0.5804(3)	5.83(15)
F(4)	0.6364(5)	0.0559(4)	0.5230(3)	5.22(15)
F(5)	0.6305(4)	0.0185(4)	0.3701(3)	3.81(12)
F(6)	0.5828(4)	-0.0228(3)	0.1315(3)	3.52(12)
F(7)	0.8030(4)	-0.0697(4)	0.0846(3)	4.59(13)
F(8)	1.0067(4)	0.0339(4)	0.1436(3)	4.60(13)
F(9)	0.9795(4)	0.1829(4)	0.2551(3)	4.18(13)
F(10)	0.7613(4)	0.2283(4)	0.3048(2)	3.29(11)
C(1)	0.4937(6)	0.2552(6)	0.1932(4)	2.20(17)
C(2)	0.3838(7)	0.2938(7)	0.1517(5)	3.5(2)
C(3)	0.4027(10)	0.3948(7)	0.1258(5)	4.6(3)
C(4)	0.5217(10)	0.4255(6)	0.1507(5)	4.5(3)
C(5)	0.5779(7)	0.3389(6)	0.1898(4)	3.1(2)
C(6)	0.5725(12)	0.1794(8)	0.0103(6)	5.1(3)
C(7)	0.6771(11)	0.2441(15)	0.0246(6)	8.6(4)
C(8)	0.6426(14)	0.3371(12)	-0.0063(8)	9.1(4)
C(9)	0.5312(12)	0.3366(11)	-0.0368(7)	7.6(3)
C(10)	0.4744(11)	0.2363(11)	-0.0291(5)	7.3(4)
C(11)	0.5187(6)	0.1718(6)	0.3381(4)	2.01(17)
C(12)	0.4640(7)	0.2571(6)	0.3722(4)	2.45(18)
C(13)	0.4730(7)	0.2795(6)	0.4518(4)	2.9(2)
C(14)	0.5308(8)	0.2126(8)	0.5027(5)	3.7(2)
C(15)	0.5812(7)	0.1251(7)	0.4742(5)	3.4(2)
C(16)	0.5753(7)	0.1071(6)	0.3938(5)	2.8(2)
C(17)	0.6572(6)	0.1072(6)	0.2204(4)	2.00(17)
C(18)	0.6787(6)	0.0309(6)	0.1654(4)	2.51(18)
C(19)	0.7931(7)	0.0054(6)	0.1397(5)	2.9(2)
C(20)	0.8939(7)	0.0563(7)	0.1682(5)	3.1(2)
C(21)	0.8808(7)	0.1328(7)	0.2250(5)	2.8(2)
C(22)	0.7650(7)	0.1536(6)	0.2487(4)	2.36(18)
C(23)	0.2531(7)	0.0990(7)	0.2743(5)	4.0(2)
C(24)	0.4064(8)	-0.0742(7)	0.2625(5)	4.2(2)
C(25)	0.3209(7)	0.0346(7)	0.1223(5)	3.5(2)

B(1)	0.5217(7)	0.1504(7)	0.2417(5)	2.08(19)
------	-----------	-----------	-----------	----------

Table 5-7: Hydrogen Parameter x, y, z and U(eq) for 3.

	<u>x</u>	<u>y</u>	<u>z</u>	<u>U(eq)</u>
H(1)	0.3096	0.256	0.1433	4.1418
H(2)	0.3446	0.4358	0.0963	5.5388
H(3)	0.5579	0.4912	0.1431	5.3998
H(4)	0.6604	0.3373	0.2106	3.7595
H(5)	0.5684	0.1088	0.0249	6.0983
H(6)	0.7539	0.2263	0.05	10.3222
H(7)	0.6945	0.396	-0.0056	10.8899
H(8)	0.4917	0.3947	-0.0611	9.14
H(9)	0.394	0.2141	-0.0456	8.7484
H(10)	0.2734	0.0996	0.3293	4.7948
H(11)	0.2331	0.1671	0.2572	4.7948
H(12)	0.1846	0.0549	0.2637	4.7948
H(13)	0.3349	-0.1149	0.2519	5.0998
H(14)	0.4743	-0.1053	0.2389	5.0998
H(15)	0.4229	-0.0698	0.3178	5.0998
H(16)	0.2904	0.0985	0.102	4.2148
H(17)	0.3842	0.0103	0.0907	4.2148
H(18)	0.2561	-0.0145	0.1217	4.2148

Table 5-8: Interatomic distances (\AA) and Angles ($^\circ$) for 3.**Distances:**

Fe(1)-C(1)	2.098(7)	C(1)-C(5)	1.42(1)
Fe(1)-C(2)	2.044(8)	C(1)-B(1)	1.61(1)
Fe(1)-C(3)	2.012(9)	C(2)-C(3)	1.40(1)
Fe(1)-C(4)	2.037(8)	C(3)-C(4)	1.40(1)
Fe(1)-C(5)	2.022(8)	C(4)-C(5)	1.43(1)
Fe(1)-C(6)	2.030(9)	C(6)-C(7)	1.42(2)
Fe(1)-C(7)	2.06(1)	C(6)-C(10)	1.44(1)
Fe(1)-C(8)	2.02(1)	C(7)-C(8)	1.36(2)
Fe(1)-C(9)	2.01(1)	C(8)-C(9)	1.30(2)
Fe(1)-C(10)	2.052(9)	C(9)-C(10)	1.45(2)
P(1)-C(23)	1.796(8)	C(11)-C(12)	1.40(1)
P(1)-C(24)	1.792(9)	C(11)-C(16)	1.386(9)
P(1)-C(25)	1.820(8)	C(11)-B(1)	1.66(1)
P(1)-B(1)	1.992(9)	C(12)-C(13)	1.383(9)

F(1)-C(12)	1.346(8)	C(13)-C(14)	1.36(1)
F(2)-C(13)	1.345(8)	C(14)-C(15)	1.36(1)
F(3)-C(14)	1.347(8)	C(15)-C(16)	1.39(1)
F(4)-C(15)	1.344(9)	C(17)-C(18)	1.390(9)
F(5)-C(16)	1.366(8)	C(17)-C(22)	1.384(9)
F(6)-C(18)	1.359(8)	C(17)-B(1)	1.64(1)
F(7)-C(19)	1.358(8)	C(18)-C(19)	1.38(1)
F(8)-C(20)	1.351(8)	C(19)-C(20)	1.35(1)
F(9)-C(21)	1.335(8)	C(20)-C(21)	1.40(1)
F(10)-C(22)	1.360(8)	C(21)-C(22)	1.37(1)
C(1)-C(2)	1.447(9)		

Angles:

C(1)-Fe(1)-C(2)	40.9(3)	F(9)-C(21)-C(22)	121.8(8)
C(1)-Fe(1)-C(3)	69.2(3)	C(20)-C(21)-C(22)	118.1(7)
C(1)-Fe(1)-C(4)	69.1(3)	F(10)-C(22)-C(17)	119.8(6)
C(1)-Fe(1)-C(5)	40.4(3)	F(10)-C(22)-C(21)	114.0(7)
C(1)-Fe(1)-C(6)	111.6(3)	C(17)-C(22)-C(21)	126.1(7)
C(1)-Fe(1)-C(7)	119.0(4)	P(1)-B(1)-C(1)	109.3(5)
C(1)-Fe(1)-C(8)	150.3(5)	P(1)-B(1)-C(11)	102.1(5)
C(1)-Fe(1)-C(9)	171.6(5)	P(1)-B(1)-C(17)	116.0(5)
C(1)-Fe(1)-C(10)	131.5(4)	C(1)-B(1)-C(11)	110.6(6)
C(2)-Fe(1)-C(3)	40.4(3)	C(1)-B(1)-C(17)	109.0(6)
C(2)-Fe(1)-C(4)	67.7(4)	C(11)-B(1)-C(17)	109.8(5)
C(2)-Fe(1)-C(5)	67.4(3)	C(4)-Fe(1)-C(7)	126.4(6)
C(2)-Fe(1)-C(6)	122.2(4)	C(4)-Fe(1)-C(8)	106.4(5)
C(2)-Fe(1)-C(7)	154.4(6)	C(4)-Fe(1)-C(9)	114.4(5)
C(2)-Fe(1)-C(8)	166.3(5)	C(4)-Fe(1)-C(10)	148.2(5)
C(2)-Fe(1)-C(9)	132.1(4)	C(5)-Fe(1)-C(6)	130.8(4)
C(2)-Fe(1)-C(10)	110.3(4)	C(5)-Fe(1)-C(7)	107.8(4)
C(3)-Fe(1)-C(4)	40.5(4)	C(5)-Fe(1)-C(8)	116.9(5)
C(3)-Fe(1)-C(5)	68.4(3)	C(5)-Fe(1)-C(9)	147.0(5)
C(3)-Fe(1)-C(6)	153.0(5)	C(5)-Fe(1)-C(10)	169.9(5)
C(3)-Fe(1)-C(7)	163.7(6)	C(6)-Fe(1)-C(7)	40.8(4)
C(3)-Fe(1)-C(8)	127.3(5)	C(6)-Fe(1)-C(8)	65.9(5)
C(3)-Fe(1)-C(9)	108.1(4)	C(6)-Fe(1)-C(9)	66.9(5)
C(3)-Fe(1)-C(10)	116.8(5)	C(6)-Fe(1)-C(10)	41.2(4)
C(4)-Fe(1)-C(5)	41.1(3)	C(7)-Fe(1)-C(8)	38.9(5)
C(4)-Fe(1)-C(6)	166.5(5)	C(7)-Fe(1)-C(9)	65.8(5)
Fe(1)-C(1)-C(5)	66.9(4)	C(7)-Fe(1)-C(10)	69.7(5)
Fe(1)-C(1)-B(1)	133.0(5)	C(8)-Fe(1)-C(9)	37.6(4)

C(2)-C(1)-C(5)	103.7(7)	C(8)-Fe(I)-C(10)	67.7(5)
C(2)-C(1)-B(1)	132.2(7)	C(9)-Fe(I)-C(10)	41.8(4)
C(5)-C(1)-B(1)	123.9(6)	C(23)-P(1)-C(24)	103.2(4)
Fe(I)-C(2)-C(1)	71.6(4)	C(23)-P(1)-C(25)	104.1(4)
Fe(I)-C(2)-C(3)	68.6(5)	C(23)-P(1)-B(1)	108.7(4)
C(1)-C(2)-C(3)	110.2(8)	C(24)-P(1)-C(25)	105.9(4)
Fe(I)-C(3)-C(2)	71.0(5)	C(24)-P(1)-B(1)	115.2(4)
Fe(I)-C(3)-C(4)	70.7(5)	C(25)-P(1)-B(1)	118.2(4)
C(2)-C(3)-C(4)	108.6(8)	Fe(I)-C(1)-C(2)	67.6(4)
Fe(I)-C(4)-C(3)	68.8(5)	Fe(I)-C(9)-C(8)	71.8(9)
Fe(I)-C(4)-C(5)	68.9(5)	Fe(I)-C(9)-C(10)	70.8(7)
C(3)-C(4)-C(5)	106.7(7)	C(8)-C(9)-C(10)	111(1)
Fe(I)-C(5)-C(1)	72.7(4)	Fe(I)-C(10)-C(6)	68.6(5)
Fe(I)-C(5)-C(4)	70.0(5)	Fe(I)-C(10)-C(9)	67.4(6)
C(1)-C(5)-C(4)	110.8(7)	C(6)-C(10)-C(9)	101(1)
Fe(I)-C(6)-C(7)	70.8(6)	C(12)-C(11)-C(16)	112.3(7)
Fe(I)-C(6)-C(10)	70.2(6)	C(12)-C(11)-B(1)	124.9(6)
C(7)-C(6)-C(10)	110(1)	C(16)-C(11)-B(1)	122.8(7)
Fe(I)-C(7)-C(6)	68.5(5)	F(1)-C(12)-C(11)	120.4(6)
Fe(I)-C(7)-C(8)	68.9(8)	F(1)-C(12)-C(13)	115.4(7)
C(6)-C(7)-C(8)	105(1)	C(11)-C(12)-C(13)	124.2(7)
Fe(I)-C(8)-C(7)	72.2(8)	F(2)-C(13)-C(12)	119.7(7)
Fe(I)-C(8)-C(9)	70.7(9)	F(2)-C(13)-C(14)	120.3(7)
C(7)-C(8)-C(9)	113(1)	C(12)-C(13)-C(14)	119.9(8)
C(22)-C(17)-B(1)	122.3(7)	F(3)-C(14)-C(13)	119.9(8)
F(6)-C(18)-C(17)	119.8(6)	F(3)-C(14)-C(15)	120.9(8)
F(6)-C(18)-C(19)	115.5(7)	C(13)-C(14)-C(15)	119.1(7)
C(17)-C(18)-C(19)	124.7(7)	F(4)-C(15)-C(14)	120.7(7)
F(7)-C(19)-C(18)	119.6(7)	F(4)-C(15)-C(16)	119.7(8)
F(7)-C(19)-C(20)	120.4(7)	C(14)-C(15)-C(16)	119.6(8)
C(18)-C(19)-C(20)	120.0(7)	F(5)-C(16)-C(11)	119.6(7)
F(8)-C(20)-C(19)	121.3(8)	F(5)-C(16)-C(15)	115.7(7)
F(8)-C(20)-C(21)	119.6(7)	C(11)-C(16)-C(15)	124.7(8)
C(19)-C(20)-C(21)	119.1(7)	C(18)-C(17)-C(22)	112.0(6)
F(9)-C(21)-C(20)	120.1(7)	C(18)-C(17)-B(1)	125.3(6)

5.5 Crystal Data Obtained for 4

Table 5-9: Atomic Parameters x, y, z and U(eq) for 4.

	<u>x</u>	<u>y</u>	<u>z</u>	<u>U(eq)</u>
Fe	0.68088(4)	0.86276(4)	0.20344(3)	0.03710(16)
B	0.7571(3)	0.6072(3)	0.1907(2)	0.0324(10)
C1	0.6361(3)	0.7618(3)	0.1095(2)	0.0437(9)
C2	0.5366(3)	0.8306(3)	0.1192(2)	0.0534(11)
C3	0.5002(3)	0.8138(3)	0.1961(2)	0.0512(10)
C4	0.5753(3)	0.7364(3)	0.2324(2)	0.0451(10)
C5	0.6609(3)	0.7009(2)	0.17867(19)	0.0362(8)
C6	0.8398(3)	0.8990(3)	0.2763(2)	0.0520(10)
C7	0.8530(3)	0.9296(3)	0.1991(2)	0.0565(11)
C8	0.7613(4)	1.0025(3)	0.1771(2)	0.0634(12)
C9	0.6914(3)	1.0152(3)	0.2425(3)	0.0578(11)
C10	0.7399(3)	0.9519(3)	0.3028(2)	0.0537(11)
C11	0.5827(3)	0.4815(2)	0.12113(18)	0.0325(8)
C12	0.5424(3)	0.3886(3)	0.08794(18)	0.0351(9)
C13	0.6186(3)	0.3054(3)	0.09041(19)	0.0360(8)
C14	0.7357(3)	0.3164(3)	0.12501(19)	0.0335(8)
C15	0.7725(3)	0.4088(3)	0.15721(18)	0.0329(8)
C16	0.7004(3)	0.4977(2)	0.15726(17)	0.0302(8)
C17	0.8989(3)	0.6199(2)	0.07240(19)	0.0348(8)
C18	1.0043(3)	0.6376(3)	0.0362(2)	0.0434(9)
C19	1.1075(3)	0.6722(3)	0.0808(2)	0.0414(9)
C20	1.1016(3)	0.6884(3)	0.1591(2)	0.0362(8)
C21	0.9941(3)	0.6693(2)	0.19324(18)	0.0331(8)
C22	0.8873(3)	0.6336(2)	0.15148(17)	0.0310(8)
C23	0.8271(7)	0.6069(5)	0.4286(3)	0.067(2)
C23'	0.837(2)	0.510(2)	0.4146(12)	0.14(2)
F1	0.49902(15)	0.55970(14)	0.11556(11)	0.0469(5)
F2	0.42686(16)	0.38017(14)	0.05293(11)	0.0528(5)
F3	0.58048(17)	0.21482(14)	0.05839(11)	0.0570(6)
F4	0.81307(17)	0.23535(14)	0.12426(11)	0.0524(5)
F5	0.88980(16)	0.41444(14)	0.19118(11)	0.0452(5)
F6	0.80090(17)	0.58560(15)	0.02392(10)	0.0496(5)
F7	1.00779(18)	0.62006(17)	-0.04190(11)	0.0659(6)
F8	1.21326(17)	0.68832(17)	0.04739(12)	0.0671(7)
F9	1.20266(16)	0.72183(14)	0.20375(11)	0.0490(5)
F10	0.99832(15)	0.68873(16)	0.27148(10)	0.0506(5)
F11	0.7892(7)	0.7047(6)	0.4247(4)	0.107(3)

F11'	0.839(3)	0.420(3)	0.3782(17)	0.154(19)
F12	0.7984(6)	0.5672(4)	0.4958(2)	0.1037(18)
F12'	0.800(2)	0.497(2)	0.4842(12)	0.150(11)
F13	0.9460(6)	0.6078(6)	0.4284(4)	0.107(2)
F13'	0.949(2)	0.5467(18)	0.4217(15)	0.100(9)
O1	0.79518(19)	0.59636(17)	0.28183(12)	0.0426(6)
O2	0.6261(7)	0.5418(7)	0.3542(7)	0.088(4)
O2'	0.6130(19)	0.5380(19)	0.346(3)	0.061(12)
O3	0.8076(9)	0.4338(5)	0.3529(5)	0.080(2)
O3'	0.732(3)	0.6886(19)	0.4014(18)	0.089(9)
S	0.75371(18)	0.5316(2)	0.34662(9)	0.0452(7)
S'	0.7268(7)	0.5928(9)	0.3589(4)	0.059(3)

Table 5-10: Hydrogen Parameters x, y, z and U(eq) for 4.

	<u>x</u>	<u>y</u>	<u>z</u>	<u>U(eq)</u>
H1A	0.6808	0.7567	0.0615	0.052
H2A	0.4982	0.8793	0.0793	0.064
H3A	0.4318	0.8493	0.2195	0.061
H4A	0.5696	0.7095	0.2864	0.054
H6A	0.8929	0.8488	0.3074	0.062
H7A	0.9179	0.9058	0.1662	0.068
H8A	0.7498	1.0404	0.1264	0.076
H9A	0.6209	1.063	0.2451	0.069
H10A	0.7098	0.9459	0.3558	0.064

Table 5-11: Interatomic Distances (Å) and Angles (°) for 4.**Distances:**

Fe-C3	2.062(3)	F9-C20	1.352(3)
Fe-C2	2.073(3)	F10-C21	1.352(3)
Fe-C8	2.071(4)	F11-C23	1.327(8)
Fe-C9	2.075(3)	F12-C23	1.315(6)
Fe-C7	2.074(4)	F13-C23	1.298(7)
Fe-C4	2.080(3)	F11'-C23'	1.309(15)
Fe-C1	2.085(3)	F12'-C23'	1.300(14)
Fe-C10	2.097(3)	F13'-C23'	1.305(15)
Fe-C6	2.091(4)	C1-C2	1.423(4)
Fe-C5	2.137(3)	C1-C5	1.421(4)
S-O3	1.392(8)	C2-C3	1.417(5)
S-O2	1.416(7)	C3-C	41.399(5)

S-O1	1.486(2)	C4-C5	1.440(4)
S-C23	1.824(6)	C6-C7	1.392(5)
S'-O2'	1.427(16)	C6-C10	1.395(4)
S'-O3'	1.430(16)	C7-C8	1.399(5)
S'-O1	1.567(7)	C8-C9	1.414(5)
S'-C23'	1.816(17)	C9-C10	1.378(5)
B-O1	1.575(4)	C11-C12	1.380(4)
B-C5	1.601(5)	C11-C16	1.388(4)
B-C16	1.624(5)	C12-C13	1.355(4)
B-C22	1.658(4)	C13-C14	1.365(4)
F1-C11	1.358(3)	C14-C15	1.357(4)
F2-C12	1.349(3)	C15-C16	1.390(4)
F3-C13	1.339(4)	C17-C18	1.372(4)
F4-C14	1.344(3)	C17-C22	1.374(4)
F5-C15	1.358(3)	C18-C19	1.374(4)
F6-C17	1.364(3)	C19-C20	1.357(4)
F7-C18	1.352(4)	C20-C21	1.377(4)
F8-C19	1.347(3)	C21-C22	1.387(4)

Angles:

C(1)-Fe(1)-C(2)	38.7(4)	Fe(1)-C(10)-C(6)	69.4(8)
C(1)-Fe(1)-C(3)	66.8(5)	Fe(1)-C(10)-C(9)	69.1(7)
C(1)-Fe(1)-C(4)	66.6(5)	C(6)-C(10)-C(9)	103.9(13)
C(1)-Fe(1)-C(5)	41.1(4)	C(12)-C(11)-C(16)	114.1(10)
C(1)-Fe(1)-C(6)	110.6(4)	C(12)-C(11)-B(1)	127.2(10)
C(1)-Fe(1)-C(7)	118.8(5)	C(16)-C(11)-B(1)	118.7(10)
C(1)-Fe(1)-C(8)	147.9(6)	F(2)-C(12)-C(11)	120.6(11)
C(1)-Fe(1)-C(9)	170.2(7)	F(2)-C(12)-C(13)	112.0(10)
C(1)-Fe(1)-C(10)	131.5(5)	C(11)-C(12)-C(13)	127.4(11)
C(2)-Fe(1)-C(3)	39.4(4)	F(3)-C(13)-C(12)	123.0(12)
C(2)-Fe(1)-C(4)	66.0(5)	F(3)-C(13)-C(14)	122.6(12)
C(2)-Fe(1)-C(5)	66.5(5)	C(12)-C(13)-C(14)	114.4(11)
C(2)-Fe(1)-C(6)	132.7(6)	F(4)-C(14)-C(13)	118.7(12)
C(2)-Fe(1)-C(7)	112.8(5)	F(4)-C(14)-C(15)	118.9(13)
C(2)-Fe(1)-C(8)	118.5(6)	C(13)-C(14)-C(15)	122.2(12)
C(2)-Fe(1)-C(9)	150.6(6)	F(5)-C(15)-C(14)	121.9(12)
C(2)-Fe(1)-C(10)	169.3(6)	F(5)-C(15)-C(16)	120.2(12)
C(3)-Fe(1)-C(4)	40.5(5)	C(14)-C(15)-C(16)	117.9(11)
C(3)-Fe(1)-C(5)	67.2(5)	F(6)-C(16)-C(11)	120.8(11)
C(3)-Fe(1)-C(6)	170.1(7)	F(6)-C(16)-C(15)	115.4(11)
C(3)-Fe(1)-C(7)	132.6(7)	C(11)-C(16)-C(15)	123.8(11)

C(3)-Fe(1)-C(8)	110.7(6)	C(18)-C(17)-C(22)	115.6(11)
C(3)-Fe(1)-C(9)	119.0(6)	C(18)-C(17)-B(1)	119.0(10)
C(3)-Fe(1)-C(10)	149.0(7)	C(22)-C(17)-B(1)	125.4(10)
C(4)-Fe(1)-C(5)	38.7(4)	F(7)-C(18)-C(17)	122.8(11)
C(4)-Fe(1)-C(6)	148.5(7)	F(7)-C(18)-C(19)	116.6(12)
C(4)-Fe(1)-C(7)	170.6(7)	C(17)-C(18)-C(19)	120.6(11)
C(4)-Fe(1)-C(8)	133.6(6)	F(8)-C(19)-C(18)	117.9(13)
C(4)-Fe(1)-C(9)	112.0(6)	F(8)-C(19)-C(20)	120.3(15)
C(4)-Fe(1)-C(10)	116.7(6)	C(18)-C(19)-C(20)	121.7(13)
C(5)-Fe(1)-C(6)	117.8(5)	F(9)-C(20)-C(19)	118.9(16)
C(5)-Fe(1)-C(7)	150.4(6)	F(9)-C(20)-C(21)	124.8(14)
C(5)-Fe(1)-C(8)	170.2(6)	C(19)-C(20)-C(21)	116.3(15)
C(5)-Fe(1)-C(9)	131.7(7)	F(10)-C(21)-C(20)	114.8(14)
C(5)-Fe(1)-C(10)	108.7(5)	F(10)-C(21)-C(22)	124.6(14)
C(6)-Fe(1)-C(7)	39.2(4)	C(20)-C(21)-C(22)	120.5(13)
C(6)-Fe(1)-C(8)	66.0(5)	F(11)-C(22)-C(17)	122.0(10)
C(6)-Fe(1)-C(9)	65.1(5)	F(11)-C(22)-C(21)	112.8(11)
C(6)-Fe(1)-C(10)	39.8(4)	C(17)-C(22)-C(21)	125.2(13)
C(7)-Fe(1)-C(8)	37.8(4)	Fe(2)-C(23)-C(24)	69.4(5)
C(7)-Fe(1)-C(9)	64.1(5)	Fe(2)-C(23)-C(27)	69.3(6)
C(7)-Fe(1)-C(10)	66.3(5)	Fe(2)-C(23)-B(2)	124.2(7)
C(8)-Fe(1)-C(9)	40.0(5)	C(24)-C(23)-C(27)	106.5(9)
C(8)-Fe(1)-C(10)	67.9(5)	C(24)-C(23)-B(2)	130.3(10)
C(9)-Fe(1)-C(10)	39.5(4)	C(27)-C(23)-B(2)	123.1(10)
C(23)-Fe(2)-C(24)	38.9(3)	Fe(2)-C(24)-C(23)	71.7(6)
C(23)-Fe(2)-C(25)	67.0(4)	C(23)-C(24)-C(25)	68.4(6)
C(23)-Fe(2)-C(26)	67.7(4)	Fe(2)-C(24)-C(25)	108.6(9)
C(23)-Fe(2)-C(27)	40.5(3)	Fe(2)-C(25)-C(24)	71.1(6)
C(23)-Fe(2)-C(28)	113.9(5)	Fe(2)-C(25)-C(26)	70.6(6)
C(23)-Fe(2)-C(29)	142.4(7)	C(24)-C(25)-C(26)	108.5(9)
C(23)-Fe(2)-C(30)	174.3(6)	Fe(2)-C(26)-C(25)	68.7(6)
C(23)-Fe(2)-C(31)	136.4(5)	Fe(2)-C(26)-C(27)	71.5(6)
C(23)-Fe(2)-C(32)	110.9(4)	C(25)-C(26)-C(27)	106.7(10)
C(24)-Fe(2)-C(25)	40.5(4)	Fe(2)-C(27)-C(23)	70.2(6)
C(24)-Fe(2)-C(26)	68.0(4)	Fe(2)-C(27)-C(26)	69.5(6)
C(24)-Fe(2)-C(27)	66.3(4)	C(23)-C(27)-C(26)	109.7(9)
C(24)-Fe(2)-C(28)	109.3(5)	Fe(2)-C(28)-C(29)	72.0(9)
C(24)-Fe(2)-C(29)	114.8(5)	Fe(2)-C(28)-C(32)	69.2(8)
C(24)-Fe(2)-C(30)	146.7(6)	C(29)-C(28)-C(32)	107.9(14)
C(24)-Fe(2)-C(31)	173.3(6)	Fe(2)-C(29)-C(28)	70.2(8)
C(24)-Fe(2)-C(32)	133.7(6)	Fe(2)-C(29)-C(30)	70.5(8)
C(25)-Fe(2)-C(26)	40.7(4)	C(28)-C(29)-C(30)	109.3(13)
C(25)-Fe(2)-C(27)	66.3(4)	Fe(2)-C(30)-C(29)	68.0(8)

C(25)-Fe(2)-C(28)	133.9(6)	Fe(2)-C(30)-C(31)	71.1(7)
C(25)-Fe(2)-C(29)	112.1(5)	C(29)-C(30)-C(31)	105.7(13)
C(25)-Fe(2)-C(30)	116.7(5)	Fe(2)-C(31)-C(30)	70.7(8)
C(25)-Fe(2)-C(31)	146.0(6)	Fe(2)-C(31)-C(32)	66.9(7)
C(25)-Fe(2)-C(32)	172.9(7)	C(30)-C(31)-C(32)	107.3(13)
C(26)-Fe(2)-C(27)	39.0(3)	Fe(2)-C(32)-C(28)	70.9(8)
C(26)-Fe(2)-C(28)	174.0(6)	Fe(2)-C(32)-C(31)	73.2(8)
C(26)-Fe(2)-C(29)	137.7(6)	C(28)-C(32)-C(31)	109.8(12)
C(26)-Fe(2)-C(30)	111.9(5)	C(34)-C(33)-C(38)	114.6(12)
C(26)-Fe(2)-C(31)	116.2(5)	C(34)-C(33)-B(2)	121.4(11)
C(26)-Fe(2)-C(32)	145.8(7)	C(38)-C(33)-B(2)	124.0(12)
C(27)-Fe(2)-C(28)	145.6(6)	F(13)-C(34)-C(33)	120.5(12)
C(27)-Fe(2)-C(29)	176.4(7)	F(13)-C(34)-C(35)	116.8(12)
C(27)-Fe(2)-C(30)	135.8(6)	C(33)-C(34)-C(35)	122.7(11)
C(27)-Fe(2)-C(31)	113.3(4)	F(14)-C(35)-C(34)	116.9(12)
C(27)-Fe(2)-C(32)	117.0(5)	F(14)-C(35)-C(36)	121.9(15)
C(28)-Fe(2)-C(29)	37.8(4)	C(34)-C(35)-C(36)	121.1(14)
C(28)-Fe(2)-C(30)	67.1(5)	F(15)-C(36)-C(35)	120.7(17)
C(28)-Fe(2)-C(31)	67.0(5)	F(15)-C(36)-C(37)	119.6(15)
C(28)-Fe(2)-C(32)	39.9(4)	C(35)-C(36)-C(37)	119.4(15)
C(29)-Fe(2)-C(30)	41.5(5)	F(16)-C(37)-C(36)	120.8(16)
C(29)-Fe(2)-C(31)	66.1(5)	F(16)-C(37)-C(38)	118.6(15)
C(29)-Fe(2)-C(32)	65.0(5)	C(36)-C(37)-C(38)	120.6(14)
C(30)-Fe(2)-C(31)	38.2(4)	F(17)-C(38)-C(33)	122.4(14)
C(30)-Fe(2)-C(32)	65.9(5)	F(17)-C(38)-C(37)	116.1(14)
C(31)-Fe(2)-C(32)	39.9(4)	C(33)-C(38)-C(37)	121.5(13)
Fe(1)-C(1)-C(2)	69.8(6)	C(40)-C(39)-C(44)	114.6(10)
Fe(1)-C(1)-C(5)	68.5(6)	C(40)-C(39)-B(2)	126.9(10)
Fe(1)-C(1)-B(1)	127.9(7)	C(44)-C(39)-B(2)	118.5(10)
C(2)-C(1)-C(5)	105.9(9)	F(18)-C(40)-C(39)	119.5(10)
C(2)-C(1)-B(1)	130.7(13)	F(18)-C(40)-C(41)	119.5(11)
C(5)-C(1)-B(1)	123.4(12)	C(39)-C(40)-C(41)	120.9(10)
Fe(1)-C(2)-C(1)	71.5(7)	F(19)-C(41)-C(40)	116.7(11)
Fe(1)-C(2)-C(3)	69.9(8)	F(19)-C(41)-C(42)	118.5(12)
C(1)-C(2)-C(3)	111.0(13)	C(40)-C(41)-C(42)	124.8(11)
Fe(1)-C(3)-C(2)	70.6(7)	F(20)-C(42)-C(41)	124.0(13)
Fe(1)-C(3)-C(4)	69.3(8)	F(20)-C(42)-C(43)	118.3(12)
C(2)-C(3)-C(4)	105.7(14)	C(41)-C(42)-C(43)	117.6(12)
C(3)-C(4)-C(3)	110.1(15)	C(42)-C(43)-C(44)	120.0(11)
Fe(1)-C(5)-C(1)	70.3(6)	F(22)-C(44)-C(39)	120.6(10)
Fe(1)-C(5)-C(4)	70.0(7)	F(22)-C(44)-C(43)	117.4(11)

C(1)-C(5)-C(4)	107.2(13)	C(39)-C(44)-C(43)	121.9(11)
Fe(1)-C(6)-C(7)	70.3(6)	F(1)-B(1)-C(1)	108.1(11)
Fe(1)-C(6)-C(10)	70.8(7)	F(1)-B(1)-C(11)	105.8(9)
C(7)-C(6)-C(10)	108.2(11)	F(1)-B(1)-C(17)	109.2(8)
Fe(1)-C(7)-C(6)	70.4(7)	C(1)-B(1)-C(11)	112.3(8)
Fe(1)-C(7)-C(8)	71.2(7)	C(1)-B(1)-C(17)	111.5(10)
C(6)-C(7)-C(8)	111.3(14)	C(11)-B(1)-C(17)	109.9(10)
Fe(1)-C(8)-C(7)	71.0(8)	F(12)-B(2)-C(23)	108.7(9)
Fe(1)-C(8)-C(9)	69.5(8)	F(12)-B(2)-C(33)	111.2(9)
C(7)-C(8)-C(9)	105.3(14)	F(12)-B(2)-C(39)	106.5(8)
Fe(1)-C(9)-C(8)	70.5(8)	C(23)-B(2)-C(33)	113.2(9)
Fe(1)-C(9)-C(10)	71.4(8)	C(23)-B(2)-C(39)	112.7(9)
C(8)-C(9)-C(10)	111.2(14)	C(33)-B(2)-C(39)	104.3(9)

5.6 Crystal Data Obtained for 5

Table 5-12: Atomic Parameters x, y, z and U(eq) for 5.

	<u>x</u>	<u>y</u>	<u>z</u>	<u>U(eq)</u>
Fe(1)	0.47424(2)	0.60533(3)	0.19642(2)	0.01850(9)
F(1)	0.58412(10)	0.24337(13)	0.52374(8)	0.0336(4)
F(2)	0.45267(11)	0.10312(14)	0.54280(10)	0.0447(5)
F(3)	0.30219(11)	0.04313(15)	0.40537(11)	0.0511(6)
F(4)	0.28586(10)	0.13217(15)	0.24537(10)	0.0419(5)
F(5)	0.41655(9)	0.27389(13)	0.22274(8)	0.0261(4)
F(6)	0.58875(9)	0.53833(13)	0.49564(8)	0.0260(4)
F(7)	0.73192(9)	0.61097(13)	0.63059(8)	0.0318(4)
F(8)	0.89648(9)	0.50797(13)	0.65393(8)	0.0322(4)
F(9)	0.91412(9)	0.32415(14)	0.53996(9)	0.0360(4)
F(10)	0.77358(9)	0.24535(13)	0.40715(8)	0.0337(4)
F(11)	0.69682(9)	0.48761(12)	0.26609(9)	0.0279(4)
F(12)	0.74000(10)	0.39110(14)	0.13829(9)	0.0373(5)
F(13)	0.68888(10)	0.13876(14)	0.07740(8)	0.0353(5)
F(14)	0.59928(10)	-0.01563(13)	0.15443(10)	0.0387(5)
F(15)	0.55900(9)	0.07630(12)	0.28498(9)	0.0295(4)
C(1)	0.53398(15)	0.5117(2)	0.32085(13)	0.0161(6)
C(2)	0.4417(2)	0.5454(2)	0.30289(14)	0.0186(6)
C(3)	0.4292(2)	0.6857(2)	0.28806(15)	0.0239(7)
C(4)	0.5129(2)	0.7420(2)	0.29664(15)	0.0242(7)
C(5)	0.5762(2)	0.6367(2)	0.31709(14)	0.0202(6)
C(6)	0.4784(2)	0.4795(3)	0.09623(15)	0.0252(7)
C(7)	0.3890(2)	0.5149(3)	0.08179(15)	0.0264(7)
C(8)	0.3823(2)	0.6562(3)	0.0753(2)	0.0309(8)
C(9)	0.4673(2)	0.7063(3)	0.0846(2)	0.0325(8)
C(10)	0.5268(2)	0.5975(3)	0.09739(15)	0.0317(8)
C(11)	0.50752(15)	0.2702(2)	0.37208(14)	0.0173(6)
C(12)	0.5111(2)	0.2212(2)	0.45129(15)	0.0220(7)
C(13)	0.4436(2)	0.1468(2)	0.4632(2)	0.0283(8)
C(14)	0.3684(2)	0.1152(2)	0.3943(2)	0.0300(8)
C(15)	0.3609(2)	0.1606(2)	0.3142(2)	0.0264(7)
C(16)	0.4287(2)	0.2344(2)	0.30459(15)	0.0213(7)
C(17)	0.67267(14)	0.3945(2)	0.43973(13)	0.0152(6)
C(18)	0.66855(15)	0.4836(2)	0.50232(14)	0.0176(6)
C(19)	0.7416(2)	0.5224(2)	0.57300(14)	0.0200(6)
C(20)	0.8241(2)	0.4686(2)	0.58612(14)	0.0199(6)
C(21)	0.83251(15)	0.3770(2)	0.52870(15)	0.0202(6)

C(22)	0.7574(2)	0.3401(2)	0.45857(14)	0.0194(6)
C(23)	0.61563(15)	0.2942(2)	0.27744(14)	0.0159(6)
C(24)	0.66612(15)	0.3627(2)	0.23832(14)	0.0181(6)
C(25)	0.6911(2)	0.3142(2)	0.17247(15)	0.0219(7)
C(26)	0.6664(2)	0.1889(2)	0.14168(15)	0.0231(7)
C(27)	0.6205(2)	0.1113(2)	0.1811(2)	0.0252(7)
C(28)	0.59823(15)	0.1641(2)	0.24738(14)	0.0187(6)
B(1)	0.5829(2)	0.3640(2)	0.3524(2)	0.0164(7)

Table 5-13: Hydrogen Parameters x, y, z and U(eq) for 5.

	<u>x</u>	<u>y</u>	<u>z</u>	<u>U(eq)</u>
H(1)	0.3944	0.4818	0.3011	0.022
H(2)	0.3724	0.7342	0.2743	0.029
H(3)	0.525	0.8364	0.2897	0.029
H(4)	0.6402	0.6478	0.3273	0.024
H(5)	0.5028	0.3887	0.1041	0.03
H(6)	0.3399	0.453	0.077	0.032
H(7)	0.3279	0.7092	0.066	0.037
H(8)	0.4827	0.8007	0.0826	0.039
H(9)	0.5907	0.603	0.1056	0.038

Table 5-14: Interatomic Distances (Å) and Angles (°) for 5.

Distances:			
Fe(1)-C(1)	2.152(2)	C(3)-C(4)	1.409(3)
Fe(1)-C(2)	2.100(2)	C(4)-C(5)	1.414(3)
Fe(1)-C(3)	2.065(2)	C(6)-C(7)	1.403(3)
Fe(1)-C(4)	2.069(2)	C(6)-C(10)	1.408(3)
Fe(1)-C(5)	2.098(2)	C(7)-C(8)	1.421(3)
Fe(1)-C(6)	2.106(2)	C(8)-C(9)	1.400(4)
Fe(1)-C(7)	2.102(2)	C(9)-C(10)	1.411(4)
Fe(1)-C(8)	2.079(2)	C(11)-C(12)	1.384(3)
Fe(1)-C(9)	2.080(2)	C(11)-C(16)	1.396(3)
Fe(1)-C(10)	2.098(2)	C(11)-B(1)	1.648(3)
F(1)-C(12)	1.356(3)	C(12)-C(13)	1.382(3)
F(2)-C(13)	1.348(3)	C(13)-C(14)	1.363(3)
F(3)-C(14)	1.345(3)	C(14)-C(15)	1.368(3)
F(4)-C(15)	1.354(3)	C(15)-C(16)	1.366(3)
F(5)-C(16)	1.359(3)	C(17)-C(18)	1.388(3)
F(6)-C(18)	1.354(3)	C(17)-C(22)	1.384(3)
F(7)-C(19)	1.353(2)	C(17)-B(1)	1.657(3)

F(8)-C(20)	1.348(2)	C(18)-C(19)	1.378(3)
F(9)-C(21)	1.354(3)	C(19)-C(20)	1.364(3)
F(10)-C(22)	1.362(2)	C(20)-C(21)	1.364(3)
F(11)-C(24)	1.362(2)	C(21)-C(22)	1.386(3)
F(12)-C(25)	1.357(3)	C(23)-C(24)	1.385(3)
F(13)-C(26)	1.339(3)	C(23)-C(28)	1.388(3)
F(14)-C(27)	1.349(3)	C(23)-B(1)	1.666(3)
F(15)-C(28)	1.355(3)	C(24)-C(25)	1.380(3)
C(1)-C(2)	1.433(3)	C(25)-C(26)	1.359(3)
C(1)-C(5)	1.434(3)	C(26)-C(27)	1.383(3)
C(1)-B(1)	1.666(3)	C(27)-C(28)	1.378(3)
C(2)-C(3)	1.428(3)		

Angles:

C(1)-Fe(1)-C(2)	39.36(8)	Fe(1)-C(8)-C(7)	71.01(13)
C(1)-Fe(1)-C(3)	67.36(9)	Fe(1)-C(8)-C(9)	70.35(14)
C(1)-Fe(1)-C(4)	67.49(9)	C(7)-C(8)-C(9)	107.8(2)
C(1)-Fe(1)-C(5)	39.41(8)	Fe(1)-C(9)-C(8)	70.30(15)
C(1)-Fe(1)-C(6)	111.54(9)	Fe(1)-C(9)-C(10)	70.96(14)
C(1)-Fe(1)-C(7)	126.73(9)	C(8)-C(9)-C(10)	108.2(2)
C(1)-Fe(1)-C(8)	161.44(10)	Fe(1)-C(10)-C(6)	70.72(14)
C(1)-Fe(1)-C(9)	158.46(10)	Fe(1)-C(10)-C(9)	69.56(15)
C(1)-Fe(1)-C(10)	124.81(10)	C(6)-C(10)-C(9)	108.1(2)
C(2)-Fe(1)-C(3)	40.10(8)	C(12)-C(11)-C(16)	112.8(2)
C(2)-Fe(1)-C(4)	66.79(9)	C(12)-C(11)-B(1)	127.3(2)
C(2)-Fe(1)-C(5)	65.29(9)	C(16)-C(11)-B(1)	119.9(2)
C(2)-Fe(1)-C(6)	125.46(10)	F(1)-C(12)-C(11)	120.8(2)
C(2)-Fe(1)-C(7)	111.23(10)	F(1)-C(12)-C(13)	115.2(2)
C(2)-Fe(1)-C(8)	125.50(10)	C(11)-C(12)-C(13)	124.0(2)
C(2)-Fe(1)-C(9)	159.87(10)	F(2)-C(13)-C(12)	120.1(2)
C(2)-Fe(1)-C(10)	159.64(10)	F(2)-C(13)-C(14)	119.8(2)
C(3)-Fe(1)-C(4)	39.86(9)	C(12)-C(13)-C(14)	120.1(2)
C(3)-Fe(1)-C(5)	66.10(9)	F(3)-C(14)-C(13)	120.5(3)
C(3)-Fe(1)-C(6)	158.86(10)	F(3)-C(14)-C(15)	120.9(2)
C(3)-Fe(1)-C(7)	123.41(10)	C(13)-C(14)-C(15)	118.7(2)
C(3)-Fe(1)-C(8)	107.72(10)	F(4)-C(15)-C(14)	119.4(2)
C(3)-Fe(1)-C(9)	123.09(10)	F(4)-C(15)-C(16)	120.8(2)
C(3)-Fe(1)-C(10)	159.18(10)	C(14)-C(15)-C(16)	119.9(2)
C(4)-Fe(1)-C(5)	39.66(9)	F(5)-C(16)-C(11)	119.3(2)
C(4)-Fe(1)-C(6)	160.96(10)	F(5)-C(16)-C(15)	116.1(2)
C(4)-Fe(1)-C(7)	156.95(10)	C(11)-C(16)-C(15)	124.6(2)

C(4)-Fe(1)-C(8)	121.08(10)	C(18)-C(17)-C(22)	112.9(2)
C(4)-Fe(1)-C(9)	107.41(10)	C(18)-C(17)-B(1)	120.9(2)
C(4)-Fe(1)-C(10)	124.52(10)	C(22)-C(17)-B(1)	126.2(2)
C(5)-Fe(1)-C(6)	127.49(9)	F(6)-C(18)-C(17)	119.7(2)
C(5)-Fe(1)-C(7)	162.43(9)	F(6)-C(18)-C(19)	115.9(2)
C(5)-Fe(1)-C(8)	156.79(9)	C(17)-C(18)-C(19)	124.3(2)
C(5)-Fe(1)-C(9)	123.48(10)	F(7)-C(19)-C(18)	120.6(2)
C(5)-Fe(1)-C(10)	111.20(10)	F(7)-C(19)-C(20)	119.7(2)
C(6)-Fe(1)-C(7)	38.96(9)	C(18)-C(19)-C(20)	119.7(2)
C(6)-Fe(1)-C(8)	66.18(10)	F(8)-C(20)-C(19)	120.3(2)
C(6)-Fe(1)-C(9)	66.06(10)	F(8)-C(20)-C(21)	120.6(2)
C(6)-Fe(1)-C(10)	39.13(9)	C(19)-C(20)-C(21)	119.1(2)
C(7)-Fe(1)-C(8)	39.73(9)	F(9)-C(21)-C(20)	119.9(2)
C(7)-Fe(1)-C(9)	66.04(10)	F(9)-C(21)-C(22)	120.6(2)
C(7)-Fe(1)-C(10)	65.56(10)	C(20)-C(21)-C(22)	119.5(2)
C(8)-Fe(1)-C(9)	39.35(10)	F(10)-C(22)-C(17)	121.6(2)
C(8)-Fe(1)-C(10)	66.07(10)	F(10)-C(22)-C(21)	114.2(2)
C(9)-Fe(1)-C(10)	39.48(10)	C(17)-C(22)-C(21)	124.3(2)
Fe(1)-C(1)-C(2)	68.38(12)	C(24)-C(23)-C(28)	111.8(2)
Fe(1)-C(1)-C(5)	68.28(12)	C(24)-C(23)-B(1)	122.2(2)
Fe(1)-C(1)-B(1)	133.13(15)	C(28)-C(23)-B(1)	125.9(2)
C(2)-C(1)-C(5)	104.4(2)	F(11)-C(24)-C(23)	119.7(2)
C(2)-C(1)-B(1)	127.1(2)	F(11)-C(24)-C(25)	114.8(2)
C(5)-C(1)-B(1)	128.0(2)	C(23)-C(24)-C(25)	125.4(2)
Fe(1)-C(2)-C(1)	72.26(13)	F(12)-C(25)-C(24)	120.3(2)
Fe(1)-C(2)-C(3)	68.62(14)	F(12)-C(25)-C(26)	120.0(2)
C(1)-C(2)-C(3)	109.7(2)	C(24)-C(25)-C(26)	119.7(2)
Fe(1)-C(3)-C(2)	71.28(14)	F(13)-C(26)-C(25)	121.4(2)
Fe(1)-C(3)-C(4)	70.22(14)	F(13)-C(26)-C(27)	120.3(2)
C(2)-C(3)-C(4)	108.0(2)	C(25)-C(26)-C(27)	118.2(2)
Fe(1)-C(4)-C(3)	69.92(13)	F(14)-C(27)-C(26)	119.2(2)
Fe(1)-C(4)-C(5)	71.28(13)	F(14)-C(27)-C(28)	121.1(2)
C(3)-C(4)-C(5)	107.1(2)	C(26)-C(27)-C(28)	119.7(2)
Fe(1)-C(5)-C(1)	72.31(12)	F(15)-C(28)-C(23)	120.7(2)
Fe(1)-C(5)-C(4)	69.06(13)	F(15)-C(28)-C(27)	114.4(2)
C(1)-C(5)-C(4)	110.9(2)	C(23)-C(28)-C(27)	124.9(2)
Fe(1)-C(6)-C(7)	70.39(14)	C(1)-B(1)-C(11)	106.0(2)
Fe(1)-C(6)-C(10)	70.14(14)	C(1)-B(1)-C(17)	105.7(2)
C(7)-C(6)-C(10)	108.0(2)	C(1)-B(1)-C(23)	112.0(2)
Fe(1)-C(7)-C(6)	70.65(14)	C(11)-B(1)-C(17)	113.2(2)
Fe(1)-C(7)-C(8)	69.25(14)	C(11)-B(1)-C(23)	110.9(2)
C(6)-C(7)-C(8)	108.0(2)	C(17)-B(1)-C(23)	108.9(2)

5.7 Crystal Data Obtained for 7

Table 5-15: Atomic Parameters x, y, z and U(eq) for 7.

	<u>x</u>	<u>y</u>	<u>z</u>	<u>U(eq)</u>
Fe(1)	0.22549(16)	0.12137(12)	0.18696(14)	0.0507(7)
Fe(2)	0.95973(15)	0.51380(12)	0.24302(14)	0.0417(6)
F(1)	0.1103(5)	0.2182(4)	0.4103(4)	0.053(2)
F(2)	0.1320(5)	-0.0922(4)	0.3631(5)	0.075(3)
F(3)	0.0951(5)	-0.1892(4)	0.4854(5)	0.080(3)
F(4)	0.1137(5)	-0.0712(5)	0.6885(5)	0.073(3)
F(5)	0.1808(6)	0.1485(5)	0.7685(5)	0.074(3)
F(6)	0.2199(5)	0.2504(4)	0.6459(5)	0.064(2)
F(7)	0.4259(5)	0.0939(5)	0.5212(5)	0.074(3)
F(8)	0.6350(6)	0.2228(6)	0.6299(6)	0.105(3)
F(9)	0.6622(7)	0.4389(6)	0.6646(6)	0.130(3)
F(10)	0.4669(6)	0.5228(5)	0.5892(5)	0.093(3)
F(11)	0.2592(6)	0.4006(4)	0.4801(5)	0.069(3)
F(12)	0.8376(5)	0.2332(4)	0.1007(4)	0.050(2)
F(13)	0.5698(5)	0.3755(4)	0.2076(5)	0.057(2)
F(14)	0.3785(6)	0.4148(5)	0.0776(5)	0.082(3)
F(15)	0.3550(7)	0.3864(5)	-0.1252(6)	0.106(3)
F(16)	0.5266(8)	0.3161(5)	-0.1958(6)	0.126(4)
F(17)	0.7196(6)	0.2782(5)	-0.0699(5)	0.079(3)
F(18)	0.7334(6)	0.3214(4)	0.3682(4)	0.061(3)
F(19)	0.6253(6)	0.1718(5)	0.4116(6)	0.089(3)
F(20)	0.5466(6)	-0.0387(4)	0.2660(5)	0.081(3)
F(21)	0.5737(6)	-0.0923(4)	0.0752(5)	0.080(3)
F(22)	0.6686(6)	0.0583(4)	0.0247(5)	0.067(3)
C(1)	0.1983(11)	0.0757(7)	0.3073(9)	0.046(4)
C(2)	0.2828(12)	0.0240(8)	0.2755(10)	0.062(5)
C(3)	0.2379(16)	-0.0397(10)	0.1656(14)	0.089(7)
C(4)	0.1182(14)	-0.0280(11)	0.1280(11)	0.082(6)
C(5)	0.0918(11)	0.0415(9)	0.2105(11)	0.070(5)
C(6)	0.2417(14)	0.2884(8)	0.2285(12)	0.069(5)
C(7)	0.3490(12)	0.2579(10)	0.2317(11)	0.064(5)
C(8)	0.3419(14)	0.1875(11)	0.1358(14)	0.072(6)
C(9)	0.2255(17)	0.1756(10)	0.0667(10)	0.076(6)
C(10)	0.1600(12)	0.2358(11)	0.1224(13)	0.082(6)
C(11)	0.1769(9)	0.0833(8)	0.4982(9)	0.034(4)
C(12)	0.1448(10)	-0.0260(8)	0.4647(9)	0.044(4)
C(13)	0.1243(10)	-0.0849(9)	0.5239(11)	0.052(5)
C(14)	0.1326(10)	-0.0219(10)	0.6259(11)	0.051(5)

Table 5-16: Hydrogen Parameters x, y, z and U(eq) for 7.

	<u>x</u>	<u>y</u>	<u>z</u>	<u>U(eq)</u>
H(1)	0.3611	0.0309	0.3223	0.074
H(2)	0.2788	-0.0821	0.1244	0.107
H(3)	0.0644	-0.0634	0.056	0.098
H(4)	0.0182	0.0635	0.2058	0.084
C(15)	0.1675(10)	0.0883(10)	0.6675(9)	0.048(5)
C(16)	0.1879(9)	0.1382(8)	0.6005(10)	0.043(4)
C(17)	0.3313(9)	0.2396(8)	0.4944(8)	0.033(4)
C(18)	0.4289(11)	0.1993(9)	0.5346(10)	0.052(5)
C(19)	0.5390(11)	0.2688(12)	0.5933(10)	0.067(6)
C(20)	0.5529(14)	0.3766(12)	0.6094(11)	0.079(6)
C(21)	0.4507(14)	0.4159(9)	0.5694(11)	0.062(5)
C(22)	0.3493(11)	0.3486(8)	0.5135(9)	0.052(4)
C(23)	0.8504(9)	0.3948(7)	0.2564(8)	0.032(4)
C(24)	0.8274(9)	0.4985(8)	0.3018(8)	0.043(4)
C(25)	0.9327(11)	0.5652(7)	0.3851(9)	0.051(4)
C(26)	1.0231(10)	0.5012(9)	0.3921(9)	0.054(5)
C(27)	0.9728(10)	0.3975(7)	0.3148(9)	0.040(4)
C(28)	0.8917(12)	0.5416(14)	0.1020(12)	0.080(7)
C(29)	0.9558(18)	0.6359(11)	0.1797(14)	0.088(7)
C(30)	1.0793(13)	0.6213(12)	0.2247(11)	0.077(6)
C(31)	1.0824(13)	0.5147(13)	0.1660(13)	0.068(6)
C(32)	0.9661(17)	0.4650(9)	0.0924(10)	0.075(6)
C(33)	0.6538(10)	0.3209(7)	0.0758(9)	0.038(4)
C(34)	0.5652(12)	0.3579(8)	0.1074(9)	0.040(4)
C(35)	0.4608(12)	0.3768(9)	0.0356(11)	0.049(5)
C(36)	0.4489(14)	0.3624(10)	-0.0610(12)	0.069(6)
C(37)	0.5358(15)	0.3302(10)	-0.0967(10)	0.062(6)
C(38)	0.6396(12)	0.3094(9)	-0.0277(12)	0.053(5)
C(39)	0.7062(9)	0.2004(8)	0.1968(9)	0.038(4)
C(40)	0.6944(10)	0.2212(8)	0.2931(9)	0.039(4)
C(41)	0.6372(11)	0.1415(10)	0.3125(10)	0.051(5)
C(42)	0.5954(11)	0.0385(10)	0.2438(11)	0.053(5)
C(43)	0.6075(10)	0.0110(9)	0.1479(11)	0.052(5)
C(44)	0.6586(10)	0.0905(9)	0.1214(9)	0.041(4)
B(1)	0.2038(12)	0.1551(9)	0.4255(12)	0.056(5)
B(2)	0.7680(11)	0.2906(9)	0.1577(10)	0.033(5)

H(5)	0.2258	0.3364	0.2876	0.083
H(6)	0.4187	0.2837	0.2942	0.077
H(7)	0.4026	0.1529	0.1181	0.086
H(8)	0.1953	0.1321	-0.0081	0.091
H(9)	0.0793	0.2404	0.095	0.098
H(10)	0.7538	0.521	0.2807	0.051
H(11)	0.9413	0.6398	0.4288	0.061
H(12)	1.1025	0.5251	0.4403	0.065
H(13)	1.0126	0.3373	0.3021	0.049
H(14)	0.8102	0.5289	0.0608	0.096
H(15)	0.9269	0.7017	0.2023	0.106
H(16)	1.1428	0.6742	0.282	0.092
H(17)	1.1498	0.481	0.1735	0.082
H(18)	0.9425	0.3909	0.0439	0.09

Table 5-17: Interatomic Distances (\AA) and Angles ($^\circ$) for 7.**Distances:**

Fe(1)-C(1)	2.094(10)	C(3)-C(4)	1.423(18)
Fe(1)-C(2)	2.073(11)	C(4)-C(5)	1.365(14)
Fe(1)-C(3)	2.064(12)	C(6)-C(7)	1.384(15)
Fe(1)-C(4)	2.052(12)	C(6)-C(10)	1.411(16)
Fe(1)-C(5)	2.070(11)	C(7)-C(8)	1.335(14)
Fe(1)-C(6)	2.061(10)	C(8)-C(9)	1.407(17)
Fe(1)-C(7)	2.060(11)	C(9)-C(10)	1.397(16)
Fe(1)-C(8)	2.063(12)	C(11)-C(12)	1.349(11)
Fe(1)-C(9)	2.050(12)	C(11)-C(16)	1.342(12)
Fe(1)-C(10)	2.079(13)	C(11)-B(1)	1.697(15)
Fe(2)-C(23)	2.101(9)	C(12)-C(13)	1.381(13)
Fe(2)-C(24)	2.071(10)	C(13)-C(14)	1.371(13)
Fe(2)-C(25)	2.036(10)	C(14)-C(15)	1.357(13)
Fe(2)-C(26)	2.061(10)	C(15)-C(16)	1.391(12)
Fe(2)-C(27)	2.088(9)	C(17)-C(18)	1.364(13)
Fe(2)-C(28)	2.058(13)	C(17)-C(22)	1.361(11)
Fe(2)-C(29)	2.080(13)	C(17)-B(1)	1.651(14)
Fe(2)-C(30)	2.114(12)	C(18)-C(19)	1.406(14)
Fe(2)-C(31)	2.120(12)	C(19)-C(20)	1.354(14)
Fe(2)-C(32)	2.037(12)	C(20)-C(21)	1.399(17)
F(1)-B(1)	1.452(12)	C(21)-C(22)	1.314(14)
F(2)-C(12)	1.361(10)	C(23)-C(24)	1.390(11)
F(3)-C(13)	1.280(10)	C(23)-C(27)	1.449(12)

F(4)-C(14)	1.323(11)	C(23)-B(2)	1.584(13)
F(5)-C(15)	1.333(10)	C(24)-C(25)	1.423(12)
F(6)-C(16)	1.377(9)	C(25)-C(26)	1.424(13)
F(7)-C(18)	1.336(10)	C(26)-C(27)	1.386(11)
F(8)-C(19)	1.380(12)	C(28)-C(29)	1.339(15)
F(9)-C(20)	1.360(14)	C(28)-C(32)	1.397(16)
F(10)-C(21)	1.332(11)	C(29)-C(30)	1.488(17)
F(11)-C(22)	1.366(12)	C(30)-C(31)	1.384(14)
F(12)-B(2)	1.434(11)	C(31)-C(32)	1.422(16)
F(13)-C(34)	1.338(10)	C(33)-C(34)	1.355(13)
F(14)-C(35)	1.364(12)	C(33)-C(38)	1.369(13)
F(15)-C(36)	1.341(14)	C(33)-B(2)	1.665(14)
F(16)-C(37)	1.315(12)	C(34)-C(35)	1.444(15)
F(17)-C(38)	1.319(12)	C(35)-C(36)	1.271(15)
F(18)-C(40)	1.331(9)	C(36)-C(37)	1.347(16)
F(19)-C(41)	1.382(10)	C(37)-C(38)	1.432(16)
F(20)-C(42)	1.325(10)	C(39)-C(40)	1.352(11)
F(21)-C(43)	1.346(10)	C(39)-C(44)	1.432(11)
F(22)-C(44)	1.337(10)	C(39)-B(2)	1.702(13)
C(1)-C(2)	1.381(13)	C(40)-C(41)	1.379(12)
C(1)-C(5)	1.463(14)	C(41)-C(42)	1.332(12)
C(1)-B(1)	1.626(15)	C(42)-C(43)	1.340(13)
C(2)-C(3)	1.396(16)	C(43)-C(44)	1.404(12)

Angles:

C(1)-Fe(1)-C(2)	38.7(4)	Fe(1)-C(10)-C(6)	69.4(8)
C(1)-Fe(1)-C(3)	66.8(5)	Fe(1)-C(10)-C(9)	69.1(7)
C(1)-Fe(1)-C(4)	66.6(5)	C(6)-C(10)-C(9)	103.9(13)
C(1)-Fe(1)-C(5)	41.1(4)	C(12)-C(11)-C(16)	114.1(10)
C(1)-Fe(1)-C(6)	110.6(4)	C(12)-C(11)-B(1)	127.2(10)
C(1)-Fe(1)-C(7)	118.8(5)	C(16)-C(11)-B(1)	118.7(10)
C(1)-Fe(1)-C(8)	147.9(6)	F(2)-C(12)-C(11)	120.6(11)
C(1)-Fe(1)-C(9)	170.2(7)	F(2)-C(12)-C(13)	112.0(10)
C(1)-Fe(1)-C(10)	131.5(5)	C(11)-C(12)-C(13)	127.4(11)
C(2)-Fe(1)-C(3)	39.4(4)	F(3)-C(13)-C(12)	123.0(12)
C(2)-Fe(1)-C(4)	66.0(5)	F(3)-C(13)-C(14)	122.6(12)
C(2)-Fe(1)-C(5)	66.5(5)	C(12)-C(13)-C(14)	114.4(11)
C(2)-Fe(1)-C(6)	132.7(6)	F(4)-C(14)-C(13)	118.7(12)
C(2)-Fe(1)-C(7)	112.8(5)	F(4)-C(14)-C(15)	118.9(13)
C(2)-Fe(1)-C(8)	118.5(6)	C(13)-C(14)-C(15)	122.2(12)
C(2)-Fe(1)-C(9)	150.6(6)	F(5)-C(15)-C(14)	121.9(12)

C(2)-Fe(1)-C(10)	169.3(6)	F(5)-C(15)-C(16)	120.2(12)
C(3)-Fe(1)-C(4)	40.5(5)	C(14)-C(15)-C(16)	117.9(11)
C(3)-Fe(1)-C(5)	67.2(5)	F(6)-C(16)-C(11)	120.8(11)
C(3)-Fe(1)-C(6)	170.1(7)	F(6)-C(16)-C(15)	115.4(11)
C(3)-Fe(1)-C(7)	132.6(7)	C(11)-C(16)-C(15)	123.8(11)
C(3)-Fe(1)-C(8)	110.7(6)	C(18)-C(17)-C(22)	115.6(11)
C(3)-Fe(1)-C(9)	119.0(6)	C(18)-C(17)-B(1)	119.0(10)
C(3)-Fe(1)-C(10)	149.0(7)	C(22)-C(17)-B(1)	125.4(10)
C(4)-Fe(1)-C(5)	38.7(4)	F(7)-C(18)-C(17)	122.8(11)
C(4)-Fe(1)-C(6)	148.5(7)	F(7)-C(18)-C(19)	116.6(12)
C(4)-Fe(1)-C(7)	170.6(7)	C(17)-C(18)-C(19)	120.6(11)
C(4)-Fe(1)-C(8)	133.6(6)	F(8)-C(19)-C(18)	117.9(13)
C(4)-Fe(1)-C(9)	112.0(6)	F(8)-C(19)-C(20)	120.3(15)
C(4)-Fe(1)-C(10)	116.7(6)	C(18)-C(19)-C(20)	121.7(13)
C(5)-Fe(1)-C(6)	117.8(5)	F(9)-C(20)-C(19)	118.9(16)
C(5)-Fe(1)-C(7)	150.4(6)	F(9)-C(20)-C(21)	124.8(14)
C(5)-Fe(1)-C(8)	170.2(6)	C(19)-C(20)-C(21)	116.3(15)
C(5)-Fe(1)-C(9)	131.7(7)	F(10)-C(21)-C(20)	114.8(14)
C(5)-Fe(1)-C(10)	108.7(5)	F(10)-C(21)-C(22)	124.6(14)
C(6)-Fe(1)-C(7)	39.2(4)	C(20)-C(21)-C(22)	120.5(13)
C(6)-Fe(1)-C(8)	66.0(5)	F(11)-C(22)-C(17)	122.0(10)
C(6)-Fe(1)-C(9)	65.1(5)	F(11)-C(22)-C(21)	112.8(11)
C(6)-Fe(1)-C(10)	39.8(4)	C(17)-C(22)-C(21)	125.2(13)
C(7)-Fe(1)-C(8)	37.8(4)	Fe(2)-C(23)-C(24)	69.4(5)
C(7)-Fe(1)-C(9)	64.1(5)	Fe(2)-C(23)-C(27)	69.3(6)
C(7)-Fe(1)-C(10)	66.3(5)	Fe(2)-C(23)-B(2)	124.2(7)
C(8)-Fe(1)-C(9)	40.0(5)	C(24)-C(23)-C(27)	106.5(9)
C(8)-Fe(1)-C(10)	67.9(5)	C(24)-C(23)-B(2)	130.3(10)
C(9)-Fe(1)-C(10)	39.5(4)	C(27)-C(23)-B(2)	123.1(10)
C(23)-Fe(2)-C(24)	38.9(3)	Fe(2)-C(24)-C(23)	71.7(6)
C(23)-Fe(2)-C(25)	67.0(4)	Fe(2)-C(24)-C(25)	68.4(6)
C(23)-Fe(2)-C(26)	67.7(4)	C(23)-C(24)-C(25)	108.6(9)
C(23)-Fe(2)-C(27)	40.5(3)	Fe(2)-C(25)-C(24)	71.1(6)
C(23)-Fe(2)-C(28)	113.9(5)	Fe(2)-C(25)-C(26)	70.6(6)
C(23)-Fe(2)-C(29)	142.4(7)	C(24)-C(25)-C(26)	108.5(9)
C(23)-Fe(2)-C(30)	174.3(6)	Fe(2)-C(26)-C(25)	68.7(6)
C(23)-Fe(2)-C(31)	136.4(5)	Fe(2)-C(26)-C(27)	71.5(6)
C(23)-Fe(2)-C(32)	110.9(4)	C(25)-C(26)-C(27)	106.7(10)
C(24)-Fe(2)-C(25)	40.5(4)	Fe(2)-C(27)-C(23)	70.2(6)
C(24)-Fe(2)-C(26)	68.0(4)	Fe(2)-C(27)-C(26)	69.5(6)
C(24)-Fe(2)-C(27)	66.3(4)	C(23)-C(27)-C(26)	109.7(9)
C(24)-Fe(2)-C(28)	109.3(5)	Fe(2)-C(28)-C(29)	72.0(9)
C(24)-Fe(2)-C(29)	114.8(5)	Fe(2)-C(28)-C(32)	69.2(8)

C(24)-Fe(2)-C(30)	146.7(6)	C(29)-C(28)-C(32)	107.9(14)
C(24)-Fe(2)-C(31)	173.3(6)	Fe(2)-C(29)-C(28)	70.2(8)
C(24)-Fe(2)-C(32)	133.7(6)	Fe(2)-C(29)-C(30)	70.5(8)
C(25)-Fe(2)-C(26)	40.7(4)	C(28)-C(29)-C(30)	109.3(13)
C(25)-Fe(2)-C(27)	66.3(4)	Fe(2)-C(30)-C(29)	68.0(8)
C(25)-Fe(2)-C(28)	133.9(6)	Fe(2)-C(30)-C(31)	71.1(7)
C(25)-Fe(2)-C(29)	112.1(5)	C(29)-C(30)-C(31)	105.7(13)
C(25)-Fe(2)-C(30)	116.7(5)	Fe(2)-C(31)-C(30)	70.7(8)
C(25)-Fe(2)-C(31)	146.0(6)	Fe(2)-C(31)-C(32)	66.9(7)
C(25)-Fe(2)-C(32)	172.9(7)	C(30)-C(31)-C(32)	107.3(13)
C(26)-Fe(2)-C(27)	39.0(3)	Fe(2)-C(32)-C(28)	70.9(8)
C(26)-Fe(2)-C(28)	174.0(6)	Fe(2)-C(32)-C(31)	73.2(8)
C(26)-Fe(2)-C(29)	137.7(6)	C(28)-C(32)-C(31)	109.8(12)
C(26)-Fe(2)-C(30)	111.9(5)	C(34)-C(33)-C(38)	114.6(12)
C(26)-Fe(2)-C(31)	116.2(5)	C(34)-C(33)-B(2)	121.4(11)
C(26)-Fe(2)-C(32)	145.8(7)	C(38)-C(33)-B(2)	124.0(12)
C(27)-Fe(2)-C(28)	145.6(6)	F(13)-C(34)-C(33)	120.5(12)
C(27)-Fe(2)-C(29)	176.4(7)	F(13)-C(34)-C(35)	116.8(12)
C(27)-Fe(2)-C(30)	135.8(6)	C(33)-C(34)-C(35)	122.7(11)
C(27)-Fe(2)-C(31)	113.3(4)	F(14)-C(35)-C(34)	116.9(12)
C(27)-Fe(2)-C(32)	117.0(5)	F(14)-C(35)-C(36)	121.9(15)
C(28)-Fe(2)-C(29)	37.8(4)	C(34)-C(35)-C(36)	121.1(14)
C(28)-Fe(2)-C(30)	67.1(5)	F(15)-C(36)-C(35)	120.7(17)
C(28)-Fe(2)-C(31)	67.0(5)	F(15)-C(36)-C(37)	119.6(15)
C(28)-Fe(2)-C(32)	39.9(4)	C(35)-C(36)-C(37)	119.4(15)
C(29)-Fe(2)-C(30)	41.5(5)	F(16)-C(37)-C(36)	120.8(16)
C(29)-Fe(2)-C(31)	66.1(5)	F(16)-C(37)-C(38)	118.6(15)
C(29)-Fe(2)-C(32)	65.0(5)	C(36)-C(37)-C(38)	120.6(14)
C(30)-Fe(2)-C(31)	38.2(4)	F(17)-C(38)-C(33)	122.4(14)
C(30)-Fe(2)-C(32)	65.9(5)	F(17)-C(38)-C(37)	116.1(14)
C(31)-Fe(2)-C(32)	39.9(4)	C(33)-C(38)-C(37)	121.5(13)
Fe(1)-C(1)-C(2)	69.8(6)	C(40)-C(39)-C(44)	114.6(10)
Fe(1)-C(1)-C(5)	68.5(6)	C(40)-C(39)-B(2)	126.9(10)
Fe(1)-C(1)-B(1)	127.9(7)	C(44)-C(39)-B(2)	118.5(10)
C(2)-C(1)-C(5)	105.9(9)	F(18)-C(40)-C(39)	119.5(10)
C(2)-C(1)-B(1)	130.7(13)	F(18)-C(40)-C(41)	119.5(11)
C(5)-C(1)-B(1)	123.4(12)	C(39)-C(40)-C(41)	120.9(10)
Fe(1)-C(2)-C(1)	71.5(7)	F(19)-C(41)-C(40)	116.7(11)
Fe(1)-C(2)-C(3)	69.9(8)	F(19)-C(41)-C(42)	118.5(12)
C(1)-C(2)-C(3)	111.0(13)	C(40)-C(41)-C(42)	124.8(11)
Fe(1)-C(3)-C(2)	70.6(7)	F(20)-C(42)-C(41)	124.0(13)
Fe(1)-C(3)-C(4)	69.3(8)	F(20)-C(42)-C(43)	118.3(12)
C(2)-C(3)-C(4)	105.7(14)	C(41)-C(42)-C(43)	117.6(12)

Fe(1)-C(4)-C(3)	70.2(8)	F(21)-C(43)-C(42)	122.1(12)
Fe(1)-C(4)-C(5)	71.4(7)	F(21)-C(43)-C(44)	117.8(12)
C(3)-C(4)-C(5)	110.1(15)	C(42)-C(43)-C(44)	120.0(11)
Fe(1)-C(5)-C(1)	70.3(6)	F(22)-C(44)-C(39)	120.6(10)
Fe(1)-C(5)-C(4)	70.0(7)	F(22)-C(44)-C(43)	117.4(11)
C(1)-C(5)-C(4)	107.2(13)	C(39)-C(44)-C(43)	121.9(11)
Fe(1)-C(6)-C(7)	70.3(6)	F(1)-B(1)-C(1)	108.1(11)
Fe(1)-C(6)-C(10)	70.8(7)	F(1)-B(1)-C(11)	105.8(9)
C(7)-C(6)-C(10)	108.2(11)	F(1)-B(1)-C(17)	109.2(8)
Fe(1)-C(7)-C(6)	70.4(7)	C(1)-B(1)-C(11)	112.3(8)
Fe(1)-C(7)-C(8)	71.2(7)	C(1)-B(1)-C(17)	111.5(10)
C(6)-C(7)-C(8)	111.3(14)	C(11)-B(1)-C(17)	109.9(10)
Fe(1)-C(8)-C(7)	71.0(8)	F(12)-B(2)-C(23)	108.7(9)
Fe(1)-C(8)-C(9)	69.5(8)	F(12)-B(2)-C(33)	111.2(9)
C(7)-C(8)-C(9)	105.3(14)	F(12)-B(2)-C(39)	106.5(8)
Fe(1)-C(9)-C(8)	70.5(8)	C(23)-B(2)-C(33)	113.2(9)
Fe(1)-C(9)-C(10)	71.4(8)	C(23)-B(2)-C(39)	112.7(9)
C(8)-C(9)-C(10)	111.2(14)	C(33)-B(2)-C(39)	104.3(9)

5.8 Crystal Data Obtained for 12.

Table 5-18: Atomic Parameters x, y, z and U(eq) for 12.

	<u>x</u>	<u>y</u>	<u>z</u>	<u>U(eq)</u>
Fe1	0.4314(2)	0.16541(12)	0.2292(2)	0.0388(7)
P1	0.0177(3)	0.2321(2)	-0.0975(4)	0.0376(10)
B1	0.2186(15)	0.2793(8)	0.0244(16)	0.028(3)
C1	0.2554(11)	0.2003(7)	0.0864(13)	0.029(3)
C2	0.2889(13)	0.1382(8)	0.0034(15)	0.039(3)
C3	0.2903(15)	0.0663(8)	0.0782(16)	0.050(4)
C4	0.2609(15)	0.0850(9)	0.1999(18)	0.049(4)
C5	0.2415(14)	0.1650(8)	0.2051(16)	0.044(4)
C6	0.5965(14)	0.2648(11)	0.338(2)	0.067(5)
C7	0.6154(16)	0.2078(14)	0.237(2)	0.074(6)
C8	0.6111(19)	0.1316(17)	0.271(3)	0.108(9)
C9	0.5858(19)	0.1377(15)	0.404(2)	0.091(7)
C10	0.5775(16)	0.2210(12)	0.4420(16)	0.060(5)
C11	0.3016(7)	0.3048(5)	-0.0774(8)	0.035(3)
C12	0.4242(8)	0.3618(5)	-0.0056(7)	0.038(3)
C13	0.5000(7)	0.3799(5)	-0.0818(9)	0.043(4)
C14	0.4532(9)	0.3411(6)	-0.2298(9)	0.039(3)
C15	0.3306(9)	0.2842(6)	-0.3016(7)	0.046(4)
C16	0.2548(7)	0.2660(5)	-0.2254(8)	0.045(4)
F1	0.4786(7)	0.3990(5)	0.1354(8)	0.053(2)
F2	0.6177(8)	0.4339(6)	-0.0106(10)	0.066(3)
F3	0.5293(9)	0.3585(5)	-0.3001(10)	0.061(2)
F4	0.2888(10)	0.2476(6)	-0.4408(9)	0.073(3)
F5	0.1433(8)	0.2120(5)	-0.2986(8)	0.057(2)
C17	0.2338(8)	0.3676(4)	0.1355(7)	0.028(3)
C18	0.2947(8)	0.3816(4)	0.2904(7)	0.031(3)
C19	0.3017(9)	0.4557(5)	0.3735(6)	0.039(3)
C20	0.2478(9)	0.5158(4)	0.3016(9)	0.045(4)
C21	0.1869(9)	0.5018(4)	0.1467(9)	0.037(3)
C22	0.1799(8)	0.4277(5)	0.0636(6)	0.030(3)
F6	0.3534(9)	0.3303(5)	0.3637(8)	0.054(2)
F7	0.3648(9)	0.4718(5)	0.5217(9)	0.060(2)
F8	0.2527(8)	0.5870(5)	0.3829(9)	0.058(2)
F9	0.1383(8)	0.5603(5)	0.0787(9)	0.053(2)
F10	0.1272(8)	0.4197(5)	-0.0800(8)	0.046(2)
C23	-0.0545(16)	0.2481(11)	0.031(2)	0.074(6)
C24	-0.0317(15)	0.1233(8)	-0.1647(17)	0.048(4)

C25	-0.0817(15)	0.2690(10)	-0.2577(18)	0.065(5)
C26	-0.069(3)	0.1025(15)	0.293(3)	0.17(3)
C27	-0.0332(17)	0.0487(9)	0.3939(14)	0.175(14)
C28	0.1005(12)	0.0539(12)	0.488(2)	0.118(9)
C29	-0.1341(9)	-0.0107(15)	0.399(2)	0.153(11)
F11	-0.198(3)	0.076(3)	0.202(4)	0.310(18)
F12	0.000(5)	0.101(3)	0.216(4)	0.310(18)
F13	-0.045(5)	0.1775(14)	0.368(5)	0.310(18)
C30	0.062(2)	0.501(2)	0.572(2)	0.155(12)
C31	0.133(4)	0.582(2)	0.691(4)	0.232(19)
C32	0.023(4)	0.626(2)	0.612(4)	0.195(16)
B2	0.5529(15)	0.1217(9)	0.7952(18)	0.101(9)
F14	0.6392(14)	0.0904(9)	0.7574(16)	0.143(6)
F15	0.604(2)	0.2025(8)	0.864(3)	0.170(11)
F16	0.521(2)	0.0792(11)	0.887(2)	0.151(10)
F17	0.4384(17)	0.1150(17)	0.667(2)	0.350(19)
F15'	0.586(3)	0.1956(13)	0.761(4)	0.056(12)
F16'	0.424(2)	0.103(2)	0.769(6)	0.11(2)

Table 5-19: Hydrogen Parameters x, y, z and U(eq) for 12.

	<u>x</u>	<u>y</u>	<u>z</u>	<u>U(eq)</u>
H2	0.3059	0.1425	-0.0787	0.047
H3	0.3078	0.0169	0.0491	0.06
H4	0.2555	0.0506	0.2644	0.059
H5	0.222	0.1922	0.2764	0.052
H6	0.5966	0.32	0.3364	0.081
H7	0.6292	0.2211	0.1566	0.089
H8	0.6217	0.0855	0.2211	0.13
H9	0.5769	0.0955	0.4544	0.11
H10	0.5622	0.2423	0.5212	0.073
H23A	-0.1429	0.2132	-0.0105	0.111
H23B	-0.0586	0.3047	0.0477	0.111
H23C	-0.0003	0.2349	0.1241	0.111
H24A	0.0099	0.0966	-0.0841	0.072
H24B	-0.0047	0.1097	-0.2414	0.072
H24C	-0.1268	0.1051	-0.2047	0.072
H25A	-0.066	0.2487	-0.3405	0.098
H25B	-0.058	0.3281	-0.2361	0.098
H25C	-0.1743	0.2497	-0.2823	0.098

Table 5-20: Interatomic Distances (Å) and Angles (°) for 12.**Distances:**

Fe1-C1	2.149(12)	C19-F7	1.330(9)
P1-C24	1.782(13)	C20-F8	1.350(9)
P1-C25	1.793(15)	C21-F9	1.329(9)
P1-C23	1.815(16)	C22-F10	1.296(9)
P1-B1	2.044(15)	C26-F13	1.314(9)
B1-C1	1.579(18)	C26-F12	1.318(9)
B1-C17	1.691(15)	C26-F11	1.324(9)
B1-C11	1.698(15)	C26-C27	1.418(8)
C1-C5	1.446(18)	C27-C28	1.397(8)
C1-C2	1.461(18)	C27-C29	1.406(8)
C2-C3	1.50(2)	C28-C29	1.382(8)
C3-C4	1.41(2)	C29-C28	1.382(8)
C4-C5	1.399(19)	C30-C30	1.542(10)
C6-C10	1.41(2)	C30-C31	1.550(10)
C6-C7	1.43(2)	C31-C32	1.539(10)
C7-C8	1.36(3)	B2-F16'	1.346(10)
C8-C9	1.48(3)	B2-F14	1.348(9)
C9-C10	1.44(3)	B2-F16	1.354(9)
C12-F1	1.314(9)	B2-F15	1.359(9)
C13-F2	1.330(10)	B2-F15'	1.361(10)
C14-F3	1.341(10)	B2-F17	1.375(9)
C15-F4	1.311(10)	F15-F15'	0.96(3)
C16-F5	1.285(9)	F16-F16'	1.40(4)
C18-F6	1.290(9)	F17-F16'	1.14(4)

Angles:

C24-P1-C25	102.3(7)	F7-C19-C20	119.0(7)
C24-P1-C23	103.9(8)	F7-C19-C18	120.9(7)
C25-P1-C23	105.0(9)	F8-C20-C19	119.7(7)
C24-P1-B1	114.9(6)	F8-C20-C21	120.3(7)
C25-P1-B1	122.9(7)	F9-C21-C20	119.7(7)
C23-P1-B1	106.0(7)	F9-C21-C22	120.3(7)
C1-B1-C17	122.8(10)	F10-C22-C21	117.1(6)
C1-B1-C11	109.3(10)	F10-C22-C17	122.8(6)
C17-B1-C11	107.0(8)	F13-C26-F12	110.7(9)
C1-B1-P1	98.0(7)	F13-C26-F11	109.8(9)

C17-B1-P1	105.0(8)	F12-C26-F11	109.9(9)
C11-B1-P1	114.9(8)	F13-C26-C27	109.5(9)
C5-C1-C2	106.1(11)	F12-C26-C27	108.6(9)
C5-C1-B1	132.2(12)	F11-C26-C27	108.3(9)
C2-C1-B1	120.8(11)	C28-C27-C29	120.0(7)
C5-C1-Fe1	66.9(7)	C28-C27-C26	120.8(8)
C2-C1-Fe1	68.6(7)	C29-C27-C26	119.2(8)
B1-C1-Fe1	137.5(8)	C29-C28-C27	120.4(8)
C1-C2-C3	105.5(12)	C28-C29-C27	118.9(8)
C4-C3-C2	109.5(12)	C30-C30-C31	119(4)
C5-C4-C3	107.0(13)	C32-C31-C30	94(3)
C4-C5-C1	111.9(13)	F16'-B2-F14	141(2)
C10-C6-C7	106.3(18)	F16'-B2-F16	62.3(18)
C8-C7-C6	113(2)	F14-B2-F16	111.0(9)
C7-C8-C9	105.7(19)	F16'-B2-F15	107(2)
C10-C9-C8	107(2)	F14-B2-F15	111.5(9)
C6-C10-C9	108.4(17)	F16-B2-F15	108.8(9)
C12-C11-B1	118.1(6)	F16'-B2-F15'	111.2(11)
C16-C11-B1	121.7(6)	F14-B2-F15'	92.9(16)
F1-C12-C13	115.8(6)	F16-B2-F15'	148.8(17)
F1-C12-C11	124.2(6)	F15-B2-F15'	41.3(14)
F2-C13-C12	119.1(7)	F16'-B2-F17	49(2)
F2-C13-C14	120.9(7)	F14-B2-F17	108.5(9)
F3-C14-C15	121.1(7)	F16-B2-F17	108.3(9)
F3-C14-C13	118.9(7)	F15-B2-F17	108.7(9)
F4-C15-C14	119.1(7)	F15'-B2-F17	81.2(16)
F4-C15-C16	120.9(7)	F15'-F15-B2	69.4(10)
F5-C16-C15	116.4(7)	B2-F16-F16'	58.6(9)
F5-C16-C11	123.6(7)	F16'-F17-B2	64.0(11)
C18-C17-B1	123.7(7)	F15-F15'-B2	69.2(11)
C22-C17-B1	116.3(7)	F17-F16'-B2	66.7(12)
F6-C18-C17	122.9(6)	F17-F16'-F16	121.5(19)
F6-C18-C19	116.9(6)	B2-F16'-F16	59.1(11)

5.9 Crystal Data Obtained for 15

Table 5-21: Atomic Parameters x, y, z and U(eq) for 15.

	<u>x</u>	<u>y</u>	<u>z</u>	<u>U(eq)</u>
Fe	-0.13253(4)	0.13364(2)	0.34607(2)	0.02807(12)
P1	0.04310(8)	0.29452(4)	0.47660(5)	0.0351(2)
P2	-0.38359(9)	-0.04858(4)	0.34952(5)	0.0412(2)
F32	-0.02909(19)	0.31179(9)	0.23533(11)	0.0509(6)
F33	-0.0558(2)	0.41546(10)	0.15193(11)	0.0631(6)
F34	-0.14743(19)	0.51795(10)	0.21143(13)	0.0665(7)
F35	-0.20771(19)	0.51383(9)	0.36003(13)	0.0608(6)
F36	-0.19472(17)	0.40776(9)	0.44313(11)	0.0487(5)
F42	-0.36511(16)	0.31405(9)	0.30575(11)	0.0468(5)
F43	-0.57048(18)	0.28569(10)	0.35194(14)	0.0657(6)
F44	-0.5662(2)	0.23215(11)	0.50001(14)	0.0751(7)
F45	-0.3458(2)	0.21604(10)	0.60622(12)	0.0691(7)
F46	-0.13849(17)	0.24601(9)	0.56285(10)	0.0463(5)
F52	-0.42870(16)	0.11713(8)	0.14829(10)	0.0414(5)
F53	-0.60678(18)	0.20001(9)	0.12934(11)	0.0540(6)
F54	-0.75333(17)	0.20989(9)	0.23948(11)	0.0536(6)
F55	-0.71480(18)	0.13340(10)	0.37208(11)	0.0557(6)
F56	-0.53838(17)	0.04925(9)	0.39253(10)	0.0496(6)
F62	-0.55198(17)	-0.03290(9)	0.17199(10)	0.0462(5)
F63	-0.54847(17)	-0.08168(9)	0.02715(10)	0.0482(5)
F64	-0.34145(18)	-0.07575(9)	-0.03524(10)	0.0515(6)
F65	-0.13607(17)	-0.02254(9)	0.05564(10)	0.0483(5)
F66	-0.13440(16)	0.02254(9)	0.20040(10)	0.0418(5)
C1	-0.1009(3)	0.22781(14)	0.33612(17)	0.0261(7)
C2	-0.1995(3)	0.20613(14)	0.27198(17)	0.0289(8)
C3	-0.1543(3)	0.15985(15)	0.22624(18)	0.0332(8)
C4	-0.0294(3)	0.15054(15)	0.26109(18)	0.0344(8)
C5	0.0026(3)	0.19147(14)	0.32841(17)	0.0297(8)
C6	-0.2464(3)	0.05911(14)	0.34728(16)	0.0261(7)
C7	-0.2626(3)	0.10457(14)	0.40627(16)	0.0313(8)
C8	-0.1503(3)	0.11422(15)	0.46278(18)	0.0354(8)
C9	-0.0614(3)	0.07506(15)	0.44084(18)	0.0385(9)
C10	-0.1199(3)	0.04092(14)	0.37079(18)	0.0348(8)
C11	0.1612(3)	0.31759(16)	0.42311(19)	0.0428(9)
C12	0.0449(3)	0.35422(16)	0.55222(18)	0.0451(10)
C13	0.1066(3)	0.22699(16)	0.53383(19)	0.0470(10)
C21	-0.3253(3)	-0.03980(17)	0.45834(18)	0.0513(10)

C22	-0.2900(4)	-0.10941(17)	0.3208(2)	0.0704(13)
C23	-0.5322(3)	-0.08443(18)	0.3414(2)	0.0640(12)
C31	-0.1162(3)	0.35252(14)	0.34298(17)	0.0290(8)
C32	-0.0797(3)	0.35903(15)	0.26881(18)	0.0335(8)
C33	-0.0909(3)	0.41299(17)	0.22428(19)	0.0387(9)
C34	-0.1359(3)	0.46496(17)	0.2544(2)	0.0444(10)
C35	-0.1677(3)	0.46240(16)	0.3292(2)	0.0410(9)
C36	-0.1589(3)	0.40724(16)	0.37062(19)	0.0354(8)
C41	-0.2376(3)	0.27908(14)	0.43045(18)	0.0299(8)
C42	-0.3536(3)	0.28898(15)	0.3820(2)	0.0369(8)
C43	-0.4628(3)	0.27449(16)	0.4041(2)	0.0460(10)
C44	-0.4604(4)	0.24897(18)	0.4788(2)	0.0497(10)
C45	-0.3500(4)	0.24041(16)	0.5316(2)	0.0456(10)
C46	-0.2441(3)	0.25626(15)	0.50697(19)	0.0370(9)
C51	-0.4759(3)	0.07629(14)	0.27009(17)	0.0271(7)
C52	-0.4987(3)	0.11766(15)	0.20529(17)	0.0303(8)
C53	-0.5896(3)	0.16172(15)	0.19436(18)	0.0335(8)
C54	-0.6634(3)	0.16710(16)	0.2497(2)	0.0366(9)
C55	-0.6453(3)	0.12828(16)	0.31541(19)	0.0365(8)
C56	-0.5538(3)	0.08476(15)	0.32354(18)	0.0335(8)
C61	-0.3445(3)	-0.00063(14)	0.19546(17)	0.0294(8)
C62	-0.4451(3)	-0.02879(15)	0.14581(18)	0.0326(8)
C63	-0.4464(3)	-0.05442(15)	0.06984(18)	0.0342(8)
C64	-0.3431(3)	-0.05147(15)	0.03884(18)	0.0358(8)
C65	-0.2399(3)	-0.02440(15)	0.08408(18)	0.0332(8)
C66	-0.2430(3)	-0.00109(14)	0.16084(18)	0.0305(8)
B1	-0.1131(3)	0.28627(17)	0.3937(2)	0.0289(9)
B2	-0.3598(3)	0.02793(17)	0.2841(2)	0.0287(9)

Table 5-22: Hydrogen Parameters x, y, z and U(eq) for 15.

	<u>x</u>	<u>y</u>	<u>z</u>	<u>U(eq)</u>
H2	-0.2859	0.2214	0.2614	0.035
H3	-0.2029	0.1374	0.1780	0.040
H4	0.0267	0.1207	0.2417	0.041
H5	0.0857	0.1945	0.3650	0.036
H7	-0.3410	0.1266	0.4070	0.038
H8	-0.1364	0.1437	0.5098	0.043
H9	0.0266	0.0719	0.4693	0.046
H10	-0.0786	0.0101	0.3412	0.042
H11A	0.1343	0.3543	0.3901	0.051
H11B	0.1765	0.2840	0.3873	0.051
H11C	0.2368	0.3269	0.4629	0.051

H12A	0.0111	0.3923	0.5250	0.054
H12B	0.1294	0.3615	0.5815	0.054
H12C	-0.0047	0.3413	0.5912	0.054
H13A	0.1094	0.1928	0.4960	0.056
H13B	0.0550	0.2155	0.5722	0.056
H13C	0.1897	0.2361	0.5642	0.056
H21A	-0.3704	-0.0069	0.4793	0.062
H21B	-0.2381	-0.0293	0.4685	0.062
H21C	-0.3360	-0.0785	0.4862	0.062
H22A	-0.3164	-0.1179	0.2621	0.085
H22B	-0.2990	-0.1467	0.3519	0.085
H22C	-0.2039	-0.0965	0.3327	0.085
H23A	-0.5702	-0.0906	0.2836	0.077
H23B	-0.5846	-0.0577	0.3667	0.077
H23C	-0.5223	-0.1243	0.3695	0.077

Table 5-23: Selected Interatomic Distances (Å) and Angles (°) for 15.**Distances:**

Fe-C1	2.087(3)	C1-C5	1.427(4)
Fe-C2	2.045(3)	C1-B1	1.615(5)
Fe-C3	2.047(3)	C2-C3	1.418(4)
Fe-C4	2.040(3)	C3-C4	1.408(4)
Fe-C5	2.031(3)	C4-C5	1.420(4)
Fe-C6	2.060(3)	C6-C7	1.433(4)
Fe-C7	2.032(3)	C6-C10	1.440(4)
Fe-C8	2.046(3)	C6-B2	1.617(4)
Fe-C9	2.057(3)	C7-C8	1.418(4)
Fe-C10	2.054(3)	C8-C9	1.411(4)
P1-C11	1.812(3)	C9-C10	1.423(4)
P1-C12	1.807(3)	C31-C32	1.391(4)
P1-C13	1.812(3)	C31-C36	1.394(4)
P1-B1	1.996(4)	C31-B1	1.666(5)
P2-C21	1.809(3)	C32-C33	1.379(4)
P2-C22	1.810(4)	C33-C34	1.373(5)
P2-C23	1.812(4)	C34-C35	1.372(5)
P2-B2	2.036(4)	C35-C36	1.376(4)
F32-C32	1.347(3)	C41-C42	1.393(4)
F33-C33	1.348(3)	C41-C46	1.388(4)
F34-C34	1.348(4)	C41-B1	1.639(5)
F35-C35	1.344(4)	C42-C43	1.381(4)
F36-C36	1.354(3)	C43-C44	1.361(5)

F42-C42	1.367(3)	C44-C45	1.370(5)
F43-C43	1.351(4)	C45-C46	1.375(4)
F44-C44	1.352(4)	C51-C52	1.389(4)
F45-C45	1.346(4)	C51-C56	1.383(4)
F46-C46	1.360(3)	C51-B2	1.645(5)
F52-C52	1.353(3)	C52-C53	1.378(4)
F53-C53	1.350(3)	C53-C54	1.365(4)
F54-C54	1.352(3)	C54-C55	1.366(4)
F55-C55	1.349(3)	C55-C56	1.377(4)
F56-C56	1.368(3)	C61-C62	1.390(4)
F62-C62	1.357(3)	C61-C66	1.376(4)
F63-C63	1.348(3)	C61-B2	1.648(4)
F64-C64	1.349(3)	C62-C63	1.384(4)
F65-C65	1.342(3)	C63-C64	1.361(4)
F66-C66	1.355(3)	C64-C65	1.371(4)
C1-C2	1.445(4)	C65-C66	1.386(4)

Angles:

C1-Fe-C2	40.92(11)	C8-C9-C10	07.6(3)
C1-Fe-C3	68.72(12)	Fe-C10-C6	69.76(17)
C1-Fe-C4	68.84(12)	Fe-C10-C9	69.85(18)
C1-Fe-C5	40.52(11)	C6-C10-C9	109.6(3)
C1-Fe-C6	152.24(12)	C32-C31-C36	113.1(3)
C1-Fe-C7	119.59(12)	C32-C31-B1	124.2(3)
C1-Fe-C8	109.24(12)	C36-C31-B1	122.6(3)
C1-Fe-C9	128.51(12)	F32-C32-C31	121.3(3)
C1-Fe-C10	166.02(12)	F32-C32-C33	114.9(3)
C2-Fe-C3	40.55(11)	C31-C32-C33	123.8(3)
C2-Fe-C4	68.16(12)	F33-C33-C32	120.5(3)
C2-Fe-C5	67.97(12)	F33-C33-C34	119.6(3)
C2-Fe-C6	117.53(12)	C32-C33-C34	120.0(3)
C2-Fe-C7	109.29(12)	F34-C34-C33	120.5(3)
C2-Fe-C8	129.80(13)	F34-C34-C35	120.4(3)
C2-Fe-C9	167.29(13)	C33-C34-C35	119.0(3)
C2-Fe-C10	151.30(12)	F35-C35-C34	119.1(3)
C3-Fe-C4	40.30(12)	F35-C35-C36	121.7(3)
C3-Fe-C5	68.01(12)	C34-C35-C36	119.3(3)
C3-Fe-C6	106.32(12)	F36-C36-C31	119.3(3)
C3-Fe-C7	128.33(12)	F36-C36-C35	116.0(3)
C3-Fe-C8	167.18(13)	C31-C36-C35	124.6(3)
C3-Fe-C9	150.82(14)	C42-C41-C46	111.6(3)

C3-Fe-C10	117.28(12)	C42-C41-B1	121.7(3)
C4-Fe-C5	40.82(11)	C46-C41-B1	126.3(3)
C4-Fe-C6	125.97(12)	F42-C42-C41	119.9(3)
C4-Fe-C7	165.08(12)	F42-C42-C43	115.1(3)
C4-Fe-C8	151.93(13)	C41-C42-C43	125.1(3)
C4-Fe-C9	117.68(14)	F43-C43-C42	120.1(3)
C4-Fe-C10	106.93(13)	F43-C43-C44	120.6(3)
C5-Fe-C6	164.88(12)	C42-C43-C44	119.3(4)
C5-Fe-C7	153.27(12)	F44-C44-C43	120.0(4)
C5-Fe-C8	119.28(12)	F44-C44-C45	120.7(4)
C5-Fe-C9	108.40(13)	C43-C44-C45	119.3(3)
C5-Fe-C10	127.82(13)	F45-C45-C44	120.2(3)
C6-Fe-C7	40.98(11)	F45-C45-C46	120.7(4)
C6-Fe-C8	69.25(12)	C44-C45-C46	119.1(3)
C6-Fe-C9	69.28(12)	F46-C46-C41	119.1(3)
C6-Fe-C10	40.98(11)	F46-C46-C45	115.4(3)
C7-Fe-C8	40.71(11)	C41-C46-C45	125.5(3)
C7-Fe-C9	68.09(13)	C52-C51-C56	112.3(3)
C7-Fe-C10	67.80(13)	C52-C51-B2	122.3(3)
C8-Fe-C9	40.24(12)	C56-C51-B2	125.1(3)
C8-Fe-C10	67.82(13)	F52-C52-C51	120.3(3)
C9-Fe-C10	40.52(11)	F52-C52-C53	115.5(3)
C11-P1-C12	104.12(16)	C51-C52-C53	124.2(3)
C11-P1-C13	103.87(16)	F53-C53-C52	120.7(3)
C11-P1-B1	107.60(15)	F53-C53-C54	119.2(3)
C12-P1-C13	105.37(16)	C52-C53-C54	120.1(3)
C12-P1-B1	115.50(16)	F54-C54-C53	120.7(3)
C13-P1-B1	118.83(16)	F54-C54-C55	120.4(3)
C21-P2-C22	103.76(18)	C53-C54-C55	118.9(3)
C21-P2-C23	104.55(17)	F55-C55-C54	120.3(3)
C21-P2-B2	113.21(16)	F55-C55-C56	120.7(3)
C22-P2-C23	103.7(2)	C54-C55-C56	119.0(3)
C22-P2-B2	107.79(16)	F56-C56-C51	119.0(3)
C23-P2-B2	122.03(16)	F56-C56-C55	115.4(3)
Fe-C1-C2	67.97(17)	C51-C56-C55	125.5(3)
Fe-C1-C5	67.62(17)	C62-C61-C66	112.2(3)
Fe-C1-B1	133.3(2)	C62-C61-B2	118.6(3)
C2-C1-C5	105.0(3)	C66-C61-B2	129.1(3)
C2-C1-B1	123.5(3)	F62-C62-C61	119.4(3)
C5-C1-B1	131.2(3)	F62-C62-C63	115.4(3)
Fe-C2-C1	71.11(17)	C61-C62-C63	125.2(3)
Fe-C2-C3	69.81(18)	F63-C63-C62	120.5(3)
C1-C2-C3	109.2(3)	F63-C63-C64	120.6(3)

Fe-C3-C2	69.64(17)	C62-C63-C64	118.9(3)
Fe-C3-C4	69.58(17)	F64-C64-C63	120.4(3)
C2-C3-C4	108.2(3)	F64-C64-C65	120.1(3)
Fe-C4-C3	70.12(18)	C63-C64-C65	119.4(3)
Fe-C4-C5	69.25(17)	F65-C65-C64	120.4(3)
C3-C4-C5	107.5(3)	F65-C65-C66	120.5(3)
Fe-C5-C1	71.85(17)	C64-C65-C66	119.1(3)
Fe-C5-C4	69.93(18)	F66-C66-C61	121.6(3)
C1-C5-C4	110.1(3)	F66-C66-C65	113.4(3)
Fe-C6-C7	68.45(17)	C61-C66-C65	125.1(3)
Fe-C6-C10	69.27(17)	P1-B1-C1	108.3(2)
Fe-C6-B2	136.3(2)	P1-B1-C31	101.4(2)
C7-C6-C10	105.0(3)	P1-B1-C41	115.7(2)
C7-C6-B2	122.9(3)	C1-B1-C31	111.8(2)
C10-C6-B2	130.7(3)	C1-B1-C41	109.4(3)
Fe-C7-C6	70.57(17)	C31-B1-C41	110.1(3)
Fe-C7-C8	70.15(18)	P2-B2-C6	99.39(19)
C6-C7-C8	109.8(3)	P2-B2-C51	114.2(2)
Fe-C8-C7	69.13(17)	P2-B2-C61	103.0(2)
Fe-C8-C9	70.31(17)	C6-B2-C51	108.1(3)
C7-C8-C9	108.0(3)	C6-B2-C61	122.0(3)
Fe-C9-C8	69.45(17)	C51-B2-C61	109.8(2)
Fe-C9-C10	69.63(17)		